TOWARD UNDERSTANDING CRANIAL SUTURES

IN ZEBRAFISH AND CHICKEN

By

Matthew Beckett

Submitted in partial fulfillment of the requirements
for the degree of Master of Science

at

Dalhousie University
Halifax, Nova Scotia
July 2015

DEDICATION

This thesis is dedicated to those who stood next to me in the past, those who stand next to me in the present, and those who will stand next to me in the future.

This thesis is dedicated to all those who may someday, somehow, benefit from this research or from my time working toward it.

This thesis is dedicated to the light at the end of the tunnel.

TABLE OF CONTENTS

LIST OF TABLES

LIST OF FIGURES

ABSTRACT

Cranial sutures are the fibrous joints between the intramembranous bones of the skull roof that enable the skull to grow in size during the development and growth of the brain. Although the skulls of vertebrate model organisms are broadly similar, mammalian models have been consistently utilized for calvariae-related studies. Zebrafish are an emerging model organism and the chicken embryo is an established model organism in developmental biology. By comparing suture development of these organisms we can gain insight into the universality of how sutures form in vertebrates. A growth series was collected for each species and stained to visualize suture formation. Using morphometric analysis, I statistically analyzed the changes in shape of the sutures over growth. In both organisms, the interfrontal suture forms first. In zebrafish, this is followed by formation of the coronal suture and then the sagittal suture. In the chicken model, suture formation occurs late and only the anterior portion of the interfrontal suture has formed by hatching. The manner in which zebrafish sutures form is more similar to that of humans than is that of chicken. I also investigated the distribution of the protein ephrin-B2a in the zebrafish skull, and compared it to that previously found in the cranial sutures of mice. No *efnb2a* was detected in the zebrafish skull roof. By comparing suture formation of these organisms and learning more about the distribution of ephrin-B2a, I have gained insight into how these organisms can be utilized to understand craniosynostosis and other disorders that affect the skull roof.

LIST OF ABBREVIATIONS USED

ANOVA – analysis of variance

BCIP – 5-bromo-4-chloro-3-indolyl phosphate

BMP – bone morphogenetic protein

DepC – Diethylpyrocarbonate

dpf – days post fertilization

efnB2a – mRNA corresponding to ephrin-B2a

FGF(R) – fibroblast growth factor (receptor)

GPI – glycosylphosphatidylinositol

HBQ – Hall, Brunt quadruple stain

HH – Hamburger & Hamilton

hpf – hours post fertilization

Hyb – hybridization

IHC – immunohistochemistry

ISH – *in situ* hybridization

NBF – neural buffered formalin

NBT – nitroblue tetrazolium

PBS – phosphate buffered saline

PBST – phosphate buffered saline with tween-20

PC – principle component

PCA – principle component analysis

PDGF(R) – platelet derived growth factor (receptor)

PF – posterior frontal

PFA – paraformaldehyde

SDS – sodium dodecyl sulphate

SL – standard length

SSC – saline sodium citrate

Tris – trisaminomethane

WB – Western blot

ZIRC – Zebrafish International Resource Centre

ACKNOWLEDGEMENTS

I would first like to thank my supervisor, Dr. Tamara Franz-Odendaal. Thank you for your knowledge, experience, and wisdom. Thank you for your high expectations. Thank you for your patience. And thank you for your endless support.

I would like to thank my supervisory committee, Dr. Kazue Semba, Dr. Frank Smith, and Dr. Michael Bezuhly. Thank you for sharing your insight and wisdom. Thank you for your invaluable guidance. And thank you for being a part of this project.

I would like to thank each member of the Franz-Odendaal Bone Development Lab. Thank you all for the inspiration, the positivity, and the comradery. Thank you, James Jabalee, for guiding me through my first Western analyses. Thank you, Karyn Jourdeuil, for guiding me through my first experiences with the chick embryo and sharing your own years of experience. Thank you, Jade Atkins, for helping ease my transition into the lab. Thank you, Christine Hammer, for sharing your experience with morphometrics. Thank you, Sewvandini Atukorala, for sharing your knowledge of all things fish-related and guiding me through the intricacies of *in situ* hybridization. Thank you, Jochen Weigele, for contributing the probe used for *in situ* hybridization. Thank you, Beverly Hymes, for guiding me through sectioning and slide preparation. I also thank Sewvandini, Beverly, Jochen, Christine, and all others who have shared the work of maintaining the fish care facility.

I would like to thank the rest of my friends and family for their endless support my journey thus far. You all know this would not have been possible without you.

And finally, I would like to thank the National Sciences and Engineering Research Council of Canada and the institutions of Dalhousie University and Mount Saint Vincent University for funding and facilitating this research.

It is through collaboration, cooperation, and positivity that all things are possible. Thank you, everyone.

1.0 INTRODUCTION

The vertebrate skeleton has evolved over millions of years to perform several important roles. It provides rigidity to the body, bears its weight, provides locations for muscle attachment, and protects vital organs. The bones themselves serve as a reservoir for minerals and, in some vertebrates, act as sites of blood cell production. The skull is a unique collection of bones that houses feeding and sensory systems, and protects the brain while accommodating its growth. Its ability to do this relies on cranial sutures, which are fibrous joints that develop between the intramembranous bone plates of the skull (Kim *et al*., 1998). In mammals, sutures typically fuse after the brain stops growing, and both premature and delayed suture fusion can cause potentially serious cranial abnormalities (Greenwald *et al*., 2000). In humans, premature suture fusion is known as craniosynostosis. Further understanding of the patterns in which cranial sutures close could allow insight into what happens when things go wrong.

1.1 THE CRANIAL NEURAL CREST

The neural crest is an assemblage of migratory, multipotent cells that forms from the dorsal region of the neural tube in the early stages of vertebrate neurulation (Gilbert, 2000). It is viewed by some as the fourth germ layer, after the three primary germ layers: ectoderm, mesoderm, and endoderm (Gilbert, 2000; Hall, 2005). As the neural folds form, populations of neural crest cells migrate from the newly forming neural tube throughout the body and act as precursors to several different cell and tissue types (Gilbert, 2000). The large population of neural crest cells is divided into four

subpopulations – the trunk neural crest, the cardiac neural crest, the vagal/sacral neural crest, and the cranial neural crest – each of which follows a unique migratory path and contributes to different tissues in different locations (Gilbert, 2000). The cranial neural crest is the primary source of craniofacial mesenchyme, and contributes to the bones, connective tissues, and nervous tissues of the skull (Sanatagi and Rijli, 2003). Uniquely, cranial neural crest cells can differentiate into bone and cartilage cells, unlike other neural crest cells (Sanatagi and Rijli, 2003). Cells of this population migrate from the fore-, mid- and hindbrain regions to form the majority of the skull bones (Sanatagi and Rijli, 2003).

Differences have been observed in the developmental potential of cranial neural crest cells depending on how early or late they emigrate from the neural tube (Baker *et al.,* 1997). An example of this has been documented in zebrafish (*Danio rerio*). In these fish, the first neural crest cells to migrate mostly give rise to neurons, and the last to migrate mostly give rise to cartilage (Schilling and Kimmel, 1994). Similar differences between early- and late-migrating neural crest cells have been observed in chicken (*Gallus gallus*) (Kitamura *et al.,* 1992).

1.2 VERTEBRATE CALVARIAE

In many vertebrates, calvariae (bones of the skull roof) form via intramembranous ossification, a process by which neural crest-derived ectomesenchymal cells aggregate to form condensations before differentiating into osteoblasts (bone-forming cells) that deposit bone matrix (Franz-Odendaal, 2011). In others, such as the chicken, some of the skull roof bones are derived from mesoderm and formed by endochondral ossification, a process whereby bone is formed via a cartilage precursor (Gross and Hanken, 2008). The

forebrain, midbrain, and hindbrain together induce osteogenesis of the squamosal, occipital, frontal, and parietal bones (Le Lievre, 1978). After initial bone matrix deposition, the bones continue to expand in size as growth proceeds (Franz-Odendaal, 2011). The frontal and parietal bones are relatively equal in size in mammals, unlike chickens and zebrafish, in which the frontal bones are larger than the parietal bones (Morriss-Kay, 2001; Quarto and Longaker, 2005).

The vertebrate skull is divided into two parts: the neurocranium and the viscerocranium. The neurocranium consists of the skull vault and base, protecting the brain and accommodating its growth and development over the course of early life (Liu *et al*., 1999). The viscerocranium refers to the part of the skull commonly known as the face, including the jaw and other branchial arch derivatives (Jiang *et al*., 2002). I will be further discussing the neurocranium, only, as it relates to my thesis.

The embryonic origins of the bones of chicken neurocranium are a subject of debate (Gross and Hanken, 2008). Some researchers have proposed that only the anterior portions of the frontal bones are derived from neural crest, and that the rest of the calvariae are of paraxial mesodermal origin (Noden, 1984). Other groups have suggested that the parietal bones are also of neural crest origin (Couly *et al*., 1993; Le Douarin and Kalcheim, 1999), thus leaving the parietal bones, the posterior portion of the frontal bones, and the sutures between these bones as regions of contention with respect to their origins (Gross and Hanken, 2008).

In zebrafish, the viscerocranium and the anterior halves of the frontal bones are of neural crest origin (Kague *et al*., 2012). The parietal bones and the posterior halves of the frontal bones are of paraxial mesodermal origin (Kague *et al*., 2012). The boundary

between regions of neural crest and mesodermal origin is at the cartilaginous epiphyseal bar (Kague *et al*., 2012). The embryonic origin of cells within individual zebrafish cranial sutures is not currently known.

Jiang *et al*. (2002) demonstrated that the mouse neurocranium is formed by embryonic tissue of both neural crest and mesodermal origin. The frontal bone is derived of neural crest and the parietal bone is derived of mesoderm (Jiang *et al.,* 2002). The caudal border of the frontal bone at the coronal suture is formed by the frontonasal neural crest as neural crest cell migration is completed (Jiang *et al.,* 2002). The neural crest tissue of the sagittal suture is present between the mesodermally derived parietal bones due to an indentation in the frontal neural crest domain caused by mesoderm of the parietal bones (Jiang *et al*., 2002). Both sutures are examples of juxtaposition between neural crest and mesoderm, as the coronal suture lies between bones of different origins, and the sagittal suture consists of neural crest tissue and is situated between bones of mesodermal origin. These sutures also make the most significant contributions to skull growth (Jiang *et al.,* 2002).

1.3 CRANIAL SUTURES

Cranial sutures are the fibrous joints between calvariae (Figure 1), and are formed when the osteogenic fronts of expanding calvarial bones approximate one another (Kim *et al*., 1998). Sutures are vital sites of both pre- and postnatal bone growth (Kim *et al*., 1998). In humans, the metopic suture is situated between the frontal bones, the sagittal between the parietal, the coronal between the frontal and parietal, and the lambdoid between the parietal and occipital (Figure 1). The coronal, sagittal, and lambdoid sutures

are named consistently in humans (Figure 1), chickens (Figure 2), zebrafish (Figure 3), and mice (Figure 4). In chicken and zebrafish, the interfrontal suture is located between the frontal bones and is analogous to the human metopic suture (Figures 2, 3). In mice (Figure 4), this suture is subdivided into the anterior frontal suture and the posterior frontal suture (Sahar *et al*., 2005). The posterior frontal suture is the only case in which the calvarial bones on either side of the suture are entirely derived from the neural crest (Figure 4; Sahar *et al*., 2005). It is also the only suture to close, as the others remain open throughout the life of the mouse (Sahar *et al*., 2005), unlike human sutures, which all close (Liu *et al*., 1999). The lambdoid and coronal sutures, which are transversely situated, overlap when fully formed (Opperman, 2000). The sagittal and interfrontal/metopic sutures do not overlap, and are therefore called “butt” sutures (Opperman, 2000).

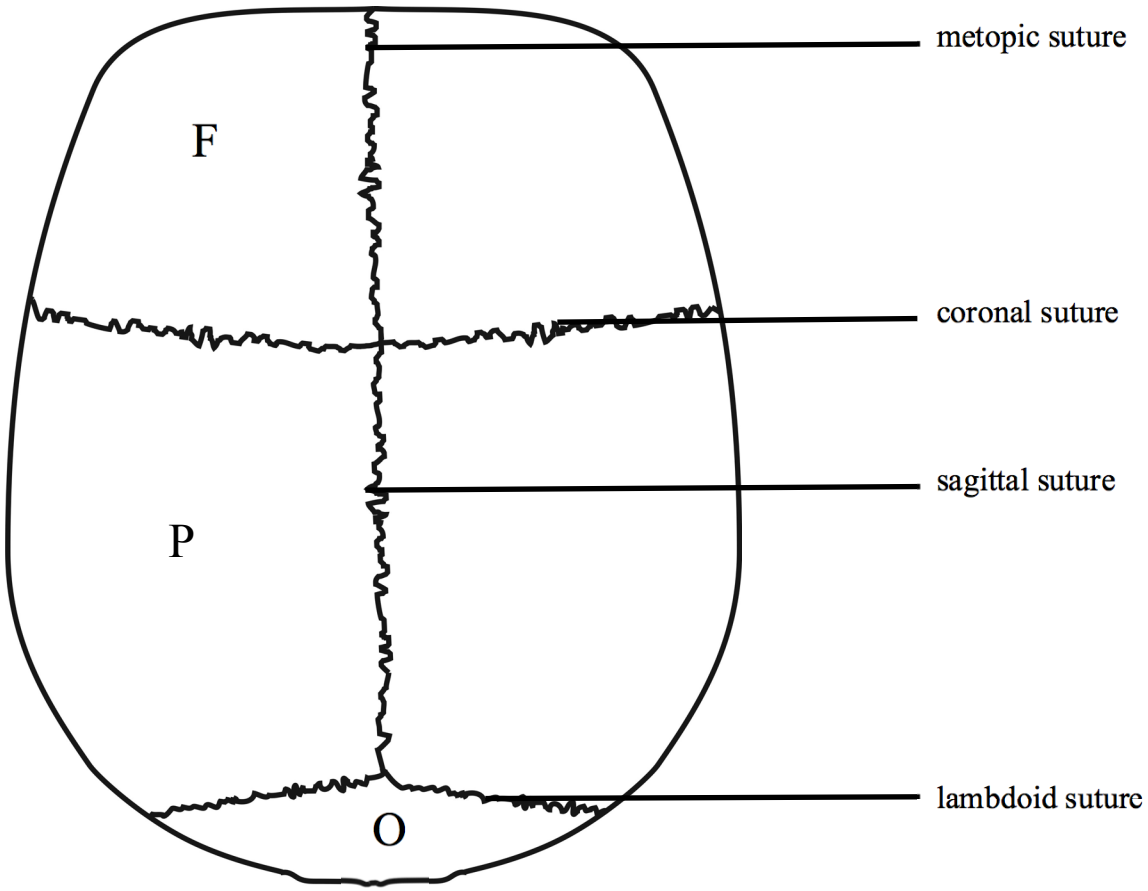

Figure 1. Rostral view of the cranial sutures of the human skull. The metopic suture is situated between the frontal bones, the sagittal between the parietal, the coronal between the frontal and parietal, and the lambdoid between the parietal and the occipital. F, frontal; P, parietal; O, occipital. Modified from Aleck (2004).

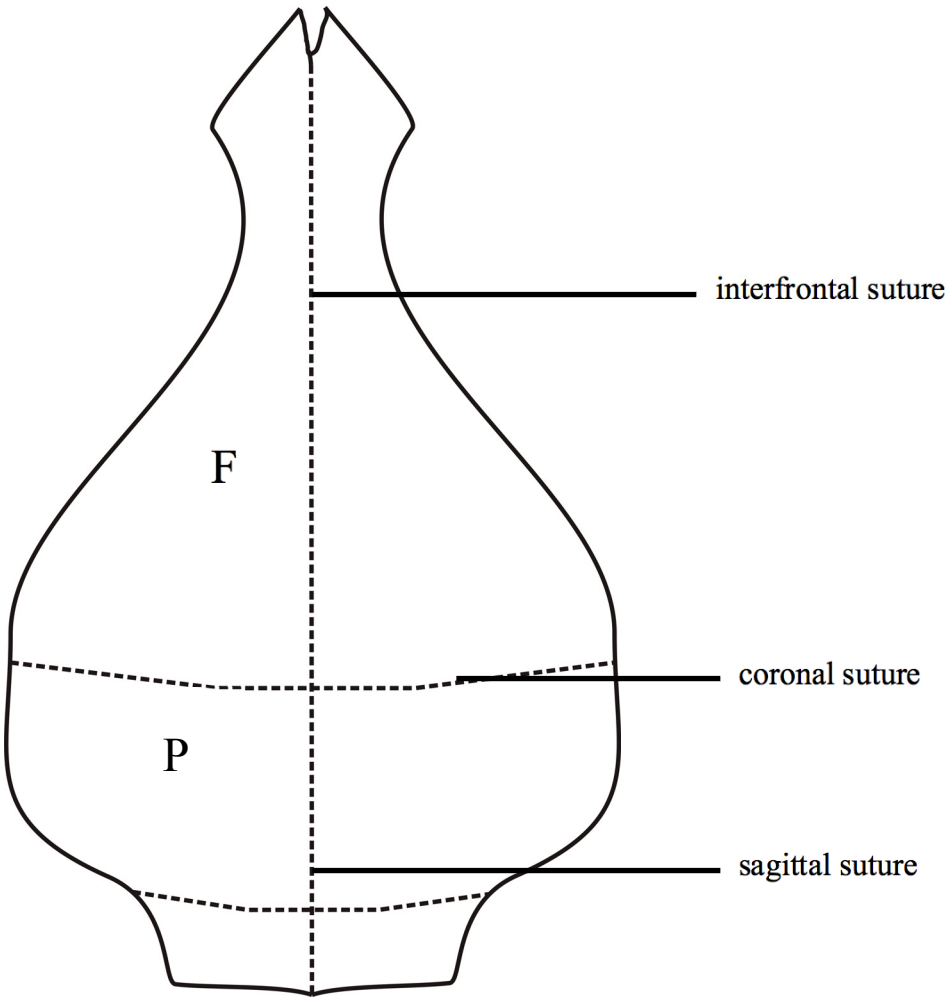

Figure 2. Dorsal view of the cranial sutures of the chicken skull, as inferred from observation of embryos. The interfrontal suture is situated between the frontal bones. The sagittal suture is situated between the parietal bones, and the coronal suture is between the frontal and parietal. F, frontal; P, parietal.

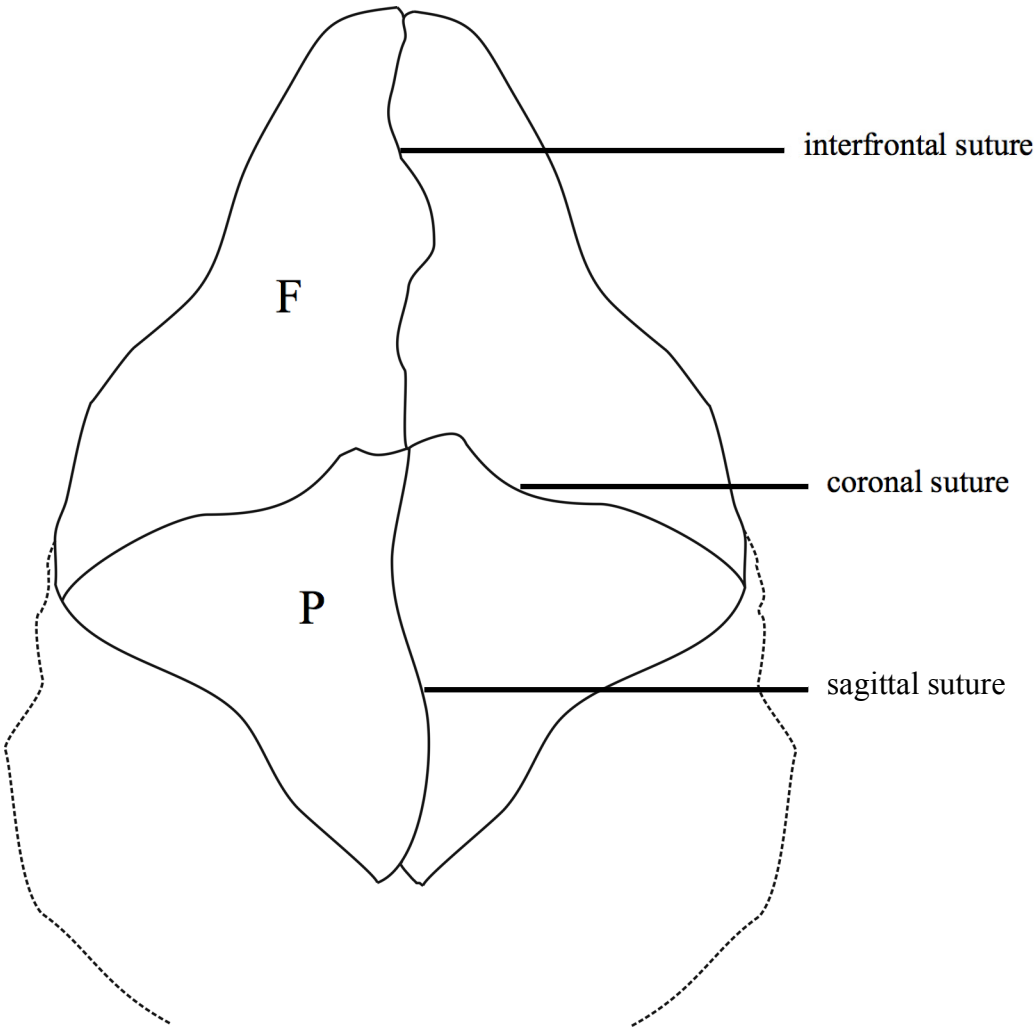

Figure 3. Dorsal view of the cranial sutures of the zebrafish skull. The interfrontal suture is situated between the frontal bones. The sagittal suture is situated between the parietal bones, and the coronal suture is between the frontal and parietal. F, frontal; P, parietal. Modified from Quarto and Longaker (2005).

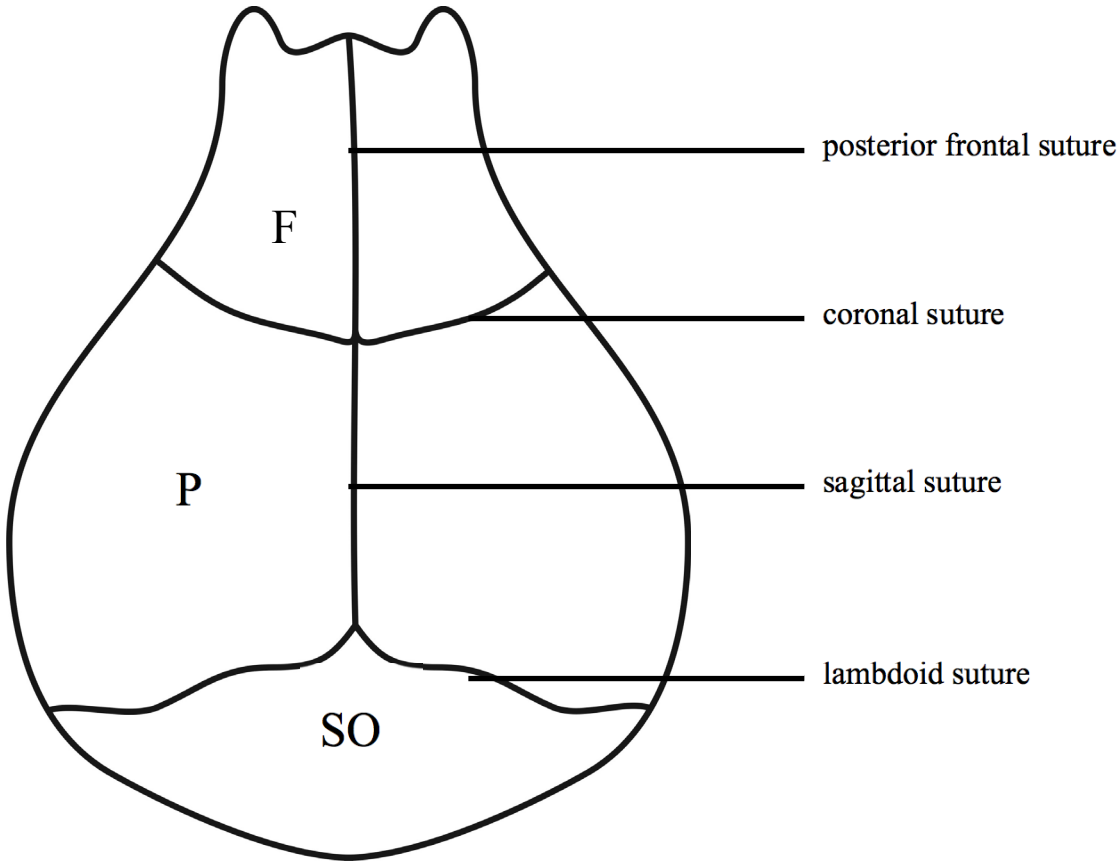

Figure 4. Dorsal view of the cranial sutures of the mouse skull. The posterior frontal (PF) suture is analogous to the human metopic suture and is situated between the frontal bones. The lambdoid suture is situated between the parietal and supraoccipital bones. The sagittal suture is situated between the parietal bones, and the coronal between the frontal and parietal. F, frontal; P, parietal; SO, supraoccipital. Modified from Sahar *et al*. (2005).

As the brain expands, sutures endure tension and are stimulated to deposit bone, resulting in osteogenesis at the edges of the calvariae (Kim *et al*., 1998). Reaction to the expanding brain is largely mediated by the underlying dura mater, which responds to tensional forces and governs suture development through fibroblast growth factor (FGF) signaling and migration of pluripotent cells into suture mesenchyme (Ogle *et al*., 2004). When brain expansion is complete, the sutures eventually close in some species, or remain open (i.e., patent) in others (Greenwald *et al*., 2000). Cranial sutures of avian

species have been observed to lose patency (i.e., close) earlier than those in mammals (Morriss-Kay, 2001). In zebrafish, all sutures remain open through adulthood (Figure 3); Quarto and Longaker, 2005).

The skull roof bones of zebrafish are of intramembranous origin, similar to mammals (Figure 3; Quarto and Longaker, 2005). Zebrafish frontal bones are larger in size than their parietal bones (Quarto and Longaker, 2005). The sutures themselves bear morphological similarity to those of mice; newly formed sutures are visible as thin plates of bone and connective tissue between the calvaria and older sutures include thickened osteogenic fronts as the bones mature (Quarto and Longaker, 2005). Zebrafish sutures do not fuse, remaining patent (i.e., open) for their entire lives (Quarto and Longaker, 2005). The extent to which zebrafish and mammals are molecularly similar in their suture development is not fully understood (Albertson and Yellock, 2007). Zebrafish are thus similar to mammals in their craniofacial structure and development, making them an effective model organism for studying these features (Quarto and Longaker, 2005).

1.4 EPHRINS AND EPH RECEPTORS

1.4.1 OVERVIEW OF EPHRINS AND EPH RECEPTORS

Ephrin ligands are expressed in developing neural tissues of frogs (Smith *et al.,* 1997), chickens (Menzel *et al.*, 2001), and zebrafish (Coulthard *et al.,* 2002). The ephrin family of proteins and receptors are involved in suture formation and bone homeostasis, angiogenesis, and several other vital biological functions (Edwards and Mundy, 2008). Very recently, ephrin-B ligands were shown to be present in embryonic and neonatal mouse sutures and sites of adult bone injury (Benson *et al*., 2012). Detailed

understanding of ephrin activity in the skull of other vertebrates will help to develop the big picture of the role of potential ephrin activity in suture development across vertebrates.

Eph receptors are the largest family of receptor tyrosine kinases (RTKs), and ephrins are the corresponding ligands that allow signaling to take place (Benson *et al*., 2012). In the human genome, eight ephrin ligands and 14 Eph receptors have been identified (Edwards and Mundy, 2008). Ephrin homologues are easily identified between different species due to their high degree of sequence conservation in key functional domains over their evolutionary history (Coulthard *et al*., 2002). They are known to play a significant role in the regulation of cell migration during embryogenesis of amphibians (Smith *et al.,* 1997), bone homeostasis in mammals (Diercke *et al.,* 2011), and healing of damaged bone tissue in mammals (Benson *et al.,* 2012). Most of this signaling occurs via phosphorylation of tyrosine residues in the Eph receptor (Coulthard *et al.,* 2002). Similar roles are played by ephrins in zebrafish and chickens (Coulthard *et al.,* 2002).

It is possible for ephrin ligands to interact with other classes of RTK. Ephrin-B ligands have been shown to be phosphorylated by platelet-derived growth factor receptors (PGDFs) and fibroblast growth factor receptors (FGFRs) (Wilkinson, 2001). Phosphorylation of ephrin-B1 by activated FGFs has been shown to decrease its ability to reduce cell adhesion (Chong *et al*., 2000). Ephrins have also been shown to mediate inhibition of FGFs in development of the motor ganglion in the *Ciona intestinalis* embryo (Stolfi *et al*., 2011).

Ephrins and Eph receptors are divided into two groups based on the nature of the attachment of the ephrin ligand to the cell membrane (Figure 5). Ephrin-A ligands are

anchored to the membrane via glycosylphosphatidylinositol (GPI) linkage and ephrin-B ligands are transmembrane proteins (Diercke *et al*., 2011).

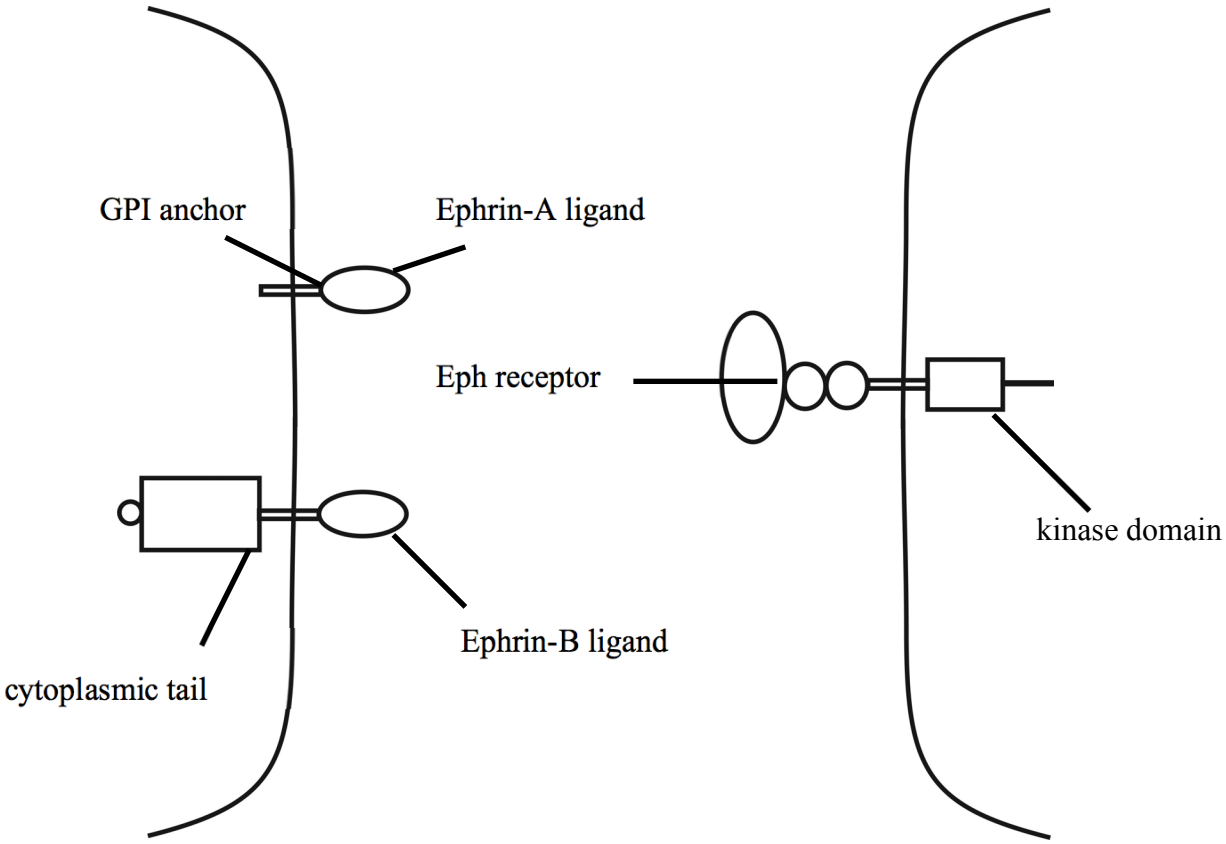

Figure 5. Ephrin-A ligand, ephrin-B ligand, and Eph receptor anchored in plasma membranes. Ephrin-A ligands are anchored via glycosylphosphatidylinositol (GPI) linkage, and ephrin-B ligands are transmembrane proteins. Eph receptors are based around the kinase domain. Modified from Edwards and Mundy (2008).

Transmembrane proteins such as Ephrin-B ligands and transmembrane receptors such as Eph receptors are individually subdivided into different domains. The extracellular domain refers to the portion of the protein outside of the cell membrane, which functions to recognize a certain molecule (in this case, the corresponding

ephrin/Eph receptor). The intracellular domain refers to the portion within the cell, on the opposite side of the cell membrane, and its function, upon activation, is to relay a specific signal in coordination with proteins within the cell. By their very nature, Eph/ephrin activity requires direct cell-to-cell contact (Diercke *et al.,* 2011).

1.4.2 INVESTIGATION OF THE EPHRIN-B CLASS IN MICE

Ephrin-B ligands appear to be particularly significant in bone health and development. Benson *et al*. (2012) observed mice to find that ephrin-B2 was expressed at its highest levels in sutures during and shortly following embryogenesis, when bone develops most quickly. Ephrin-B2 was also expressed within sutures and at sites of injury later in life (Benson *et al.,* 2012). Osteoblasts are known to develop at suture sites, generated from undifferentiated mesenchymal cells (Benson *et al*., 2012). Stem cells present in the sutures of uninjured skulls migrate to injury sites when necessary in order to differentiate into osteoblasts and synthesize the bone matrix needed to control damage and maintain skull integrity (Benson *et al*., 2012). Benson *et al*. (2012) found Ephrin-B2 to be present in these locations and hypothesized that it stimulates this response. These investigators also dissected and cultured embryonic calvariae in a method determined to allow for continued growth (Benson *et al*., 2012). They showed that bone content was doubled in these cultured embryonic calvariae when they were exposed to ephrin-B2/Fc while maintaining normal suture and skull morphology (Benson *et al*., 2012). Benson *et al*. (2012) concluded that their data supported a role for ephrin-B2 in bone health and development.

Interestingly, EphB4, the typical receptor for the ephrin-B2 ligand, was not found to be present in adult or embryonic murine skulls, but EphB1 and EphB2 were both found in these skulls (Benson *et al*., 2012). EphB1 expression increases in adult mice as ephrin-B2 levels significantly decrease (Benson *et al*., 2012). Suppressing EphB1 expression resulted in calvarial bone content reduction in adult but not neonatal stages (Benson *et al.,* 2012). This finding implies that receptors differ in their expression patterns and change roles over the course of the development and growth of the animal (Benson *et al*., 2012). It appears that EphB1 and EphB2 are potential receptors for the ephrin-B2 ligand in bone (Benson *et al*., 2012), implying that ephrin-B ligands are capable of binding "promiscuously" to various EphB receptors, and are not limited to an exclusive ligand-receptor relationship (Chan *et al*., 2001).

Ephrin-Eph bidirectional signaling plays a role in the complex relationship between osteoblast and osteoclast formation in mice (Zhao et al., 2006). This group used gain- and loss-of-function experiments to demonstrate that ephrin-Eph bidirectional signaling patterns stimulate bone formation and suppress osteoclast formation in mice. Those mice with increased EphB4 expression displayed higher femoral bone density, lower than average osteoclast counts and typical osteoblast counts (Zhao *et al*., 2006). For bone homeostasis to be maintained, osteoclast and osteoblast populations are often complimentary, but these findings indicate that the EphB4 increase shifted the balance in favour of osteoblast function (Zhao *et al.,* 2006).

A version of ephrin-B1 has been observed in developing chicken retinas, and antibodies specific for this ephrin do not react with the corresponding mouse ephrins (Kalo *et al*., 2001), suggesting a fundamental difference between ephrins in the two

species. Analogous ephrin activity has been observed in retinal development in mice (Coulthard *et al*., 2002).

1.4.3 INVESTIGATION OF THE EPHRIN-B CLASS IN ZEBRAFISH

Ephrin-B ligands in zebrafish have been determined to parallel the mammalian ephrin-B class, and, similarly, are capable of promiscuously binding to multiple EphB receptors (Chan *et al*., 2001). The homology between mammalian and zebrafish ephrin-B classes is approximately 58%, and four cysteines in particular have been completely conserved in the extracellular domain (Chan *et al*., 2001). Eph-ephrin interaction occurs during zebrafish embryogenesis (Aizawa, 2007; Kawahara, 2008; Pi-Roig *et al*., 2014), but little is known about post-natal ephrin expression in zebrafish.

Due to a teleost genome duplication event, zebrafish have two types of ephrin-B2, known as ephrin-B2a and ephrin-B2b (Chan *et al.,* 2001). Ephrin-B2a has been shown in the developing eye, dorsal artery, and central nervous system in zebrafish embryos (Chan *et al*, 2011). Ephrin-B2b has been shown to interact with EphB2 before gastrulation begins (i.e., in the first five hours post fertilization), aiding in cell-cell recognition (Chan *et al*., 2001). Ephrin-B2a is more closely related to mammalian ephrin-B2 with 65% amino acid identity as opposed to ephrin-B2b, which has 55% identity (Chan *et al*., 2001). The latest stage at which ephrin-B2a has been observed in zebrafish is 60 hpf (Aizawa, 2007; Kawahara, 2008; Pi-Roig *et al*., 2014), and ephrin-B2b has not been observed later than 36 hpf (Chan *et al*., 2001). Further investigation is required into the expression of ephrins in zebrafish bone development, especially post-embryogenesis.

1.5 NEUROCRISTOPATHIES OF THE SKULL

Disruption of the fates of neural crest cells can occur in isolation or as parts of larger syndromes (Parisi, 2002). Pathologies arising from this disruption are collectively referred to as neurocristopathies. This is a broad and diverse class of conditions, many of which are not yet fully understood.

Calvarial foramina are unossified areas in the skull vault caused by defects in differentiation and proliferation of cranial neural crest cells (Ishii *et al.,* 2003). Various genes may be linked to this neurocristopathy, including various FGFRs, HLG gene, *Twist*, and homeobox genes *Msx2* and *Alx4* (Ishii *et al.,* 2003). Ishii *et al*. (2003) traced the origin of the foramen defect to genes that regulate the differentiation and proliferation of skeletogenic mesenchyme.

Another well-known neurocristopathy is craniofrontonasal syndrome, which is an X-linked disorder caused by a mutation in the gene for ephrin-B1. This neurocristopathy is unusual in that it affects females far more severely than males (Wieland *et al*., 2004). It is characterized by orbital hypertelorism, bifid nasal tip, dry curly hair, splitting of the nails, thoracic abnormalities, facial asymmetries, and craniosynostosis (fusion) of the coronal suture (Wieland *et al*., 2004).

Craniosynostosis refers to early fusion of calvarial bones, and, in humans, most commonly involves the fusion of a single suture, although fusion of multiple sutures is also possible (Stamper *et al*., 2011). This can manifest as a result of developmental and/or metabolic abnormalities, or problems such as stunted brain growth or application of external pressure (Aleck, 2004). Cases of syndromic craniosynostosis, which include such disorders as Crouzon syndrome, Apert syndrome, and Muenke syndrome, typically

involve not only sutures but also the central nervous system and extracranial skeletal deformities (Aleck, 2004).

Stamper *et al.* (2011) utilized microarray analysis of extracted RNA to compare gene expression of humans with multiple forms of craniosynostosis with one another and with a control population. They found significant changes in expression of FGF7, SFRP4, and VCAM1 genes in individuals with single-suture craniosynostosis (Stamper *et al*., 2011). This finding coincides with the accepted notion that human syndromic craniosynostosis is most often, but not always (Aleck, 2004), the result of FGFR mutations (Robin *et al*., 1998). These receptors play a vital role in the migration, proliferation, and survival of neural crest cells, regulating early pharyngeal skeletal development (Creuzet *et al*., 2004). Although genetic factors have been identified in the pathology of craniosynostosis and other neurocristopathies, the underlying causes are complex and require further study.

1.6 MODELS

Many different animal models have been utilized in attempt to gain understanding of suture development and craniosynostosis. Mammalian models have included mice, rats, and rabbits. The mouse is an attractive mammalian model due to the similarities in calvarial arrangement (Opperman, 2000) and genetic pathways (Wilkie and Morriss-Kay, 2001) shared by mice and humans. The murine interfrontal suture, which is analogous to the human metopic suture, closes at roughly 7-12 days old, and the other sutures remain patent through the entire life of the mouse (Sahar *et al*., 2005). The mouse therefore provides opportunity for study of both fused and patent sutures (Grova *et al*., 2012). Rice

et al. (2003) investigated murine calvariae and cranial sutures to conclude that craniosynostosis may result from disruption of certain signaling pathways during osteoblast differentiation. Various transgenic mice have been developed based on genes associated with certain manifestations of craniosynostosis, and have provided valuable insight into factors at work in these disorders (Grova *et al*., 2012). The rat is also a useful model, as it bears many of the advantages of the mouse model while being a larger animal (Grova *et al.,* 2012). Studies that have separated rat cranial sutures from the underlying dura mater have shown delays or differences in suture fusion (Levine *et al*., 1998; Roth *et al*., 1996), suggesting that the dura mater plays a role in governing suture fate (Grova *et al.,* 2012). Manipulation of the dura mater (Mooney *et al.,* 2001) and application of anti-TGF-β2 antibodies (Mooney *et al*., 2007) in a certain strain of New Zealand white rabbits have shown potential for reducing suture fusion and may therefore provide a basis for human therapies (Grova *et al.,* 2012). Although these mammalian models have helped us to understand cranial suture development, non-mammalian models would also have their advantages.

1.6.1 CHICKEN

The chick embryo, *Gallus gallus*, has been used as a model in developmental biology for thousands of years, since ancient Egyptians first cracked eggs open to observe the growing organisms therein (Stern, 2005). As chickens have remained everyday elements of human society, so have their eggs remained common models in many facets of biology.

Due to the long history of the chick embryo as a model organism, their development is well documented and protocols for staining, immunological analysis, and embryological manipulation are all well established. As they grow in eggs, incubation allows researchers to mimic their natural conditions so that they can develop in a controlled environment and be analyzed or manipulated at desired stages. Their generally low cost and wide availability makes them particularly accessible to many researchers.

The chick embryo has been instrumental in the study and understanding of human development. For my thesis I elected to use this model to further understanding of cranial suture formation. By understanding suture development in one of the gold standards of developmental biology models, I can better understand of the universality of the patterns that I see.

1.6.2 ZEBRAFISH

The zebrafish, *Danio rerio*, is a more recently established model organism in developmental biology and medical research. The zebrafish genome has been well analyzed and compared to other vertebrates (Bier and McGinnis, 2004). Zebrafish development is well understood and easily observable, as embryos develop quickly and externally. Zebrafish are relatively easy to care for, breed, and raise, as they have relatively short life cycles and yield large clutches of young. Protocols for staining and immunological analysis have been well established, and many mutant strains are available.

Laue *et al*. (2011) analyzed zebrafish with genetically altered retinoic acid to conclude that craniosynostosis is a consequence of abnormal osteoblast differentiation.

Zebrafish have also been used to explore the roles of FGF8 (Albertson and Yelick, 2007), Glypican 4 (LeClair *et al*., 2009), and many other genes implicated in craniofacial abnormalities. Noting the similarities of the zebrafish cranial anatomy and that of mammalian organisms (Quaro and Longaker, 2005) and the versatility of the zebrafish in developmental biology, the zebrafish is an ideal organism in which to explore cranial suture formation.

By understanding suture development in this model organism, I can gain a greater appreciation of how this organism can be utilized to understand craniosynostosis and other disorders affecting the skull roof.

1.7 OBJECTIVES

In order to gain insight into such disorders as craniosynostosis, it is imperative that we further understand cranial suture development. My goal was to investigate suture formation in zebrafish and chicken, two established models for study of craniofacial development. To do this, I had three objectives:

1. The first was to qualitatively analyze suture formation patterns in both species, and compare them to one another. This was done by visualizing cranial ossification via bone staining, and observing the sutures at various developmental points in a growth series.
2. The second objective was to statistically analyze the changes in shape of the cranial sutures by means of morphometric analysis, quantifying the variation between sutures at various time points in both species.

3. The third objective was to determine ephrin distribution in the osteogenic fronts of developing zebrafish calvariae. This was attempted using Western analysis, immunohistochemistry, and *in situ* hybridization.

My approach to the second objective will involve outline morphometrics. This is more appropriate than landmark morphometrics due to the lack of consistently identifiable homologous landmarks around the closing sutural space.

By further understanding the patterns and factors at work in the chosen model organisms, we can gain insight into their universality and come closer to understanding and treating such disorders as craniosynostosis in our fellow humans.

I hypothesize that both zebrafish and chicken will be similar to humans in the manner and order of their suture development, and that organisms at different developmental stages will be significantly different from one another with regard to their suture formation. I also hypothesize that ephrin-B2a will be present in the sutures of the zebrafish skull roof as has been observed in mice (Benson *et al*., 2012). Several researchers have argued that the zebrafish is a good model for craniosynostosis (Gart *et al*., 2014; Quarto and Longaker, 2005) and I hope that my research will contribute to this debate by demonstrating whether zebrafish suture formation is similar to that of other vertebrates.

2.0 METHODS

2.1 CHICKEN: STAGING AND SAMPLE COLLECTION

Fertilized chicken (*Gallus gallus*) eggs were obtained from Cox Brothers Farm (Maitland, Nova Scotia) and ACA Poultry (Upper Sackville, Nova Scotia) and refrigerated at 4°C for no more than one week before being incubated with humidity control at 37°C. Staging was done according to Hamburger and Hamilton's (1951) guidelines. One day before a set of eggs was expected to reach the desired stage, a single egg was opened and the embryo was staged. It was generally assumed that all eggs incubated at the same time were at the same developmental stage, so if the test embryo appeared to be younger or older than expected, plans for sample collection were adjusted accordingly.

Chick embryos were sacrificed by cracking the egg into a large petri dish and swiftly severing the neck of the embryo using small, sharp scissors. The head was moved into a separate petri dish partially filled with chick saline solution (0.85% NaCl) and assessed for features indicative of developmental stage according to Hamburger and Hamilton (1951). For embryos at stage 40 (approximately 14 dpf) and older, the relevant criteria primarily consisted of beak and toe length.

For optimization of the staining protocol, chick embryo heads were fixed in 10% neutral buffered formalin (NBF) overnight at room temperature before being either transferred through a graded ethanol series for storage in 70% ethanol or stained immediately. Those embryos used for subsequent staining after optimization were fixed in 4% paraformaldehyde (PFA) at 4°C overnight and stored in phosphate buffered saline (PBS) at 4°C. For further details on fixation solutions, see Appendix B.

2.2 CHICKEN: GROWTH SERIES AND STAINING

Eleven chick embryos at stages 38-44 were fixed for optimization of the whole-mount double staining protocol. Samples were prepared for staining by removal of the eyes and brain. It was easiest to remove the brain through an incision in the caudal region of the skull, as not to disrupt the bones of the skull roof. Samples were rinsed and cartilage was stained using a solution of 1% Alcian blue in 20% acetic acid/80% ethanol. Following the cartilage stain, samples were rehydrated through an ethanol series and bleached with 1% KOH and 3% H_2O_2. They were then rinsed and placed in 30% saturated sodium tetraborate overnight before being stained for bone using a saturated Alizarin Red in 1% KOH solution. After staining and rinsing, 1% trypsin/2% borax was used to digest soft tissue and a glycerol series was used to clear the remaining tissue before the specimens were stored in 70% glycerol in 70% ethanol. Further details can be found in Appendix C. I later decided to switch to a whole-mount bone-only stain (Franz-Odendaal *et al*., 2007), which made it easier to observe and photograph the ossification of the calvarial bones. Based on this procedure, I decided to create a bone-stained growth series to better understand calvarial development in the final stages before hatching.

One chick embryo at each of Hamburger and Hamilton (HH) stages 40, 41, 42,43, 44, and 45 (n=6) was bone-stained (Franz-Odendaal *et al*., 2007) to create a growth series. Samples were prepared for staining by removal of the eyes and brain the same way they were prepared for the whole-mount double stain described above. Bone staining followed the same protocol used for zebrafish. Further details can be found in Appendix C. By observing this growth series, the following stages were selected for further

analysis: HH 40, HH 42, and HH 45. These stages show the progression of the calvarial bones from early stages of ossification (HH 40) through to the point of hatching (HH 45), with the gradual progression of ossification in between (HH 42).

After the stages of interest were selected, the whole mount bone staining protocol (Franz-Odendaal *et al*., 2007) was performed on heads of embryos at HH 40 (n=8), HH 42 (n=8), and HH 45 (n=8) in order to visualize ossification of the calvariae and so that a morphometric analysis could be conducted.

2.3 CHICKEN: OBSERVATION AND PHOTOGRAPHY

All stained chick samples were stored and observed in 70% glycerol in 70% ethanol. Samples were large enough to be viewed without the use of a microscope. For photographing, the samples were placed in a 5 cm plastic petri dish with their storage solution, oriented so that the beak faced upwards when photographed from the dorsal surface. Using a Canon Rebel T4i camera on its manual flash setting, the images were photographed from directly above. Self-consistency was achieved by lining up the edges of the petri dish with the lines inside the viewfinder of the camera in the same fashion for every sample.

2.4 ZEBRAFISH: STAGING AND SAMPLE COLLECTION

Wild-type zebrafish (*Danio rerio*) were bred in the Franz-Odendaal Aquatic Facility at Mount Saint Vincent University from AB stock populations obtained originally from the Zebrafish International Research Centre (ZIRC) (University of Oregon, Eugene, Oregon, USA). These zebrafish were maintained according to animal

care protocols approved by the Canadian Council for Animal Care and the MSVU-SMU Animal Care Committee and were euthanized upon reaching designated developmental stages.

After approximately 40 days post fertilization (dpf), zebrafish were anesthetized approximately once a week for measuring. Anesthesia was accomplished by immersion in 0.01% Ethyl 3-aminobenzoate, methane sulfonic salt, 98% (MS-222) buffered to a pH of 7.0 in zebrafish system water. While under anesthesia, the standard length (SL) of the zebrafish was measured using a ruler. SL is defined as the distance from the snout to the caudal peduncle (Parichy *et al*., 2009). Those within approximately 0.5 mm of a whole number were classified as that whole number. Upon reaching the desired SL, zebrafish were euthanized by immersion in 0.1% MS-222 in zebrafish system water. Euthanized samples were fixed in 4% PFA overnight at 4°C and moved into 1x PBS the following day for storage at 4°C. For a complete list of all collected zebrafish samples, see Appendix A. For further details on fixation solutions, see Appendix B.

2.5 ZEBRAFISH: GROWTH SERIES AND STAINING

Fourteen zebrafish at 7-14 mm SL were fixed to optimize the staining protocols and determine the approximate stages at which sutures develop. An initial growth series was generated by visualizing bone and cartilage in one zebrafish at each of 8 mm, 9 mm, 10 mm, 11 mm, 12 mm, 13mm, and 14 mm SL (n=7). These zebrafish were initially stained using the established whole-mount acid-free double stain (Walker and Kimmel, 2007 modified according to Franz-Odendaal *et al.*, 2007). This acid-free stain avoids potential bone demineralization resulting from the acetic acid used in cartilage staining

(Walker and Kimmel, 2007). Fixed samples were rinsed in 50% ethanol before immersion in a staining solution overnight that contained 0.5% Alizarin Red and 0.02% Alcian Blue, to stain bone and cartilage, respectively. Samples were rinsed and bleached with 1.5% H_2O_2/1% KOH before being transferred through a glycerol series in 1% KOH and stored in 100% glycerol. Further details can be found in Appendix C. After observing these stained samples, three sizes were selected as stages for analysis, namely 8 mm, 10 mm, and 12 mm. By observing these stages, I could visualize calvarial development from the beginning of ossification (8 mm) through an intermediate phase in which various sutures were at different developmental points (10 mm) to a point when all suture development was nearly complete (12 mm).

After the stages of interest were selected, whole mount bone-only staining (Franz-Odendaal *et al*., 2007) was conducted on fish at 8 mm SL (n=8), 10 mm SL (n=8), and 12 mm SL (n=8) in order to visualize ossification of the calvariae and for morphometric analysis of skull development. The single bone stain was used from this point onward because it was a more straightforward protocol and resulted in clearer pictures. Samples were bleached with 1% KOH and 3% H_2O_2. They were then rinsed and placed in 30% saturated sodium tetraborate overnight before being stained using a saturated Alizarin Red in 1% KOH solution. After staining and rinsing, 1% trypsin/2% borax was used to digest soft tissue and a glycerol series was used to clear the remaining tissue before the specimens were stored in 70% glycerol in 70% ethanol. Further details are provided in Appendix C.

2.6 ZEBRAFISH: OBSERVATION AND PHOTOGRAPHY

All stained zebrafish samples were stored and observed in 100% glycerol. Under a Nikon SMZ1000 microscope, samples were oriented using fine forceps so that the skull roof could be viewed and photographed dorsally and ossification could be observed. In most cases, the mandibles were removed so that staining of the skull roof could be seen more clearly. In some 8 mm SL samples, the skull roof bones were separated from the rest of the skull in order to clearly observe ossification. The bones were not flattened (which may have reduced quality) in order to maintain their natural orientation and alignment. The skull roof was aligned so that its anterior portion was facing up for all photographs. All photographs were taken using a Nikon DXM 1200 camera and NIS Elements Software.

2.7 MORPHOMETRICS: ANALYSIS OF STAINED SKULLS

Morphometrics allow for statistical analysis and quantification of changes in shape amongst samples. Zebrafish and chicken samples were processed separately but using similar procedures. Photographs of skull roofs for all samples (n=8 per stage) were imported into CorelDraw. In CorelDraw, the developing sutures (the negative space between the stained calvarial bones) were outlined using the drawing tool. This often required varying the magnification, tracing in short segments, and carefully adjusting the lines to precisely follow the edges of the calvariae. The original photograph was then deleted, leaving behind the trace of the sutures between the calvariae. The outline was coloured red, and the shape created by the outline was filled in using the same red colour. These images were saved as “CorelDraw X3 Graphic” files before being imported into

CorelPaint, where they were converted to bitmap files, which were necessary for compatibility with the morphometrics program. For each organism, all bitmap images were loaded into the SHAPE version 1.3 morphometrics program (Iwata and Ukai, 2002). The program consists of four subprograms: Chain Coder, CHC2NEF, PrinComp and PrinPrint.

The first subprogram, Chain Coder, analyzed the contours of the imported bitmap shapes to produce chain codes. These chain codes were then normalized for size and orientation by an Elliptic Fourier test in the second program, CHC2NEF, producing a NEF file. By normalizing the shapes in this way, the shapes are more comparable to one another and not skewed by differences in overall size. The Elliptic Fourier test produced a covariance matrix and eigenvalues. The third subprogram, PrinComp, used these eigenvalues to perform a principle component analysis (PCA), resulting in a set of principle components (PCs) that represented specific changes in shape that accounted for the largest degrees of variation amongst the original samples. The proportion of variation corresponding to each PC was provided. PCs were considered significant, or "effective," if they accounted for more than 1/77 of the total variation, 77 being the number of coefficients analyzed by the program. The two most significant PCs for each of zebrafish and chicken were graphed using Microsoft Excel. For a schematic of the scatterplots and labeling of quadrants, see Figure D1 in Appendix D.

PrinPrint visualized the PCs by generating contour diagrams showing the average shape of each principle component as well as images representing shapes two standard deviations removed from the mean in both the positive and negative direction. These images representing shapes two standard deviations removed from the average were

carefully traced using CorelDraw (this was done for clarity, as they were shown overlapping in the PrinPrint output) and placed on either end of the corresponding axes of the PC graphs made in Excel to represent the extremes of that PC. For more information regarding morphometric analysis, see Appendix D.

To determine if there were significant differences amongst the groups, Minitab 14 was used to conduct at One-Way Analysis of Variance (ANOVA). Tests were conducted for each group for each PC, and those with p-values less than 0.05 were considered to be statistically significant. For those cases in which the ANOVA found the PC to be significant, a Tukey's comparison test was done to compare each group of samples to one another, allowing for analysis and interpretation of the differences between developmental time points. For full Minitab outputs, see Appendix E.

2.8 EPHRIN-B2A ANALYSIS

Western analysis and immunohistochemistry were unsuccessful. They are addressed only briefly here, and are not addressed in the Results section. Further details regarding both methods and results can be found in Appendices G (Western analysis) and H (immunohistochemistry).

2.8.1 EXPLORATION OF EPHRIN-B2A IN ZEBRAFISH: WESTERN ANALYSIS

Western analysis was attempted to determine the presence or absence of ephrin-B2 in the zebrafish skull roof. A total of 129 zebrafish was used, ranging from 6 mm to 12 mm SL. The strategy was to test brain, eye, and skull roof tissue for ephrin-B2 and β-tubulin, a loading control protein. Though little is known of ephrin-B2 distribution post-

embryogenesis, it is present in developing neural and retinal tissue in zebrafish (Chan *et al*., 2001). After several attempts and modifications to the protocol, I was only able to detect β-tubulin in the brain, and was unable to detect ephrin-B2 in any zebrafish tissue. Using a Ponceau rouge stain, I was able to confirm that the fractionated proteins were successfully transferred to the nitrocellulose membrane. It is possible that there were underlying issues with protein concentration, tissue homogenizaiton, or antibodies that were not formally guaranteed for use in zebrafish. Further details of strategies attempted, including antibody information, kit information, and troubleshooting, can be found in Appendix G. After approximately six months of troubleshooting Western analysis, attention was redirected to immunohistochemistry (IHC) as a method of analyzing ephrin-B2 in the zebrafish skull.

2.8.2 EXPLORATION OF EPHRIN-B2A IN ZEBRAFISH: IMMUNOHISTOCHEMISTRY

Both paraffin section and whole-mount IHC were attempted to detect ephrin-B2 distribution or lack thereof in suture tissue of zebrafish at 8 mm and 10 mm SL. Paraffin IHC yielded inconclusive results as no staining could be differentiated from the background or from negative controls, even after modifications to several steps of the protocol. Before every paraffin IHC run, a Hall, Brunt Quadruple (HBQ) (Hall, 1986) stain was performed on various slides from the same series in order to determine which sections showed the sutures and would therefore be best suited for IHC. Further details regarding paraffin IHC, including preparation of slides, HBQ staining, antibody information, and troubleshooting can be found in Appendix H. After approximately three

months of troubleshooting paraffin IHC for sections of the zebrafish skull, attention was redirected to whole-mount IHC. Since I did not have a confident positive control for paraffin IHC, I decided to perform whole-mount IHC on 36 hours post fertilization (hpf) zebrafish embryos. Chan *et al*. (2001) had detected ephrin-B2 in the developing brain at this stage and I was hoping to use these as a positive control in subsequent IHC runs.

Whole-mount IHC was done on 36 hpf zebrafish embryos (n = 45). Negative controls were included in these IHC runs that omitted primary and/or secondary antibodies. After attempts to optimize two whole-mount IHC protocols, these results were also inconclusive. Since neither protocol was successful, I decided that the antibodies may be the problem, as the antibody used was not guaranteed for use in IHC. At this point, attention was redirected to *in situ* hybridization (ISH). More detail regarding the two whole-mount IHC protocols, including antibody information and troubleshooting, can be found in Appendix I.

2.8.3 EXPLORATION OF EPHRIN-B2A IN ZEBRAFISH: *IN SITU* HYBRIDIZATION

In situ hybridization (ISH) was conducted to visualize the distribution of the mRNA *efnB2a* in the zebrafish skull roof. Twenty zebrafish at 8 mm (n = 7), 10 mm (n = 6), and 12 mm (n = 7) SL and approximately 20 embryos at 36 hpf were used for this protocol. Samples were fixed in 4% PFA in 1x Diethylpyrocarbonate (DepC) PBS at 4°C overnight before being dehydrated through a series of solutions of MeoH in 1x DepC treated PBS and stored in 100% MeOH at -20°C for several weeks. Full details of the ISH protocol are found in Appendix J.

The first day of ISH began with rehydration of the samples through a series of MeOH/1x DepC treated PBS solutions and multiple washes in a PBS/Tween (PBST) solution. Samples were then bleached in a solution of 0.5% KOH, 0.09% H_2O_2 in DepC treated water. Following the bleach step, samples were washed in PBS and dehydrated as they had been previously before being stored again at -20°C overnight.

The second day of ISH began with the same rehydration and washing steps as the first day. The samples were then permeabilized with Proteinase K (10 µg/mL DepC treated water), fixed again in 4% PFA in DepC treated PBS, and treated with acetic anhydride before incubation in a pre-hybridization(-) solution at 70°C rotating at 35 rpm. This incubation was followed by overnight incubation in the hybridization(+) solution, to which the *ephrin-B2a* probe was added (note that no probe was added to the negative controls), at 70°C and 35rpm. This probe was prepared by Dr. Jochen Weigele, a post-doctoral fellow in the lab.

The third day consisted of a series of washes in hybridization(-) solution, saline sodium citrate (SSC), and PBST. These were followed by incubation in a blocking buffer of 2% heat-inactivated sheep serum and 2% bovine serum albumin in 1x PBST. An anti-digoxigenin antibody (1:10000) was then added for an overnight incubation at 4°C with agitation.

The fourth day began with washes in PBST before incubation in a TRIS staining buffer. This was followed by overnight incubation in a nitro blue tetrazolium/5-bromo-4-chloro-3-indolyl phosphate (NBT/BCIP) colour detection solution at 4°C in the dark. Samples were monitored the following day and the colour detection was stopped by

rinses in PBST. The samples were fixed in 4% PFA and dehydrated through to 100% MeOH for storage.

2.8.4 EXPLORATION OF EPHRIN-B2 IN CHICKEN: WESTERN ANALYSIS

Western analysis was attempted to determine the presence or absence of ephrin-B2 in the chick embryo skull roof. The plan, similar to that in the zebrafish Western analysis, was to test brain, eye, and skull roof tissue for ephrin-B2 and β-tubulin, a loading control protein. A total of four chick embryos at HH stage 41 and two at HH stage 43 were used for this protocol. After several attempts and modifications to the protocol, β-tubulin was detected in all three tissues, and ephrin-B2 was detected in none. It is possible that this was an issue with the antibodies being used, as they were not guaranteed for use in this protocol with this organism. Further details regarding this protocol, including antibody information, kit information, and troubleshooting, can be found in Appendix G.

3.0 RESULTS

I will first describe the shapes of cranial sutures in chicken, followed by zebrafish. For both organisms, morphology is described first and then the morphometric analysis. I also describe interpretation of *in situ* hybridization results visualizing the distribution of ephrin-B2a in the zebrafish skull.

3.1 THE CHICKEN SKULL

3.1.1 OBSERVATION OF CRANIAL SUTURE FORMATION IN CHICKEN

Early staining trials showed that ossification of the chicken skull roof begins at HH 38, at approximately 12 dpf. To better understand cranial suture formation patterns in chicken, skulls of chicken embryos at HH stages 40, 42, and 45 were whole-mount bone stained with Alizarin red (Figure 6) and the development of their cranial sutures was observed (Figure 7). At HH stage 40, the skull, and therefore the space between the developing calvariae, was proportionately wider than it was at HH stages 42 and 45.

Figure 6. Chicken skull samples whole-mount bone stained with Alizarin red, dorsal view. Anterior is to the top. Arrow indicates point where frontal bones first met. IF, interfrontal suture; C, coronal suture; S, sagittal suture. A) HH stage 40 (approx. 14 dpf). B) HH stage 42 (approx. 16 dpf). C) HH stage 45 (approx. 19 dpf). Scale bar = 5 mm

Figure 7. Tracings of chicken cranial sutures. Eight embryos were traced for each stage. After staging, the tracings were arranged in order of increasing maturity from left to right in each row.

The interfrontal suture appeared to have begun forming in the HH 40 samples.

The HH stage 42 and 45 samples showed increasingly narrow interfrontal sutures. The

coronal sutures of the HH stage 40 samples displayed a noticeably broader gap than those of the HH 42 and 45 samples. The sagittal suture was more narrow in samples of greater maturity, but the differences between sagittal sutures were less extreme than those amongst the interfrontal and coronal sutures.

From morphological observations, I concluded that the interfrontal suture appears to be the first to develop, followed by the coronal suture and then the sagittal suture (Figures 7 and 8). When observing the interfrontal and coronal sutures, it is helpful to think of them closing somewhat like "zippers". The interfrontal suture formed by the meeting of osteogenic fronts at a midpoint between the eyes, and "zipping" in the anterior direction, toward the beak, before developing posteriorly and partially closing the larger gap in the center of the skull roof (Figure 6A). The coronal suture was the second to form. This suture "zipped" unidirectionally inward, toward the midline of the skull roof, also contributing to the narrowing of the large gap between the calvariae (Figure 6). The sagittal suture was the last to develop, and was different from the interfrontal and coronal sutures in that the calvariae on either side of this suture approached uniformly, instead of narrowing gradually from one or more end points (Figure 8C). When a chick hatches at HH 46 (approximately 21 dpf) the sutures have not fully formed and there is still a gap between the calvariae.

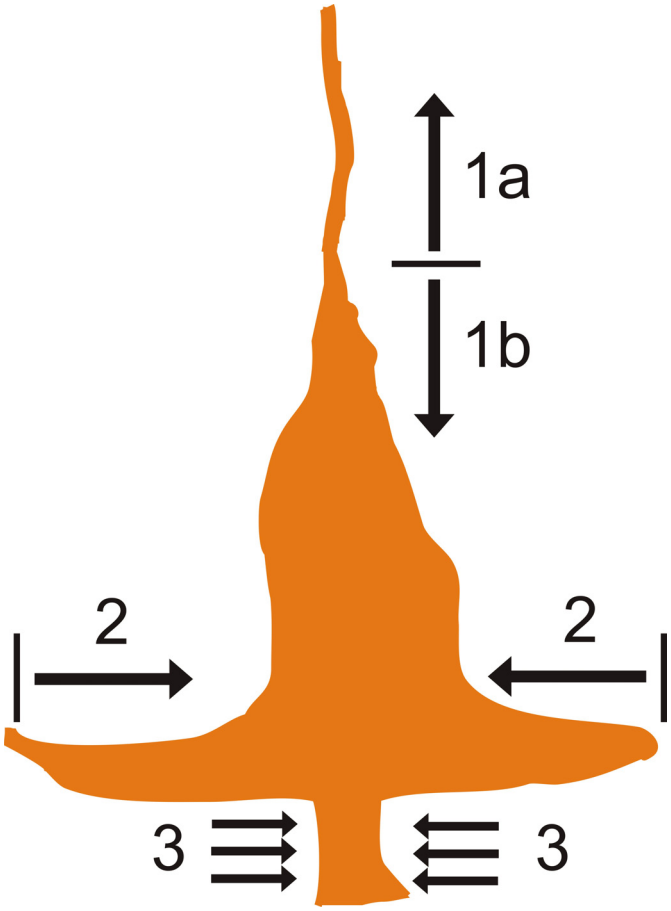

Figure 8. Schematic showing how the sutures come together in the chicken embryonic skull. 1) The interfrontal formed first, zipping in the anterior and then posterior direction. 2) The coronal suture formed second, developing inward toward the midline of the skull. 3) The sagittal suture formed last, narrowing uniformly along its lengeth.

3.1.2 MORPHOMETRIC ANALYSIS OF CHICKEN CRANIAL SUTURES

Morphometric shape analysis was performed using the SHAPE software program (Iwata and Ukai 2002) to statistically analyze the differences in shape between the cranial sutures of embryonic chicken skulls at HH stages 40, 42, and 45. The variation in shape amongst the sutures of the three different groups was characterized by principle components (PCs), each of which represented a specific variation in shape amongst the samples. As per standard convention, the PCs that each accounted for more than 1/77

(1.29%) of the total variation were considered effective components, influencing the variation in shape (Table 1). In this instance, eight PCs were identified this way, cumulatively accounting for 94.7% of the variation between the samples (Figure 9).

Table 1. Eigenvalues and proportions of the eight effective PCs of chicken cranial sutures at HH stages 40, 42, and 45. Eigenvalues were rounded to the nearest third decimal and percentages were rounded to the second decimal.

PC	Eigenvalue	Percentage	Cumulative %
PC1	0.012	33.10	33.10
PC2	0.010	28.35	61.45
PC3	0.006	15.60	77.05
PC4	0.002	5.69	82.74
PC5	0.002	4.53	87.28
PC6	0.002	4.04	91.33
PC7	0.001	2.01	93.34
PC8	0.001	1.37	94.70

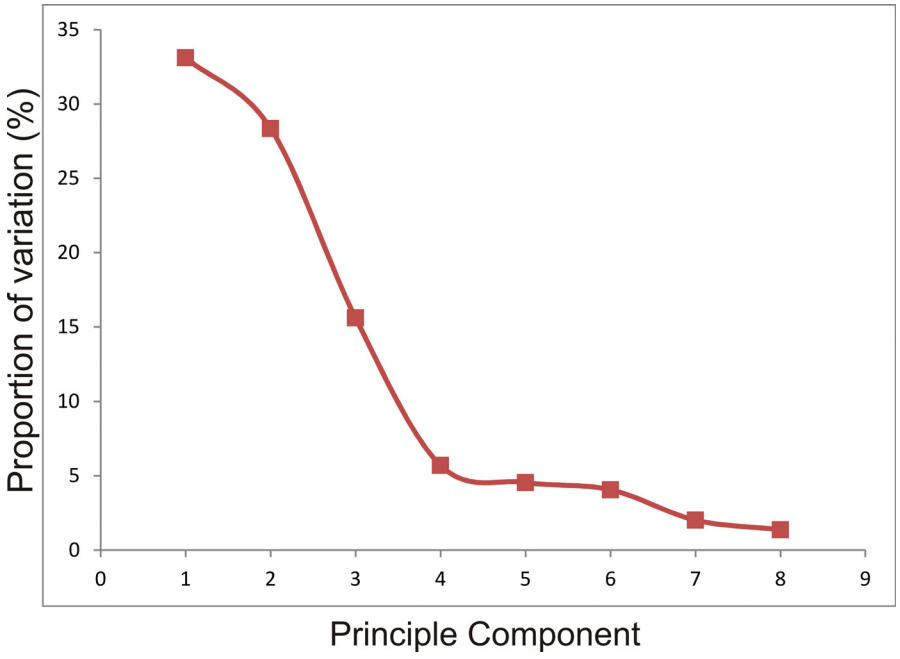

Figure 9. The proportion of variation accounted for by the eight significant principle components of the chicken cranial sutures. PC1 accounted for 33.1% of the total variation, PC2 accounted for 28.3%, PC3 accounts for 15.6%, PC4 accounts for 5.7%, and PC5-8 account for less than 5% of the observed variation.

PC1 and PC2 were the two most substantial PCs, accounting for 33.1% and 28.3% of the total variation, respectively (Table 1; Figure 9). Therefore together, these two PCs accounted for more than half of the observed variation (61.4%). PrinPrint was used to visualize the contours of these two PCs (Figure 10). Both PC1 and PC2 corresponded to the narrowing of all three sutures, however, PC1 captured more narrowing of the interfrontal suture, as well as a twisting or asymmetry of the sutural space between the developing calvariae. This analysis therefore showed that amongst all the samples over all time points (HH 42 – HH 45), the major shape variation was twisting and narrowing of the sutures.

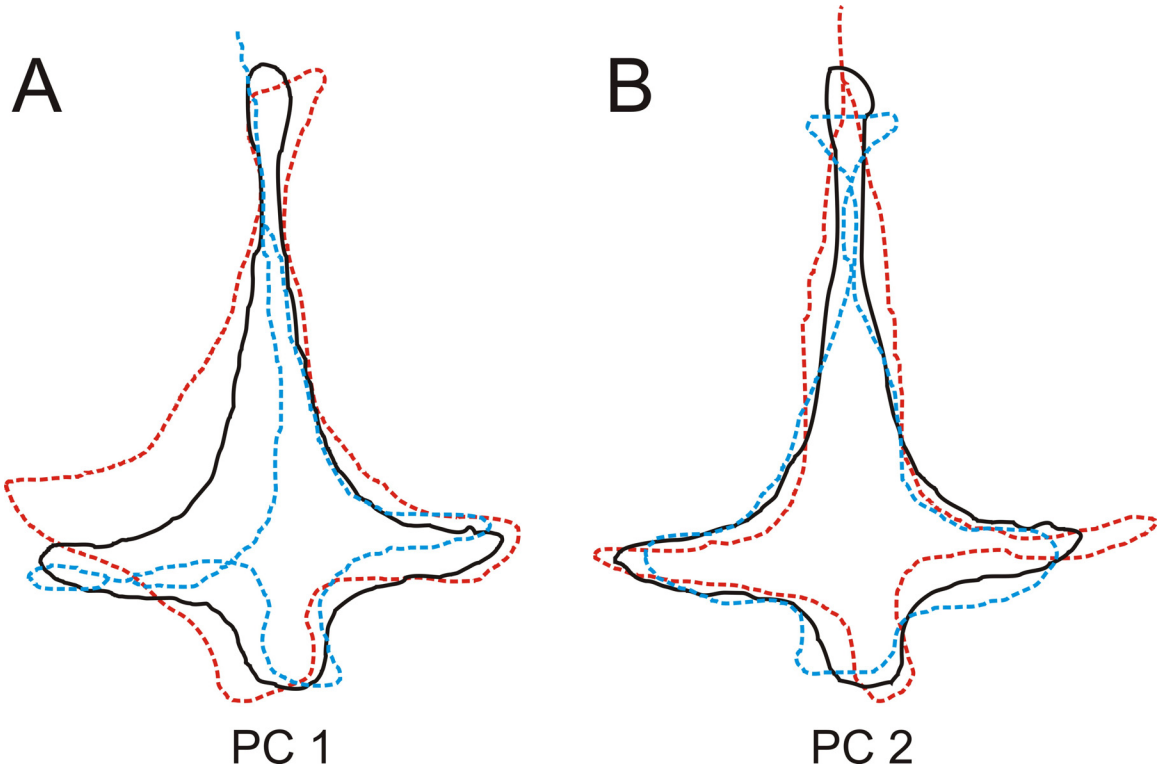

Figure 10. Variations in suture shape of chicken cranial sutures for the first (A) and second (B) principle components. The black solid line, red broken line, and blue broken line show the mean shape, +2 standard deviations, and -2 standard deviations, respectively.

In order to visualize these major shape axes and how they change in each embryonic stage examined, the samples were plotted using Excel with PC1 on the x-axis and PC2 on the y-axis (Figure 11). The HH 40 samples and HH 45 samples were clustered with respect to both PCs, though more so with respect to PC2. The HH 40 samples were largely grouped lower along the PC2 axis (quadrant IV). The HH 42 samples, however, wee not grouped distinctly from the other two groups, showing a wider spread along the PC2 axis (quadrants II, III, IV). HH 42 samples were scattered amongst the HH 40 and HH 45 clusters, and one specimen in this group had a higher PC1 value than any other specimen (Figure 11, arrow). To definitively prove that this was a true outlier, it would have had to fall outside two standard deviations from the middle. Observations of the shapes and the contours showed that it did not. I will, however, refer to this specimen as the outlier from here onwards in this thesis.

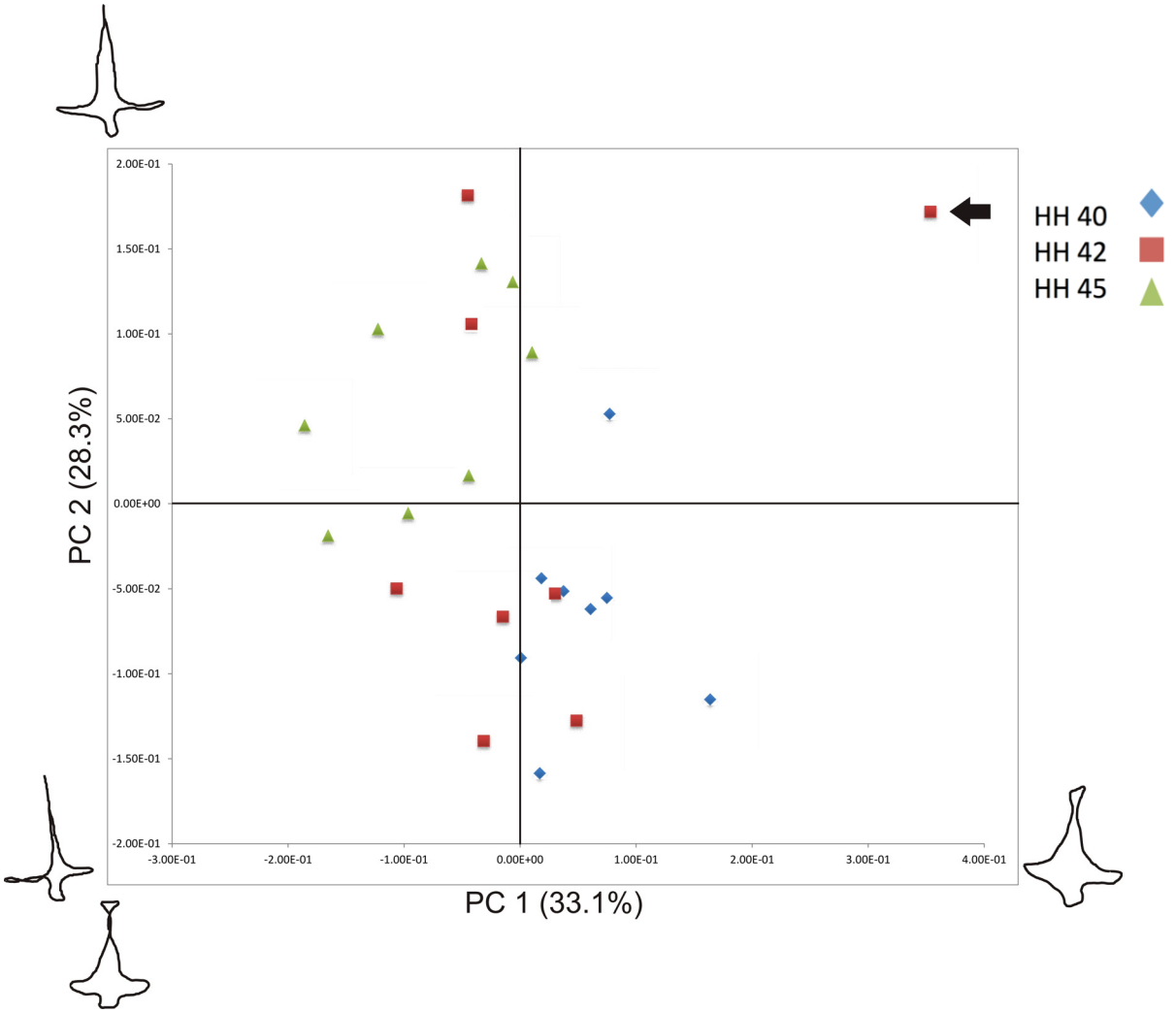

Figure 11. The relationship between the first and second principle components of the chicken cranial sutures. Arrow indicates the outlier. Schematics at the end of each axis show the shapes representing -2 and +2 standard deviations from the mean shape of each principle component.

Because the outlier may have been biasing the analysis, a second morphometric analysis was completed without this specimen. Again, eight PCs accounted for more than 1/77 (1/29%) of the total variation and were considered effective components (Table 2). Cumulatively, these eight PCs accounted for 94.4% of the variation between these samples (Figure 12). It is important to note that this suite of PCs are different to the ones

in the previous analysis and capture potentially different aspects of the shape variation in the cohort of samples examined.

Table 2. Eigenvalues and proportions of the eight effective PCs of chicken cranial sutures at HH stages 40, 42, and 45 after removal of the HH 42 outlier. Eigenvalues were rounded to the nearest third decimal and percentages were rounded to the second decimal.

PC	Eigenvalue	Percentage	Cumulative %
PC1	0.011	38.02	38.02
PC2	0.007	25.02	63.04
PC3	0.004	14.19	77.23
PC4	0.002	5.90	83.13
PC5	0.002	5.31	88.44
PC6	0.001	2.61	91.05
PC7	0.001	1.77	92.82
PC8	0.001	1.55	94.37

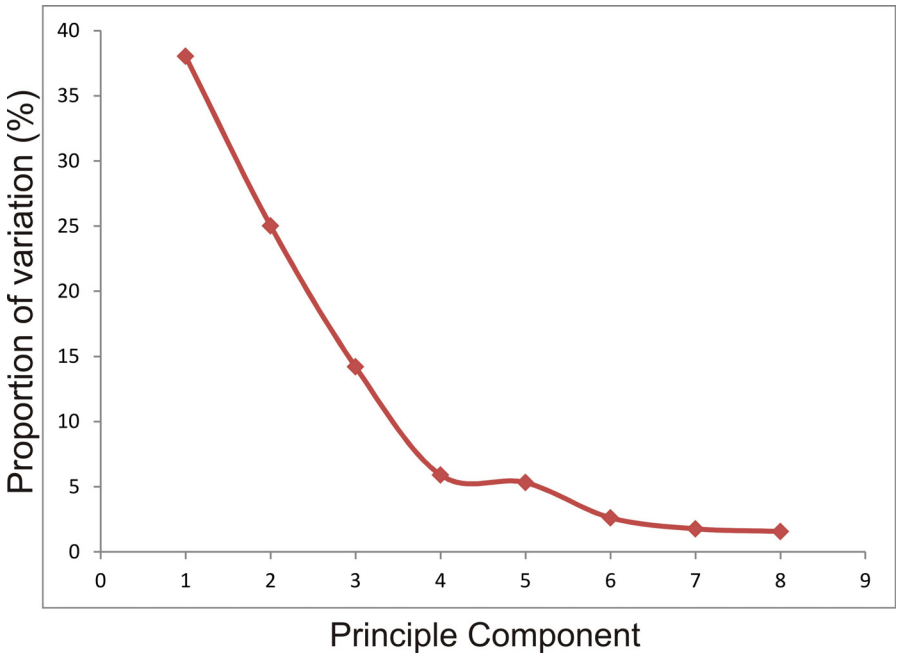

Figure 12. The proportion of variation accounted for by the eight significant principle components of the chicken cranial sutures after removal of the outlier. PC1 accounts for 38.0% of the total variation, PC2 accounts for 25.0%, PC3 accounts for 14.2%, PC4 accounts for 5.9%, PC5 accounts for 5.3%, and PC6-8 account for less than 6% of the observed variation.

The two most substantial PCs, PC1 and PC2, accounted for 38.0% and 25.0% of the total variation amongst the samples, respectively (Table 2; Figure 12). Together, these two PCs accounted for 63.0%. of the total variation PrinPrint was used to visualize the contours of these new PCs and assess the shapes that they represented (Figure 13). As in the first morphometric analysis, PC1 showed a twist or asymmetry in the narrowing of the sutural space. In this analysis, however, PC2 was different in that it appeared to represent a more complete narrowing of the interfrontal suture than PC2 of the original analysis. Both PCs represented an overall narrowing of all three featured sutures. This analysis again showed that the sutures are closing and twisting (PC1) and closing (PC2) amongst all samples.

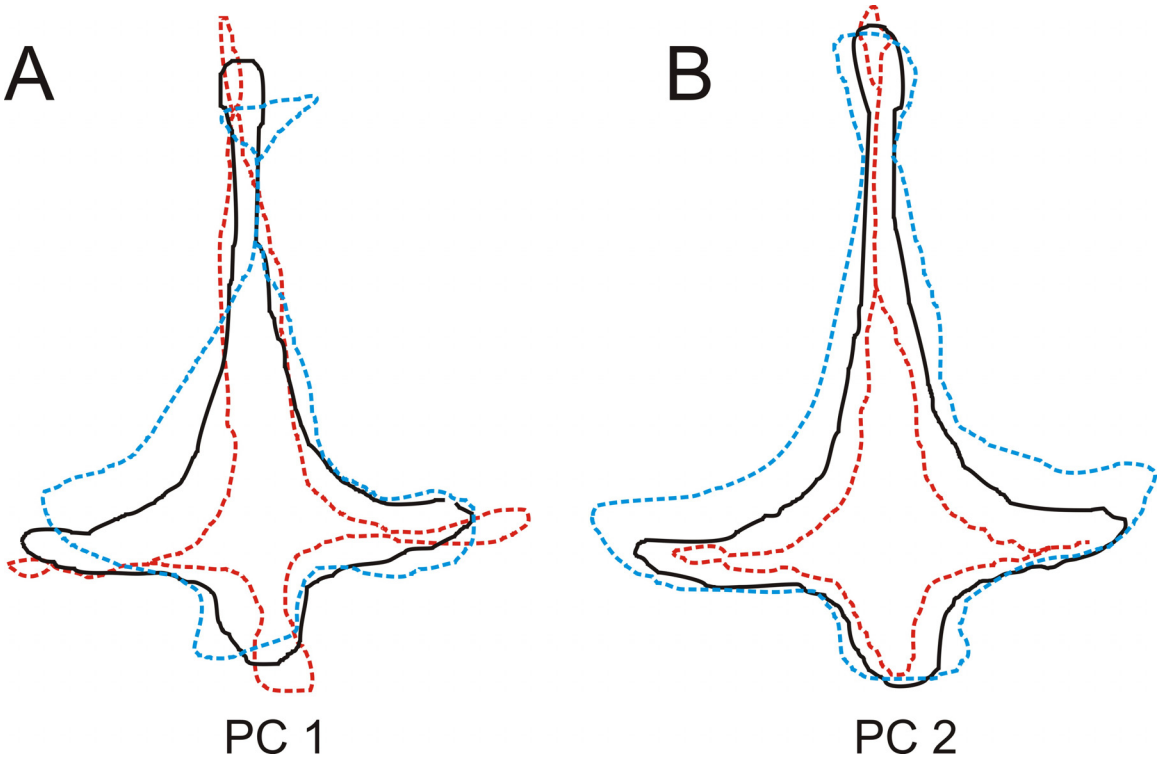

Figure 13. Variations in suture shape of chicken cranial sutures for the first (A) and second (B) principle components, after removal of the outlier. The black solid line, red broken line, and blue broken line show the mean shape, +2 standard deviations, and -2 standard deviations, respectively.

PC1 and PC2 were again plotted along the x and y axes, respectively (Figure 14). In this scatterplot, the HH 40 and HH 45 samples were, again, separated into distinct clusters and grouped with respect to both PCs. The HH 40 samples had lower PC1 values and, as a whole, lower PC2 values than the HH 45 samples. The HH 40 samples were entirely within quadrants II and III, and the HH 45 samples were entirely within quadrants I and IV (Figure 14). The HH 42 samples were, again, scattered amongst the HH 40 and HH 45 samples, suggesting that they were not a distinct group with respect to suture shape.

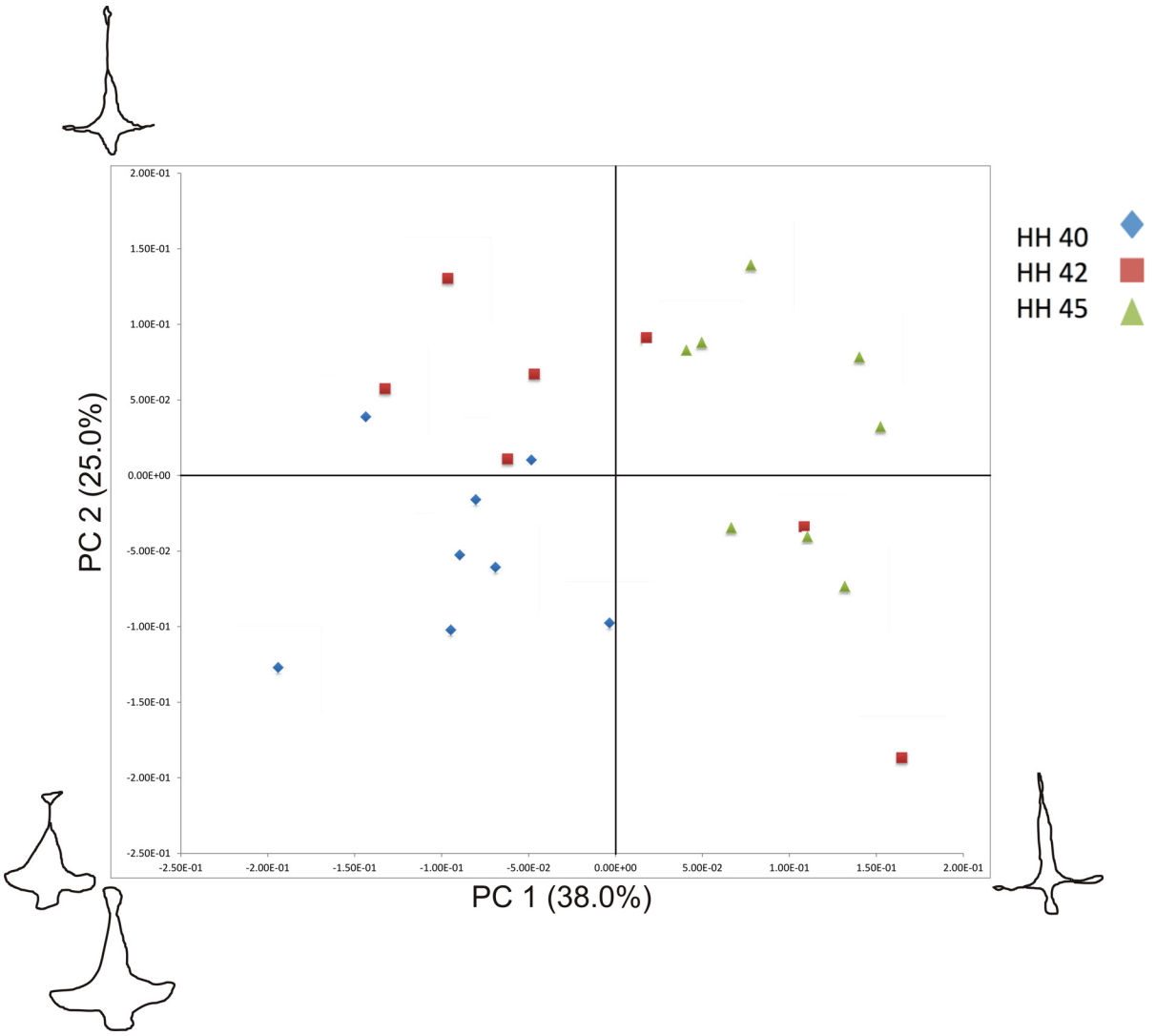

Figure 14. The relationship between the first and second principle components of the chicken cranial sutures after removal of the outlier. Schematics at the ends of each axis show the shapes representing -2 and +2 standard deviations from the mean shape of each principle component.

A third morphometric analysis for chicken cranial sutures removed the HH 42 samples entirely, with hopes that an analysis of the statistically different HH 40 and HH 45 samples would yield a more informative shape analysis. Eight PCs each accounted for more than 1/77 (1.29%) of the total variation and were deemed effective (Table 3). These

eight effective PCs together accounted for 97.2% of the total variation amongst the samples (Figure 15).

Table 3. Eigenvalues and proportions of the eight effective PCs of chicken cranial sutures at HH stages 40 and 45. Eigenvalues were rounded to the nearest third decimal and percentages were rounded to the second decimal.

PC	Eigenvalue	Percentage	Cumulative %
PC1	0.014	48.63	48.63
PC2	0.006	22.07	70.70
PC3	0.004	12.63	83.32
PC4	0.002	5.67	89.00
PC5	0.001	2.78	91.78
PC6	0.001	2.41	94.19
PC7	0.001	1.69	95.88
PC8	0.000	1.37	97.25

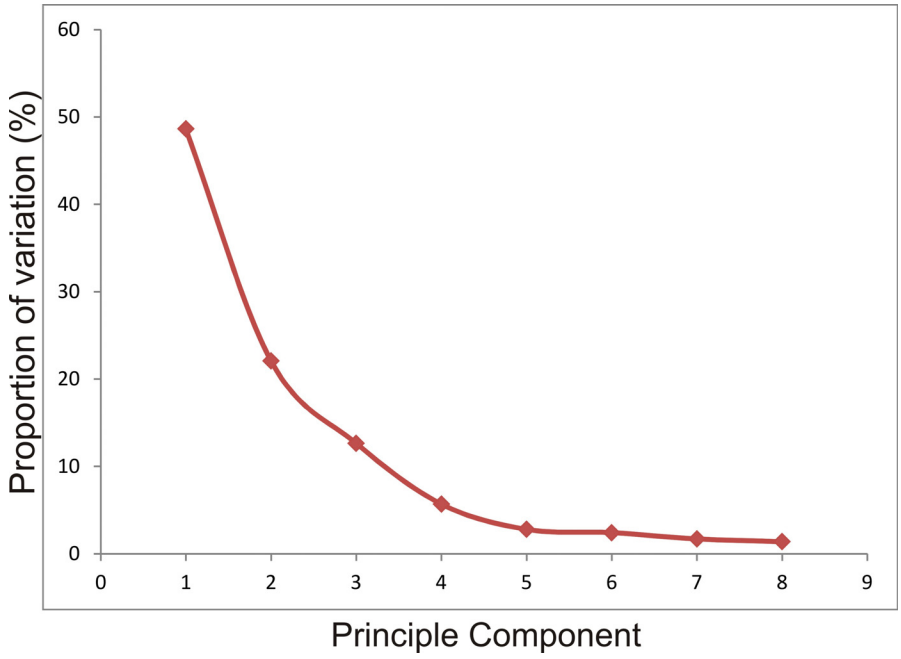

Figure 15. The proportion of variation accounted for by the eight significant principle components of the chicken cranial sutures at HH stages 40 and 45. PC1 accounts for 48.6% of the total variation, PC2 accounts for 22.1%, PC3 accounts for 12.6%, PC4 accounts for 5.7%, and PC5-8 account for less than 5% of the observed variation.

PC1 and PC2, the two most substantial PCs, respectively represented 48.6% and 22.1% of the total variation amongst the samples (Table 3; Figure 15). These two PCs together accounted for 70.7% of the total shape variation. Using PrinPrint, these two PCs were visualized and assessed in terms of what shapes they represented (Figure 16). In this analysis, PC1 most clearly represented a gross change in the narrowing of all sutures after the osteogenic fronts of the frontal bones originally meet between the eyes. PC2 represents a fine-tuning of the narrowing sutures.

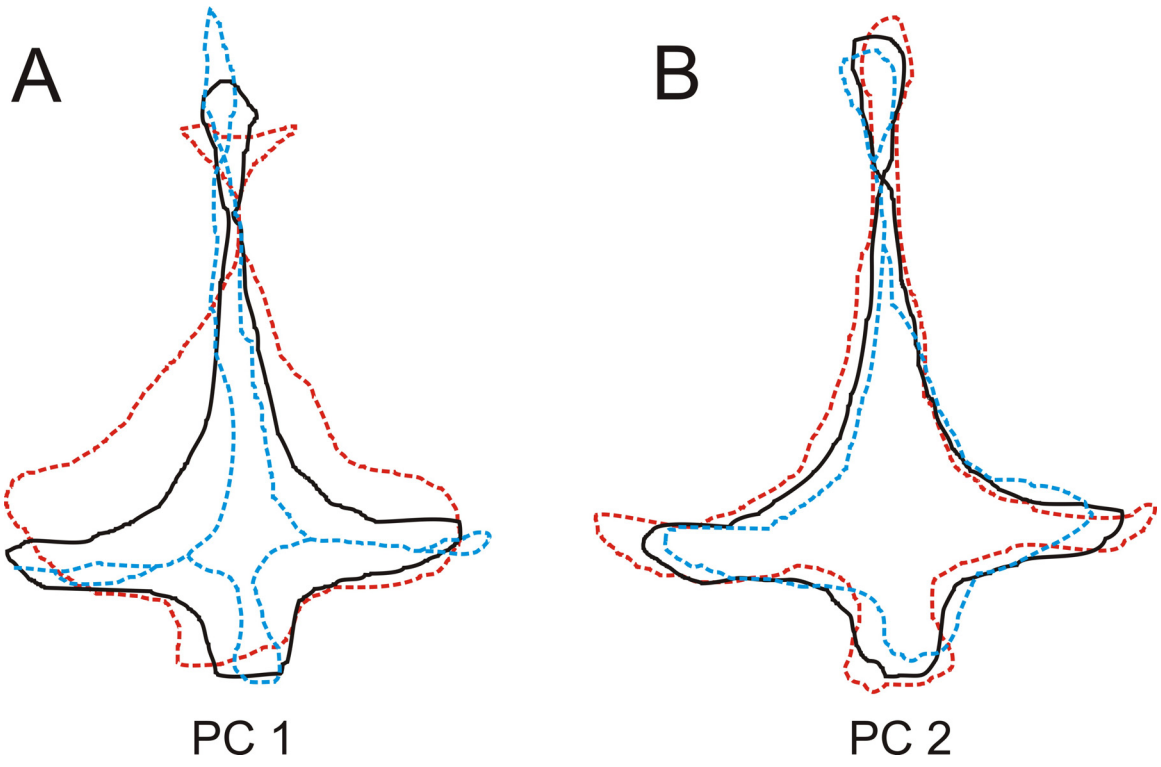

Figure 16. Variations in suture shape of chicken cranial sutures of stages 40 and 45 for the first (A) and second (B) principle components. The black solid line, red broken line, and blue broken line show the mean shape, +2 standard deviations, and -2 standard deviations, respectively.

PC1 and PC2 were plotted as in the previous two morphometric analyses (Figure 17). The two groups of samples were clustered separately from one another with respect to PC1, but not PC2. HH 45 samples had lower PC1 values than the HH 40 samples. HH 40 samples are entirely within quadrants II and III, and HH 45 samples were entirely within quadrants I and IV (Figure 17). There did not appear to be a distinction between the two age groups with respect to PC2, which is unsurprising as the fine-tuning is similar for each stage.

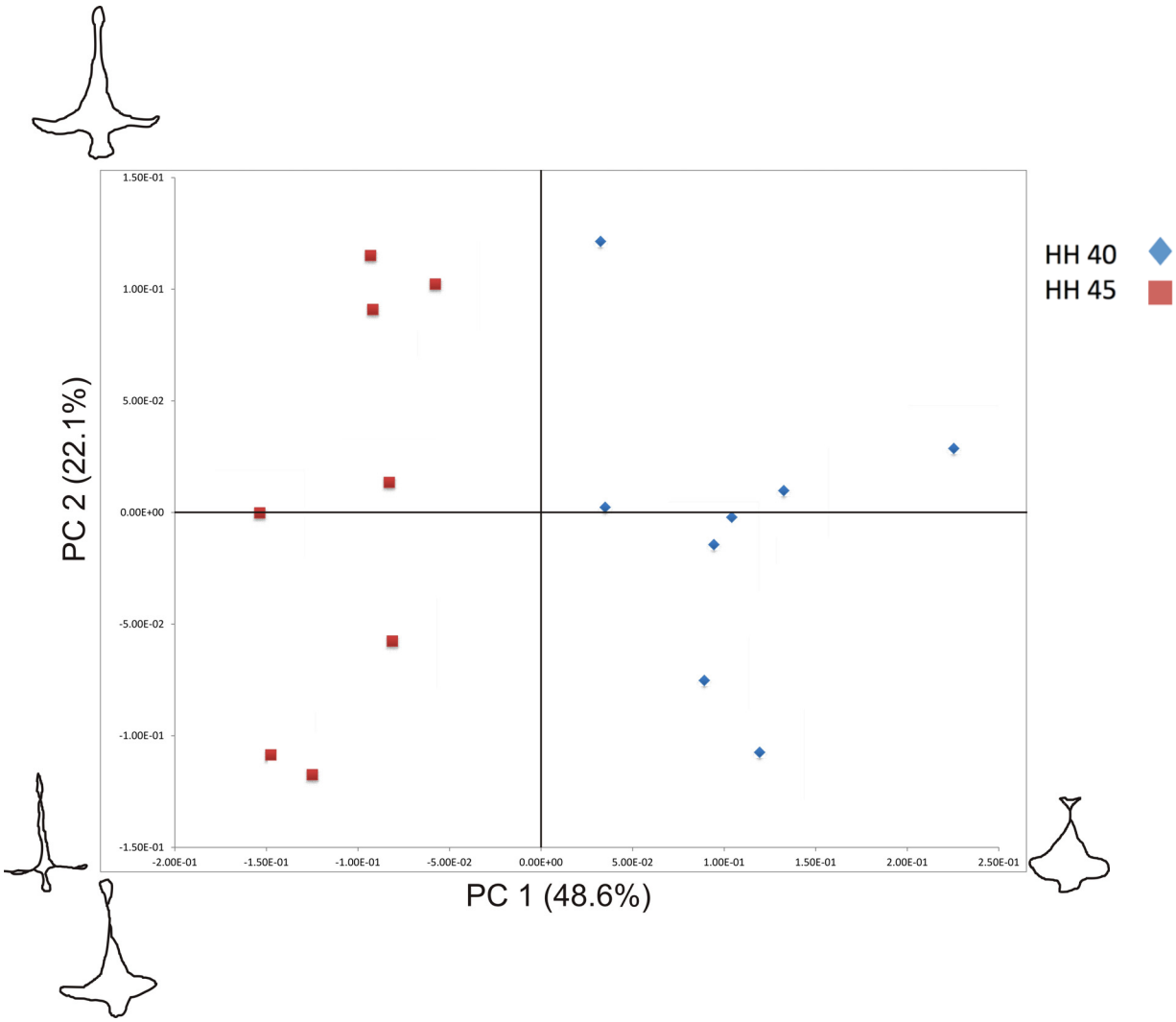

Figure 17. The relationship between the first and second principle components of the chicken cranial sutures at HH stages 40 and 45. Schematics at the ends of each axis show the shapes representing -2 and +2 standard deviations from the mean shape of each principle component.

3.1.3 STATISTICAL ANALYSIS OF CHICKEN MORPHOMETRICS

In order to determine whether there was a significant difference between the three different stages in each scenario above, a one-way analysis of variance (ANOVA) and a Tukey's comparison test were completed (see Appendix E for full Minitab output). The

results for each of the three scenarios above (all data points, no outlier in HH42 group, no HH42 group) are described below.

In the first morphometric analysis, there was significant difference between the HH 40 and HH 45 age groups for PC1 (ANOVA df = 2, F = 4.37, $p < 0.05$) and PC2 (ANOVA df = 2, F = 4.01, $p < 0.05$) (see Appendix F for all p-values). A Tukey's comparison test found significant differences between the HH 40 and HH 45 groups, but did not find that the HH 42 age group was significantly different from the other two. This suggests that the HH 42 samples did not comprise a distinct group with respect to suture development, which is in keeping with the scatterplot data (Figure 11).

With the HH 42 outlier removed, PC1 remained significant (ANOVA df = 2, F = 12.9, $p < 0.05$), but PC2 (ANOVA df = 2, F = 2.50, $p > 0.05$) did not. A Tukey's comparison test for PC1 confirmed that the HH 45 group was significantly different from both the HH 40 group and the HH 42 group, but that the latter two groups were not significantly different from one another. There was no significant difference between the three groups for PC2 in this analysis. This suggests that the HH 45 samples comprised a distinct group with respect to suture development, but that there was not a significant difference between the suture development of HH 40 and HH 42 chick embryos when the outlier is removed.

When the entire HH 42 age group was removed, a significant difference remained between HH 40 and HH 45 groups for PC1 (ANOVA df = 1, F = 71.05, $p < 0.05$). There was no significant difference between these two groups for PC2 (ANOVA df = 1, F = 0.05, $p > 0.05$). This analysis showed that there was significant difference in cranial

suture development between HH 40 and HH 45 chick embryos, again agreeing with the scatterplot data (Figure 17).

3.1.4 SUMMARY OF CHICKEN SKULL ANALYSES

Analysis of gross morphology of the chicken embryonic skull at HH stages 40, 42, and 45 showed that cranial sutures of the chick embryo developed in the following order: interfrontal suture, followed by coronal suture, followed by sagittal suture. The interfrontal and coronal sutures closed in a zipper-like fashion, and the sagittal suture closes uniformly. Morphometric analysis showed that the HH 40 and HH 45 samples were distinct groups with respect to suture development, but that HH 42 samples were not. This suggests that, while there was a clear difference in suture development between HH 40 and HH 45, the progression of suture development between these two stages was not uniform. Also, similar fine-tuning occurs at both HH 40 and HH 45.

In future analysis of this data, the full data set (i.e., the first morphometric analysis) and the set including only samples at HH 40 and HH 45 (i.e., the third morphometric analysis) should be used. The full data set gave the most information regarding overall shape variation, and the third set showed that the observed asymmetry was present only in the HH 42 samples.

3.2 THE ZEBRAFISH SKULL

3.2.1 OBSERVATION OF CRANIAL SUTURE FORMATION IN ZEBRAFISH

Skulls of zebrafish at 8 mm, 10 mm, and 12 mm SL were whole-mount bone stained with Alizarin red and observed to gain insight into their suture formation patterns (Figure 18). The sutures between their calvariae were traced and observed to learn the pattern of their development (Figure 19). This data shows how the sutures developed as the zebrafish increased in length.

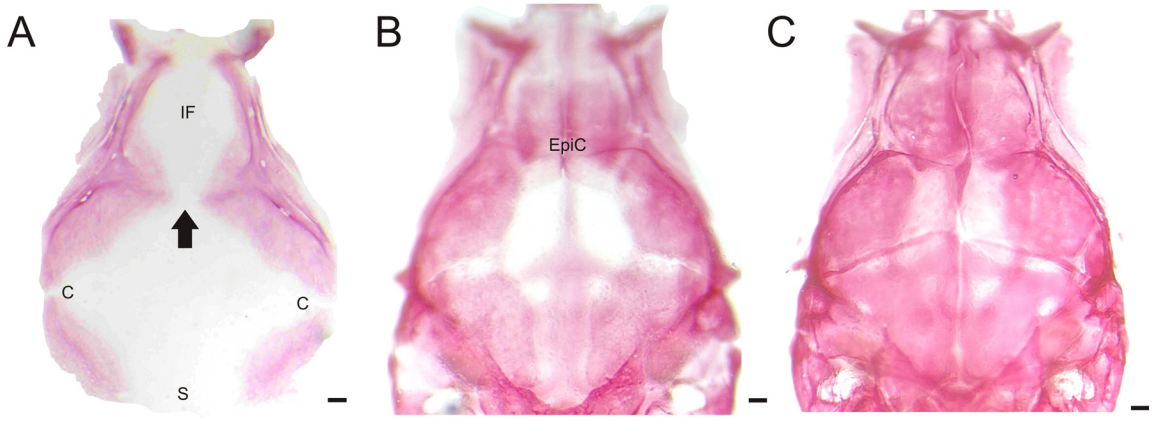

Figure 18. Zebrafish skull samples whole-mount bone stained with Alizarin red, dorsal view. Arrow indicated where interfrontal suture first formed, directly dorsal to the epiphyseal bar. IF, interfrontal suture; C, coronal suture; S, sagittal suture; EpiC, epiphyseal cartilaginous bar. Anterior is to the top. A) 8 mm SL. B) 10 mm SL. C) 12 mm SL. Scale bar = 100 μm.

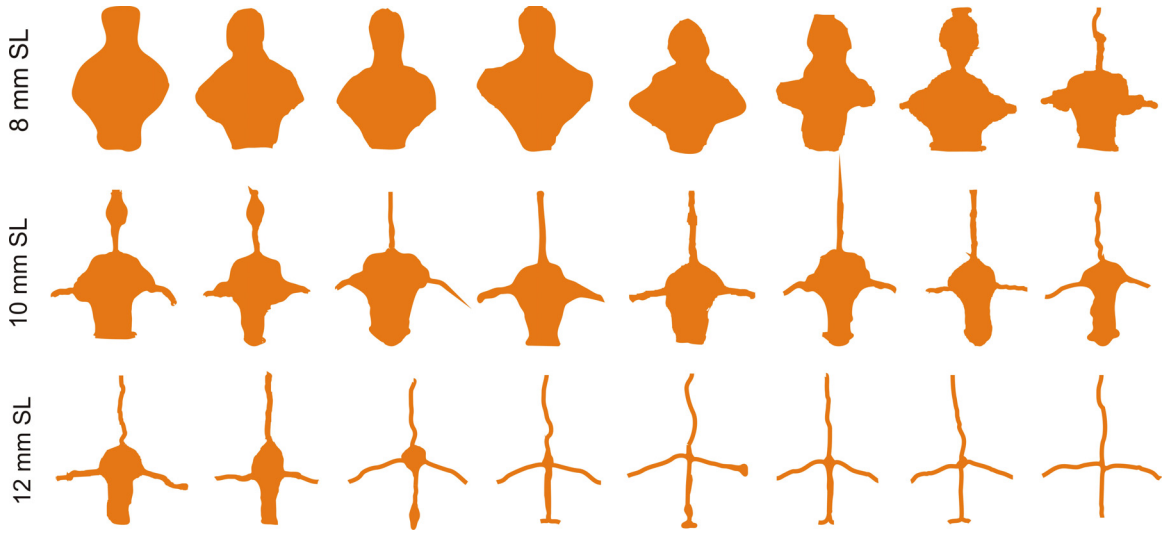

Figure 19. Tracings of zebrafish cranial sutures. Eight zebrafish were traced for each stage. After staging, the samples were arranged in order of increasing maturity from left to right in each row.

All sutures appear to be fully formed at approximately the 12 mm SL size (Figure 19). The interfrontal suture was observed to be the first to develop, followed by the coronal and sagittal sutures (Figure 4, Figure 20). Again, it is helpful to think of the interfrontal and coronal sutures closing as if they were zippers. The interfrontal suture appears to form first where the frontal bones meet superficial to the cartilaginous epiphyseal bar (Figure 18). The suture continues to develop by zipping in the posterior direction and then the anterior direction (Figure 20). There is a point where there is a noticeable gap in the anterior half of the developing interfrontal suture. After this gap is replaced by the anterior portion of the interfrontal suture, the posterior portion of the suture forms completely. This further closes the central gap in the midline of the skull roof. The coronal suture develops more slowly than the interfrontal suture, zipping unidirectionally inward, toward the center of the skull roof as it does in the chicken

embryo (Figure 20). Finally, the sagittal suture forms by a gradual narrowing of the space between the parietal bones (Figure 20).

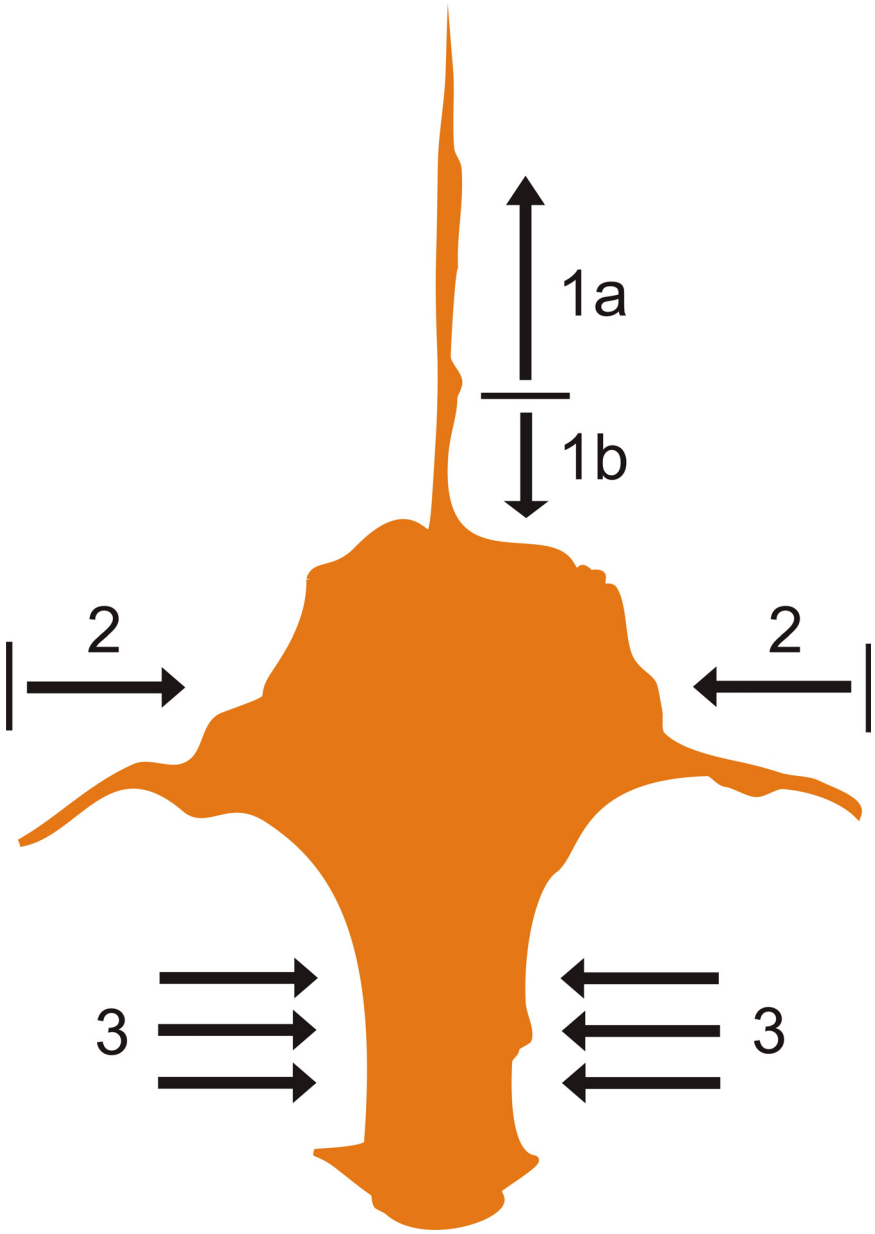

Figure 20. Schematic showing how the sutures come together in the zebrafish skull. 1) The interfrontal suture formed first, beginning superficially to the epiphyseal bar and zipping anteriorly, then posteriorly. 2) The coronal suture formed second, inward toward the midline of the skull. 3) The sagittal suture formed last, narrowing uniformly.

3.2.2 MORPHOMETRIC ANALYSIS OF ZEBRAFISH CRANIAL SUTURES

In order to quantitatively analyze the differences in shape amongst the cranial sutures of zebrafish at 8, 10 and 12 mm SL, a morphometric analysis was conducted using SHAPE morphometrics program (Iwata and Ukai 2002). Seven PCs each accounted for more than 1/77 (1.29%) of the total variation amongst the samples and were considered effective components (Table 4). These seven PCs cumulatively represented 96.0% of the total shape variance (Figure 21).

Table 4. Eigenvalues and proportions of the eight effective PCs of zebrafish cranial sutures at 8, 10, and 12 mm SL. Eigenvalues were rounded to the nearest third decimal and percentages were rounded to the second decimal.

PC	Eigenvalue	Percentage	Cumulative %
PC1	0.043	53.80	53.80
PC2	0.014	17.95	71.75
PC3	0.009	10.66	82.41
PC4	0.005	5.98	88.39
PC5	0.004	4.45	92.86
PC6	0.002	1.84	94.67
PC7	0.001	1.36	96.03

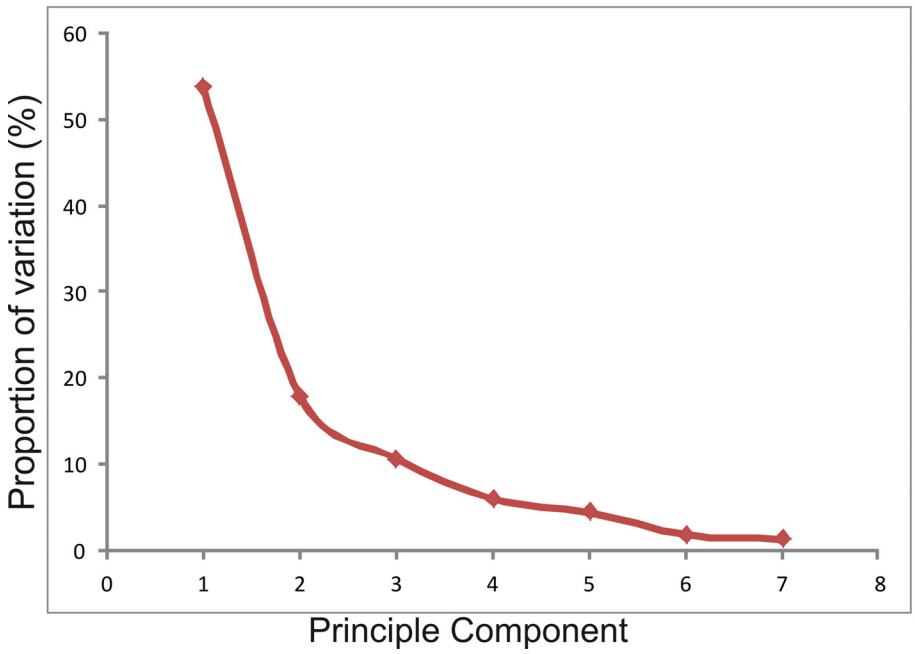

Figure 21. The proportion of variation accounted for by the seven significant principle components of the chicken cranial sutures. PC1 accounts for 53.8% of the total variation, PC2 accounts for 17.9%, PC3 accounts for 10.6%, PC4 accounts for 5.9%, and PC5-7 cumulatively account for less than 8% of the observed variation.

The two most significant PCs, PC1 and PC2, accounted for 53.8% and 17.9% of the total shape variation, respectively (Table 4, Figure 21). PC1 accounted for most of the observed variation. Using PrinPrint, the shape contours represented by PC1 and PC2 were visualized. Both PCs showed the narrowing of all three observed sutures. PC1 represented overall development from the virtually shapeless open calvarial space of the 8 mm SL samples to the much more defined sutures of the 12 mm SL samples. PC2 represented a narrowing of the coronal and sagittal sutures and an asymmetry of the sutural space. PC2 also captured asymmetry in the sutural space of all samples. This analysis therefore showed that amongst all the samples over all time points (8 mm SL – 12 mm SL), the major shape variation was twisting and narrowing of the sutures (i.e., fine tuning).

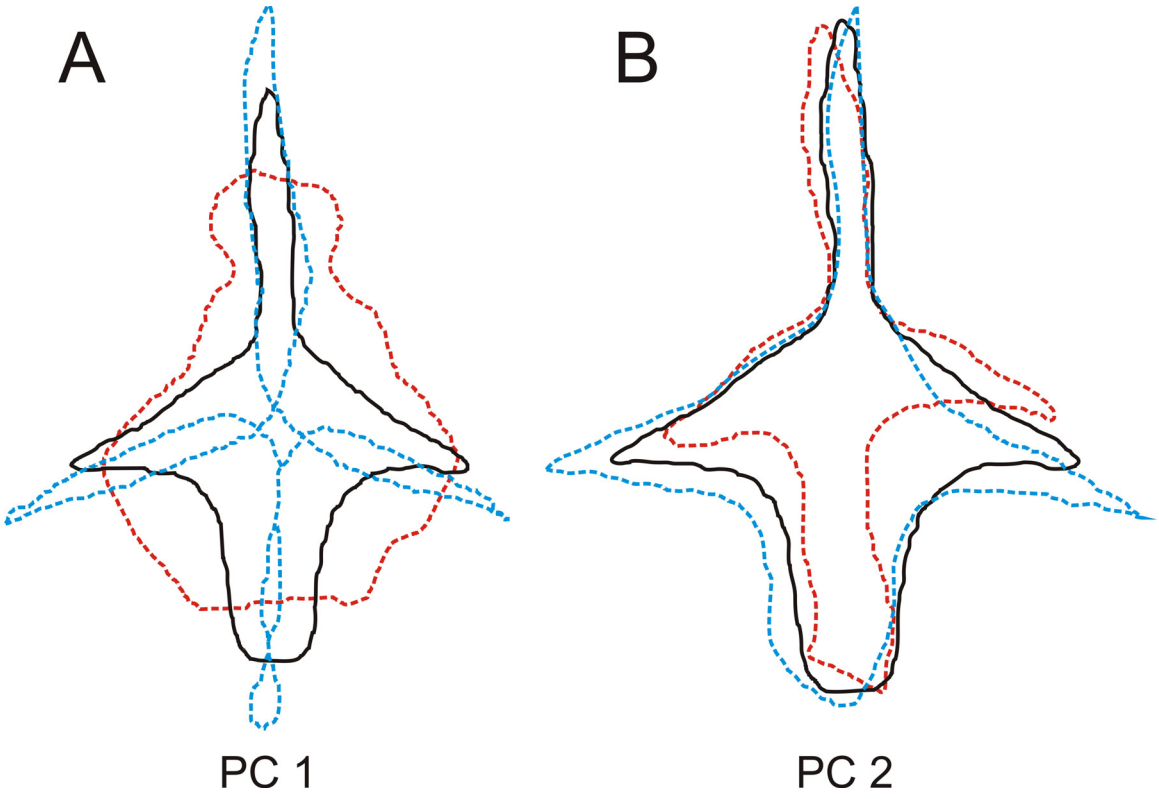

Figure 22. Variations in suture shape of zebrafish cranial sutures for the first (A) and second (B) principle components. The black solid line, red broken line, and blue broken line show the mean shape, +2 standard deviations, and -2 standard deviations, respectively.

These first two PCs, accounting for 71.8% % of a total shape variation, were plotted as they were in the chicken analyses described above. Each of the three groups was clustered together with respect to PC1 (Figure 23). The samples were arranged from 8 mm through to 12 mm along the PC1 axis. The 8 mm SL samples were grouped in quadrants I and IV, the 10 mm SL samples were present in all four quadrants, and the 12 mm SL samples were grouped in quadrants II and III (Figure 23). The 12 mm SL samples showed the widest spread in both the PC1 and PC2 dimensions, but were still grouped

separately from the other two groups, suggesting that the fine-tuning of sutural shape was more variable in larger samples than in smaller ones.

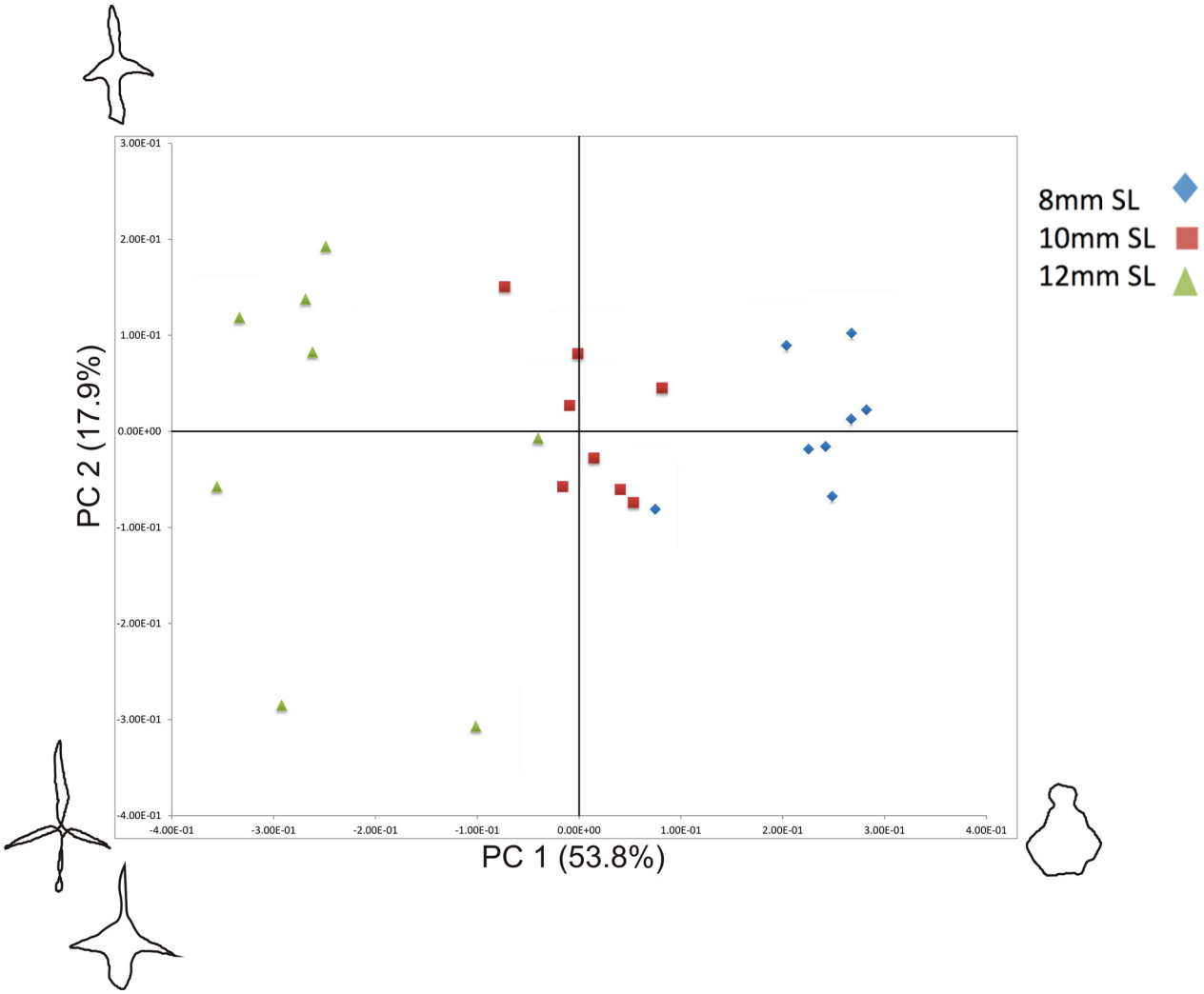

Figure 23. The relationship between the first and second principle components of the zebrafish cranial sutures. Schematics at the ends of each axis show the shapes representing -2 and +2 standard deviations from the mean shape of each principle component.

3.2.3 STATISTICAL ANALYSIS OF ZEBRAFISH MORPHOMETRICS

To determine the statistical significance of the differences amongst these three age groups, a one-way ANOVA (with a Tukey's comparison test was performed for both PC1 and PC2 (see Appendix E for full Minitab output). A significant difference was found with respect to PC1 between the three groups (ANOVA $df = 2$, $F = 68.69$, $p < 0.05$) (see Appendix F for all p-values). The subsequent Tukey's comparison test confirmed that all three groups were significantly different from one another with respect to PC1. There was no significant difference between the groups with respect to PC2 (ANOVA $df = 2$, $F = 0.10$, $p > 0.05$). This agrees with the scatterplot data represented in Figure 23, in which the 8 mm SL and 10 mm SL samples displayed similar PC2 values and the 12 mm SL samples displayed a wider range of PC2 values. These tests indicate that there is significant difference with respect to suture narrowing between these three developmental stages.

3.2.4 SUMMARY OF ZEBRAFISH SKULL ANALYSIS

Analysis of the zebrafish embryonic skull at 8 mm, 10 mm, and 12 mm SL showed that zebrafish cranial sutures developed in the following order: interfrontal suture, followed by coronal suture, followed by sagittal suture. The interfrontal suture first formed dorsally to the epiphyseal bar before zipping posteriorly and then anteriorly. The coronal suture zipped inward and the sagittal suture narrows uniformly. Morphometric analysis showed that the primary variation in suture shape between the three age groups was the narrowing of all three sutures. Fine-tuning of sutural shapes occured in all samples but with more variation in the larger samples. There is a

statistically significant difference with respect to suture development between zebrafish at 8 mm, 10 mm, and 12 mm SL.

3.2.5 INVESTIGATION OF EPHRIN-B2A IN ZEBARFISH

In situ hybridization was utilized to visualize *ephrin-B2a* (*efnB2a*) distribution in the zebrafish skull at the stages 8 mm, 10 mm, and 12 mm SL. In addition, zebrafish embryos at 36 hpf were used as an initial positive control since *efnB2a* expression has been described at this stage (Chan *et al.,* 2001)

My results showed the presence of *efnB2a* in the developing telencephalon, eye, and pharyngeal region of 36 hpf zebrafish (Figure 24A), as expected based on the findings of Chan *et al.* (2001). In the 8 mm SL samples (n = 7), *efnB2a* expression was present in the gill region (Figure 24B-D). Further examination of the gill region showed expression at the cellular level, in the gill filaments (Figure 26). No other expression was seen at this time point. No expression was observed in the 10 (n = 6) and 12 mm SL (n = 7) samples (Figure 24E-J). Similarly, no expression was seen in the skull roof of the 8, 10, or 12 mm SL samples, as can be seen quite clearly in Figure 24 D, G, and F, where the brain and skull roof can be seen unstained. Dissection of brain tissue from the 8 mm SL sample confirmed that there was also no expression in the brain (Figure 27). No expression was seen in the no-probe controls (Figure 25).

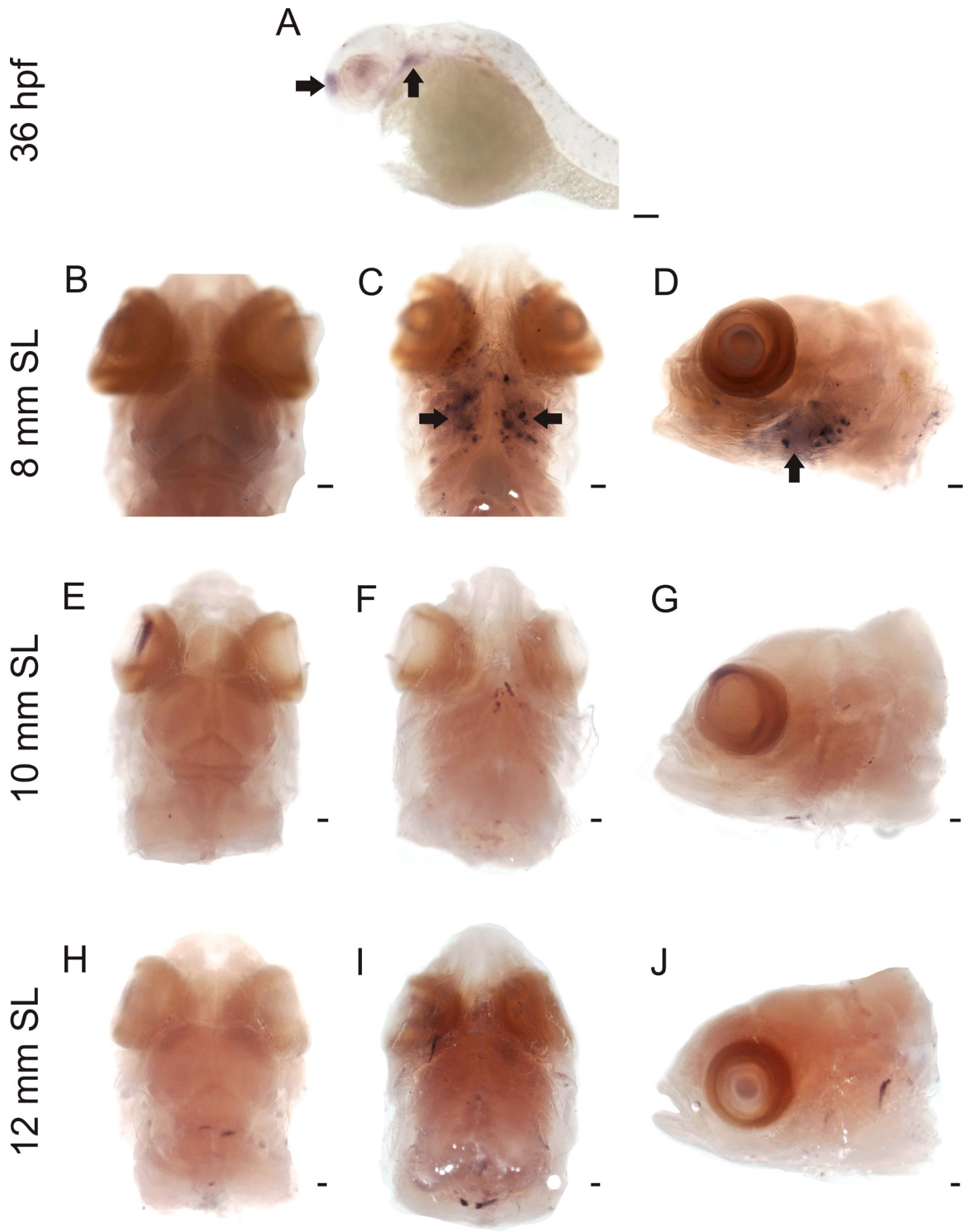

Figure 24. Expression of *efnb2a* by *in-situ* hybridization. A) *efnb2a* expression in the developing forebrain, eye, and pharyngeal region of 36 hpf zebrafish. B-D) *efnb2a* expression in 8 mm SL zebrafish, dorsal, ventral, and lateral views. Expression is strong in the gill region. E-G) *efnb2a* expression in 10 mm SL zebrafish, dorsal, ventral, and

lateral views. Expression is seen faintly in the left eye and the gill region. H-J) *efnb2a* expression in 12 mm SL zebrafish, dorsal, ventral, and lateral views. Expression is seen faintly in the gill region and at the anterior end of the skull roof. The strongest expression is seen in the gills of 8 mm SL zebrafish. All scale bars = 100 μm.

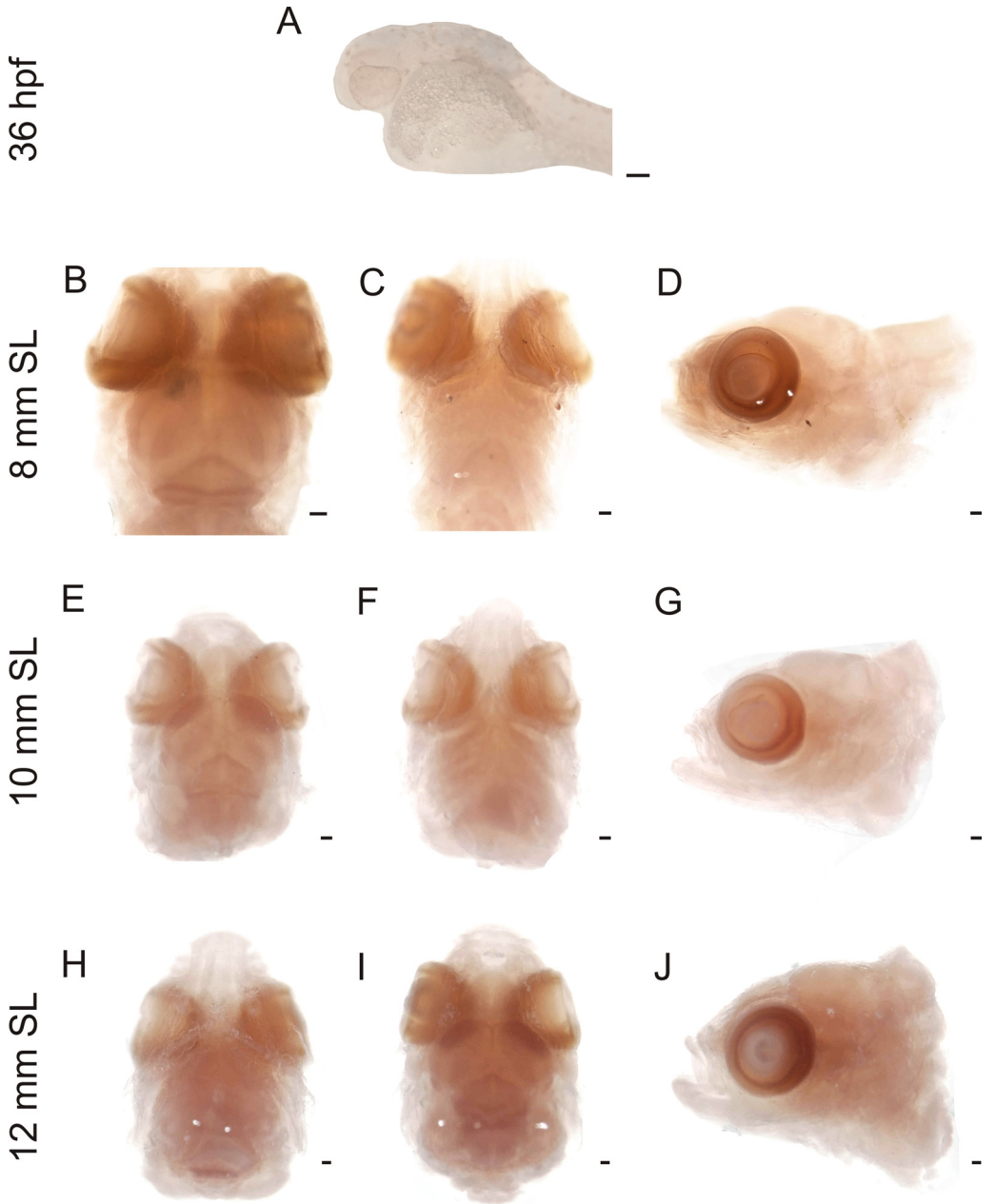

Figure 25. Negative controls for zebrafish *in-situ* hybridization for *efnB2a*. A) 36 hpf zebrafish. B-D) 8 mm SL zebrafish, dorsal, ventral, and lateral views. E-G) 10 mm SL zebrafish, dorsal, ventral, and lateral views. H-J) 12 mm SL zebrafish, dorsal, ventral, and lateral views. All scale bars = 100 μm.

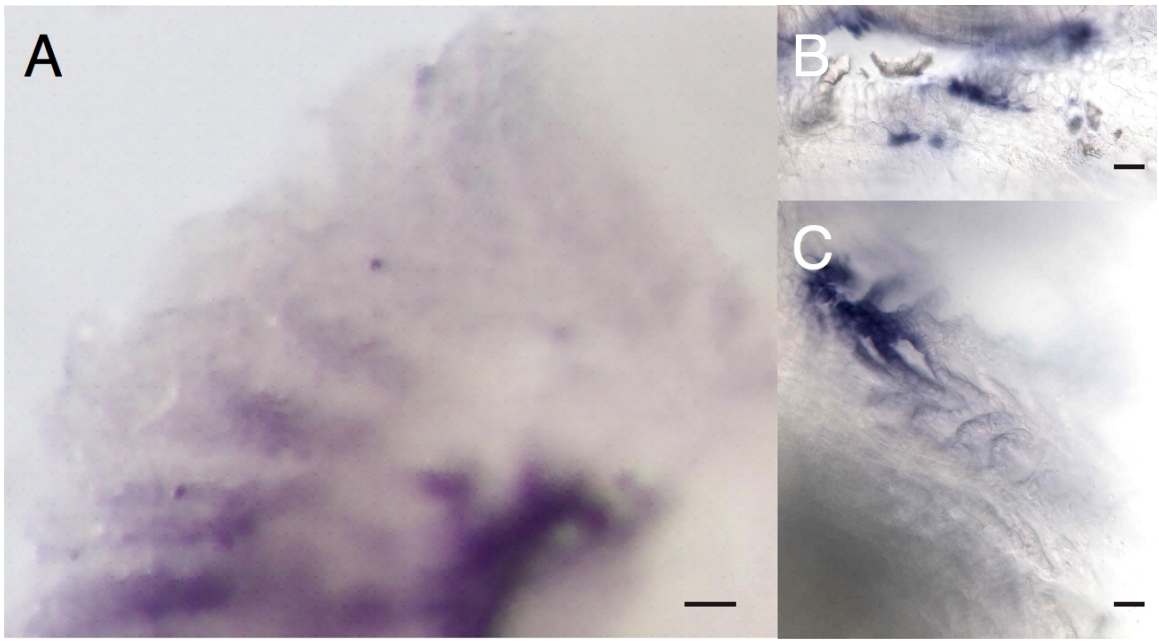

Figure 26. *Efn-b2a* expression in the gills of an 8 mm SL zebrafish. A) Expression is strong in the gill filaments. Scale bar = 100 μm. B, C) Higher magnification shows expression on the cellular level. Scale bars = 10 μm

Figure 27. Dissected brain tissue from an 8 mm SL zebrafish sample tested for presence of *efnB2a* via *in situ* hybridization. No expression is visible. Scale bar = 100 μm.

4.0 DISCUSSION

This thesis elucidates the manner of shape change of the cranial sutures of zebrafish and chicken using outline morphometric analysis. In brief, my results show that, in both models, the sutures form in the same order (interfrontal suture, followed by coronal suture, followed by sagittal suture) and in a similar manner. In addition, this pattern is also similar to that of humans. My results also show sutural asymmetry in both organisms.

Morphometric analysis has previously been employed for analyses of skull shape in several models, including dolphins (Monteiro *et al.,* 2002), turtles (*Claude et al*., 2004), dogs (Onar, 2001), rats (Monteiro *et al.,* 2003), and humans (Benfer, 1975). Jaw shape has been analyzed in this way in rodents (Zelditch, 2008), cichlid fishes (Albertson et al., 2003), Mexican tetra (Hammer, 2014), and zebrafish (Hammer, 2014). The orbital bones of zebrafish (Chang and Franz-Odendaal, 2011; Dufton *et al.*, 2012) and Mexican tetra (Dufton *et al.*, 2012) have also been analyzed using morphometrics. Albertson and Kocher's (2001) study of the oral jaw bones and neurocranium of cichlids used landmark-based morphometrics to analyze shape differences amongst species with different feeding habits. Powder *et al*. (2015) used morphometrics to compare the morphological ontogeny of six species of cichlids. Landmark-based morphometrics have also been used to analyze changes in shape of the maturing human face (Bastir *et al.,* 2006). Outline morphometrics have been used to analyze shape variation in the jaws of Mexican tetra and zebrafish in relation to tooth development and growth of the two different species (Hammer, 2014). Until this time, outline morphometric analysis has not been used to study suture formation and closure in any vertebrate.

4.1 CHICKEN CRANIAL SUTURE ANALYSIS

My thesis illustrates how cranial sutures of the chick embryo approach closure under normal conditions. Until this time, neither a qualitative nor quantitative study of cranial sutures in chicken had been completed.

My observations showed that ossification of the chicken skull roof began at approximately HH stage 38, or roughly 12 dpf. Ossification of the calvaria was not complete by the time of hatching at HH stage 46, or roughly 20 dpf. This is similar to humans, which are born with areas of incomplete ossification of the skull roof where the sutures meet, known as fontanelles. When staging chick embryos, the primary staging characteristics at HH 40 and above are beak and toe lengths. When taken by hand, there is always potential for human error in these measurements. Errors in measurement could lead to slightly inaccurate staging when coupled with the fact that eggs of the same batch do not always develop at a uniform rate due to the timing of their collection by the farmer. I am confident, however, that, because the selected developmental stages were two to three stages apart, any significant errors in measurement are highly unlikely to have an effect on my results.

Of the cranial sutures of the embryonic chick, the first to form was the interfrontal suture, followed by the coronal suture and then the sagittal suture. This is the same order in which human sutures typically close (Kumar *et al*., 2012; Opperman, 2000), and confirms my original hypothesis. In humans, the metopic (interfrontal) suture disappears within the first few years of life, and the coronal and sagittal sutures close slowly, over a period of several years, often beginning in the third decade of life (Kumar *et al*., 2012;

Opperman, 2000). The ventral portion of the human coronal suture fuses first (Kumar *et al.,* 2012), similarly to how the coronal suture of the chicken closes inward, toward the centre of the skull. In humans, the middle third of the sagittal suture is the first to fuse, followed by the anterior third and then the posterior third (Kumar *et al.,* 2012). As the sagittal sutures of the chicken have not completely formed at the time of hatching, we can not be certain if it follows the same pattern as suture closure in humans. Up until hatching, however, it appears that the osteogenic fronts on either side of the sagittal suture come together uniformly, which would be different from the pattern seen in human sagittal suture closure. As this study focuses on the shape changes of the sutural region as the sutures develop, further insight could be gained by analysis of fully formed cranial sutures of chickens post-hatching.

I conducted three analyses of chicken cranial sutures. The first included all data from all three selected developmental stages, the second removed an outlier from the HH 42 group, and the third removed the entire HH 42 group. In the first analysis, we can see that both PCs represented an overall closing of all three sutures, which appears to be indicative of global sutural development (Figure 10). The clustering of the HH 40 samples higher along the PC1 axis and lower along the PC2 axis, primarily in quadrant IV (Figure 11), compared to the HH 45 samples primarily in quadrant II (Figure 11), was unsurprising as the HH 40 samples exhibit less developed calvariae and broader sutural space (Figures 6, 7). The HH 42 samples, according to this analysis, were not significantly different enough from the other two groups with respect to suture development to be a distinct group. The removal of the HH 42 outlier confirmed that HH 45 chick embryos are significantly different from the other two groups, but showed that

the HH 40 and HH 42 samples were not significantly different from one another. In this analysis, the HH 40 and HH 42 samples were generally found to be lower on the PC1 axis than the HH 45 samples (Figure 14), again demonstrating that embryos at these stages consistently displayed broader, less developed sutural space than those at HH 45. Removal of the entire HH 42 group again confirmed the significant difference between the HH 40 and HH 45 groups, and observation of the visualized PC contours and the scatterplot showed that this difference was with respect to overall development of all sutures. In summary, chick embryos at HH 45 had more developed cranial sutures than those at HH 40, but those at HH 42 did not, and a similar fine-tuning occured at both HH 40 and HH 45 that was not significantly different between the two groups.

In all three sets of PCs, the first and most significant component, PC1, represented general suture development by the narrowing of all observed sutures (Figures 10, 13, 16). An interesting finding in both the first analysis and the analysis following removal of the HH 42 outlier was the asymmetry of the interfrontal and coronal sutures represented by PC1. In both analyses, the HH 40 and HH 45 groups were significantly different with respect to this PC, implying that there was an asymmetry in suture formation during the early stages of suture formation that was somewhat corrected by the time an embryo reached HH 45. This asymmetry was not present, however, in the third analysis, which removed the HH 42 samples. This suggested that asymmetrical patterns may appear and disappear between the points in suture development displayed in HH 40 and HH 45 embryos.

In humans, an asymmetrical distortion of the skull is referred to as plagiocephaly, and is often diagnosed at birth (Kane *et al.,* 1996). One potential cause of this is

unicoronal synostosis, or the premature fusion of only the left or right coronal suture (Kane *et al.,* 1996; Lo *et al*., 1996). In normal human development, coronal suture closure shows no significant difference in rate or pattern between the left and right sides (Kumar *et al*., 2012). By learning more about the temporary asymmetry present in developing chicken cranial sutures, it is possible that new findings could be of clinical significance to patients with unicoronal synostosis or other cranial asymmetries, and that the chick embryo would be a useful model to study asymmetry in human sutures.

The chick embryo has its advantages as a model organism in its accessibility for many researchers and well-documented development. However, as the sutures have not completed development by the time of hatching, and post-hatching chicks are far more complicated to study, there is a limit to how useful the chicken embryo can be as a model for human suture development. The differences between human and chicken suture closure, such as the differences in interfrontal suture closure discussed above, are also worth considering. Further analysis of post-hatching chicken skulls may provide further insight into the reliability of the chick embryo as a model for human suture development.

Addtional applications of the chicken model are possible due to the fact that it is a living descendant of the dinosaurs. Of the birds examined by Romanov *et al*. (2014), the chicken genome appears to be the most closely related to the dinosaur avian ancestor. Therefore, analysis of chicken sutures may be a way to study suture development of the chicken's prehistoric ancestors. Analysis of suture closure in archosaur fossils has proven useful in assessment of maturity (Brochu, 1996). Rayfield (2005) used finite-element analysis to investigate potential for stress accommodation by sutures during feeding. A

greater understanding of cranial suture formation in embryonic and juvenile chickens could lend insight into the form and function of cranial sutures in young dinosaurs.

4.2 ZEBRAFISH CRANIAL SUTURE ANALYSIS

4.2.1 GROSS MORPHOLOGY AND SHAPE OF ZEBRAFISH CRANIAL SUTURES

Zebrafish have been established as a model for study of craniofacial development and suture formation (Albertson and Yelick, 2007; Gart *et al*., 2014; Laue *et al*., 2011; LeClair *et al*., 2009; Quarto and Longaker, 2005). Previously, cranial sutures of extant fish species *Polypterus endlicherii* have been studied for quantification of their morphology and function during feeding (Markey and Marshall, 2007). Quarto and Longaker (2005) and Gart *et al*. (2014) have investigated zebrafish sutures to assess the potential of zebrafish as a model for craniosynostosis. This thesis analyzes the manner of zebrafish cranial suture formation under normal conditions.

My morphological observations showed that ossification of the zebrafish skull roof begins at approximately 7 mm or 8 mm SL, and is completed at roughly 12 or 13 mm SL. When staging zebrafish, SL was measured by hand using a ruler, and small discrepancies in measurement could lead to slightly inaccurate staging. However, because the selected stages were separated by one to two developmental stages, I am confident that any minor errors in staging would not have a significant impact on the validity of the results.

The first suture of the zebrafish cranium to develop was the interfrontal suture. Quarto and Longaker (2005) noted that osteogenesis of the zebrafish skull roof first

occurs in the frontal bones. The expanding frontal bones first met to form the interfrontal suture between the eyes, directly dorsal to the cartilaginous epiphyseal bar. Note that this point is the boundary between regions of neural crest origin (the anterior portion of the frontal bones) and paraxial mesoderm origin (the posterior portion of the frontal bones and the parietal bones in their entirety) (Kague *et al*., 2012). I observed that the posterior portion of the suture formed earlier than the anterior portion. In humans, it is common to observe patency of the anterior third of the metopic suture of fetuses or infants (Ajmani *et al*., 1983). Skrzat *et al*. (2004) found that the posterior half of the human metopic suture displays a significantly more complex shape than the anterior half in individuals in which metopic sutures persisted into adulthood. My data therefore suggests that the zebrafish interfrontal suture forms in a similar manner to the closure of the human metopic suture. Note that this is different from the interfrontal suture of the chicken (see above), in which the anterior portion forms before the posterior portion. Also note that zebrafish sutures do not fully close (Quarto and Longaker, 2005). Future research could compare the morphology and shape complexity of the anterior and posterior halves of the zebrafish interfrontal suture, using the epiphyseal bar as the dividing line.

In zebrafish, I also showed that the coronal and sagittal sutures follow the interfrontal suture in order of development, developing more slowly. The coronal suture of the zebrafish skull zipped inward in the same direction as that of the embryonic chick skull; both were similar to what is found in humans (Kumar *et al.,* 2012). Morphological observation showed that fully formed sutures of the zebrafish cranium did not occur as straight lines, but instead occur as sinusoidal, potentially asymmetrical curves (Figure 19). Human sutures do not occur as perfectly straight lines, either, but with small curves

and serrations (Ajmani *et al*., 1983). It is difficult to determine conclusively whether the sagittal suture of the zebrafish cranium forms in the same manner as the human sagittal suture, partially due to the more complex sinusoidal shape in zebrafish.

Where the coronal and sagittal sutures of zebrafish met, a small gap persisted although all sutures appear to be fully developed. In humans, the anterior fontanelle is present at this location during infancy, and the intersection between the coronal and sagittal sutures is known as the bregma after the anterior fontanelle closes. Zebrafish cranial sutures remain patent, unlike human cranial sutures (Morriss-Kay, 2001), possibly allowing for indefinite skull growth. The fontanelle-like region in the zebrafish calvaria possibly functions similarly to the fontanelles of human crania in allowing for further expansion of the skull roof bones to accommodate the growing brain.

Morphometric analysis of zebrafish cranial sutures showed that all three groups (8 mm, 10 mm, and 12 mm SL samples) were significantly different from one another with respect to PC1, which represented overall suture development (Figure 23). This showed that zebrafish at these developmental stages are distinct with respect to the progress of their suture development. The 12 mm SL samples displayed the widest spread with respect to PC2 (Figure 23, quadrants II and III), which represented fine-tuned narrowing of the coronal and sagittal sutures and an asymmetry of the sutural space (Figure 22). This asymmetry may be representative of the sinusoidal shape of zebrafish sutures noted above. Further investigation into the asymmetry of zebrafish cranial sutures may provide insight into factors governing the small curves of human sutures, or may lend insight regarding human cranial asymmetries, as discussed above with respect to asymmetry of chicken cranial sutures.

In summary, zebrafish show great potential as a model for human suture formation. The advantages of the zebrafish model are well known, including straightforward care, fully observable life cycles, large clutch sizes, and a fully sequenced genome. Gross morphology tells us that, despite differences in suture patency, zebrafish cranial sutures bear notable similarity to those of humans. By gaining knowledge of zebrafish suture formation under normal conditions, there is potential to better appreciate what may change when things go wrong. Zebrafish are an exciting model as we strive to better understand cranial sutures and the disorders that affect them.

4.2.2 EPHRIN-B2A IN THE ZEBRAFISH SKULL

The latest stage in which *efnB2a* has been observed in zebrafish until this point has been at 60 hpf, at which point expression has been found in the dorsal aorta (Kawahara, 2008), the dorsal retina (Pi-Roig *et al*., 2014) and the optic tectum (Aizawa, 2007). Expression of *efnB2a* has not, until now, been explored in juvenile zebrafish.

The 36 hpf zebrafish used as a positive control in this study showed *efnB2a* expression in the developing telencephalon, eye, and pharyngeal region. Chan *et al*. (2001) had also observed *efnB2a* in these regions, in addition to the optic tectum, which was not observed in my samples. It is possible that either Chan *et al*. or I misidentified the brain regions where expression is observed. It is also possible, as I used a probe made in our lab, that there are different splice forms of *efnB2a* and the form present in the optic tectum was not compatible with the probe that I used.

Furthermore, I could not detect *efnB2* expression in the cranial sutures of zebrafish, as had previously been observed in embryonic mice (Benson *et al*., 2012).

Benson *et al*. (2012) found that *efnB2* was expressed within sutures and sites of bone injury in embryonic and neonatal mice, respectively. No *efnB2a* expression was seen in the sutures or skull roof of zebrafish at 8 mm, 10 mm, and 12 mm SL (Figure 24). *EfnB2a* was found solely in the gill region of the 8 mm SL samples (Figure 24C), and was not clearly expressed anywhere in the 10 mm and 12 mm SL samples. (Figure 24E-J). It is important to note that Benson *et al*. (2012) observed *efnB2* in developing osteogenic fronts in embryonic mice, whereas I studied post-embryonic zebrafish.

There are several explanations as to why detection was possible in the gills and not the skull roof. The probe was able to penetrate the gill tissue and detect *efnB2a* at the cellular level, but it is possible that the layer of skin over the skull roof prevented the probe's penetration into the skull roof and the sutural space. The skin of juvenile fish is tough compared to that of embryonic mice. This could potentially be remedied by optimization of the permeabilization step in terms of length and proteinase-K concentration. It is also possible that a false positive could have occurred in the gills if excess probe was not properly washed away in the subsequent washing steps. Increased washing steps could decrease the chances of non-specific binding. Another run of *in situ* hybridization should be conducted to ensure penetration of the probe. This could be done by using another probe at the same stages and observing whether it penetrates the same tissues.

It is important to recall that zebrafish have two isoforms of *efnB2*, known as *efnB2a* and *efnB2b*, as a consequence of a teleost genome duplication event (Chan *et al*., 2001, Coulthard *et al*., 2002). The decision to test for *efnB2a* was made because *ephrin-B2a* is more closely related to the mammalian *efnB2* than is *efnB2b*. Furthermore, *efnB2a*

was shown to be present in the zebrafish embryo as late as 60 hpf (Aizawa, 2007; Kawahara, 2008; Pi-Roig *et al*., 2014), whereas *efnB2b* has been observed to be most active during gastrulation, and has not been observed past 36 hpf (Chan *et al*., 2001). A future direction for research should be to analyze *efnB2b* expression in the zebrafish skull roof, before concluding that the ephrin expression observed by Benson *et al*. (2012) in mice is entirely absent in zebrafish.

Another class of receptor tyrosine kinase with which ephrin ligands have been shown to interact is the FGFR family (Wilkinson, 2001). FGF signaling is involved in regulation of suture development by the dura mater (Ogle *et al*., 2004). Cross-talk between ephrin ligands and FGFRs has been observed multiple times (Arvanitis and Davy, 2008). Some studies report an antagonistic relationship between ephrins and FGFRs, an example of which was reported by Jones *et al.* (1998). *Xenopus* embryos in the two-cell stage displayed blastomere dissociation after ephrin-B1 injections, but this phenotype could be rescued by FGFs (Jones *et al*., 1998). Other studies report an agonistic relationship between ephrins and FGFs, an example of which is the co-stimulation of mitogen-activated protein kinase (MAPK) (Yokote *et al.* 2005), likely by interactions between Eph-A4 and FGFRs (Park *et al.,* 2005). Gain-of-function mutations of FGFRs are the cause of approximately 20% of cases of craniosynostosis (Eswarakumar *et al.,* 2006). If *efnB2b* is found to be present in the cranial sutures, investigation into the distribution of *efnB2b* and FGFRs in the zebrafish cranium may provide insight into whether their presence mirrors that displayed in mammals.

4.3 POTENTIAL ERROR IN MORPHOMETRIC ANALYSIS

Consistency of sample orientation is essential for morphometric analysis, as the images represent the samples and are used to trace the shapes that will later be analyzed. Despite efforts to be consistent in the capture of these images, discrepancies in orientation could potentially contribute to the observed asymmetry in both models. Human error is also a possible factor when tracing the sutural space. The larger the difference between the shapes, the less likely it is that subtle inaccuracies would influence the results. In my zebrafish analysis, in which all three size groups examined are significantly different from one another, it is unlikely that any small human errors would be significant. In the chick embryo analysis, in which the HH 42 samples are not significantly different from the other two groups, it is more possible that differences in tracing the HH 42 samples may have made them slightly more similar to one group or the other. However, it is unlikely that errors would be made in only one sample group and not all. Nevertheless, this could potentially be reduced by having multiple people trace the shapes and using the averages between the different attempts as the final trace versions used in the morphometric analysis.

4.4 CONCLUSIONS AND FUTURE DIRECTIONS

In both zebrafish and chicken, the cranial sutures approach one another in the same order and in a similar manner, with the interfrontal suture forming most quickly, followed by the coronal sutures and then the sagittal suture. The interfrontal suture formation pattern of zebrafish is more similar to what is found in humans than is that of chicken. This supports my hypothesis that zebrafish and chicken are similar to humans in

the manner of their suture closure, though zebrafish are more similar. Morphometric analysis of suture development allowed for the differences between the selected developmental stages to be analyzed statistically, shedding light on which stages are significantly different from another in terms of suture formation. The major shape variation is suture closure over time, and this variation is statistically significant amongst the different stages, supporting my hypothesis that there is a significant difference in suture development between developmental stages. Investigation into the temporary asymmetry observed in chicken suture development between HH 40 and HH 45 may be useful as a model to study human cranial asymmetries. Similarly, the sinusoidal shape of zebrafish cranial sutures bears resemblance to irregularities in those of humans, and may be useful in attempting to understand these irregularities.

I hypothesized that *efnB2a* would be present in zebrafish cranial sutures as it is in mice (Benson *et al*., 2012). The expression of *ephrin-B2a* in the zebrafish skull did not reproduce the results found by Benson *et al*. (2012) in their observations of the mouse skull, as *ephrin-B2a* was not found in zebrafish cranial sutures. Future research should investigate expression of *ephrin-B2b* and the potential for FGFR activity in zebrafish calvariae, with hopes of learning more of how zebrafish can be utilized to better comprehend skull roof disorders such as craniosynostosis.

In my opinion, zebrafish is superior to chicken as a model organism for the study of cranial suture development relevant to humans. This is because zebrafish are more similar to humans in the manner of their suture formation, and their suture development can be observed from beginning to end in the lab, unlike in the chick embryo, in which the sutures are not fully formed at the time of hatching. My analysis of suture

development agrees with previous reports that zebrafish is a useful model for cranial suture development and craniosynostosis (Gart *et al*., 2014; Quarto and Longaker, 2005). The similarity between the zebrafish interfrontal suture and the human metopic suture make the zebrafish a particularly appropriate model for the study of metopic synostosis. It should be noted, however, that the asymmetry observed in chicken suture development makes the chick embryo as a potentially promising model for the study of unicoronal synostosis, specifically.

Hopefully this research has helped to paint a larger picture that can be used by future researchers to further the field of craniofacial development. By analyzing suture formation in these two organisms using a novel method, I have obtained a greater appreciation for how zebrafish and chicken can be utilized to understand the skull roof and disorders that affect it.

REFERENCES

Aizawa, H., Hitoshi, O., and Tomomi, S., 2007. Genetic single-cell mosaic analysis implicates ephrinB2 reverse signaling in projections from the posterior tectum to the hindbrain in zebrafish. Journal of Neuroscience. 27(20): 5271-5279.

Ajmani, M.L., Mittal, R.K., and Jain, S.P., 1983. Incidence of the metopic suture in adult Nigerian skulls. Journal of Anatomy. 137(1): 177-183.

Albertson, R.C., Streelman, J.T., and Kocher, T.D., 2003. Genetic basis of adaptive shape differences in the cichlid head. Journal of Heredity. 94(4): 291-301.

Aleck, K., 2004. Craniosynostosis syndromes in the genomic era. Seminars in Pediatric Neurology. 11(4): 256-261.

Arvanitis, D. and Davy, A., 2008. Eph/ephrin signaling: networks. Genes & Development. 22: 416-429.

Baker, C.V.H., Bronner-Fraser, M., Le Douarin, N.M., and Teillet, M.A., 1997. Early- and late-migrating cranial neural crest cell populations have equivalent developmental potential in vivo. Development. 124: 3077-3087.

Balling, R., Mutter, G., Gruss, P., and Kessel, M., 1989. Craniofacial abnormalities induced by ectopic expression of the homeobox gene *Hox-1.1* in transgenic mice. Cell. 58(2): 337-347.

Bastir, M., Rosas, A., and O'Higgins, P., 2006. Craniofacial levels and the morphological maturation of the human skull. Journal of Anatomy. 209(5): 637-654.

Benson, M.D., Opperman, L.A., Westerlund, J., Fernandez, C.R., San Miguel, S., Henkemeyer, M., and Chenaux, G., 2012. Ephrin-B stimulation of calvarial bone formation. Developmental Dynamics. 241(12): 1901-1910.

Bier, W. and McGinnis, W., 2004. Model Organisms in the Study of Development and Disease. Inborn Errors of Development. Oxford University Press. New York, New York, 10016, USA.

Brochu, C.A., 1996. Closure of neurocentral sutures during crocodilian ontogeny: Implications for maturity assessment in fossil archosaurs. Journal of Vertebrate Paleontology. 16(1): 49-62.

Chan, J., Mably, J.D., Serluca, F.C., Chen, J.N., Goldstein, N.B., Thomas, M.C., Cleary, J.A., Brennan, C., Fishman, M.C., and Roberts, T.M., 2001. Morphogenesis of prechordal plate and notochord requires intact Eph/ephrin B signaling. Developmental Biology. 234(2): 470-482.

Chang, C.T., and Franz-Odendaal, T.A., 2014. Perturbing the developing skull: using laser ablation to investigate the robustness of the infraorbital bones in zebrafish (*Danio rerio*). BMC Developmental Biology. 14: 44.

Chong, L.D., Park, E.K., Latimer, E., Friesel, R., and Daar, I.O., 2000. Fibroblast growth factor receptor-mediated rescue of x-ephrin-B1-induced cell dissociation in *Xenopus* embryos. Molecular Cellular Biology. 20:724-734.

Claude, J., Pritchard, P.C.H., Tong, H., Paradis, E., and Auffray, J.C., 2004. Ecological correlates and evolutionary divergence in the skull of turtles: a geometric morphometric assessment. Systematic Biology. 53(6): 933-948.

Coulthard, M.G., Duffy, S., Down, M., Evans, B., Power, M., Smith, F., Stylianou, C., Kleikamp, S., Oates, A., Lackman, M., Burns, G.F., and Boyd, A.W., 2002. The role of the Eph-ephrin signalling system in the regulation of developmental patterning. International Journal of Developmental Biology. 46: 375-384.

Creuzet, S., Schuler, B., Couly, G., and Le Douarin, N.M., 2004. Reciprocal relationships between FGF8 and neural crest cells in facial and forebrain development. Proceedings of the National Academy of Sciences of the United States of America. 101(14): 4843-4847.

Diercke, K., Kohl, A., Lux, C.J., and Erber, R., 2011. Strain-dependent up-regulation of ephrin-B2 protein in periodontal ligament fibroblasts contributes to osteogenesis during tooth movement. Journal of Biological Chemistry. 286: 37651-37664.

Dufton, M., Hall, B.K., and Franz-Odendaal, T.A., 2012. Early lens ablation causes dramatic long-term effects on the shape of bones in the craniofacial skeleton of *Astyanax mexicanus*. PLoS One. 7(11): e50308. DOI: 10.1371/journal.pone.0050308.

Eames, B.F., Sharpe, P.T., and Helms, J.A., 2004. Hierarchy revealed in the speciation of three skeletal fates by Sox9 and Runx2. Developmental Biology. 274(1): 188-200.

Edsall, S.C., 2011. An assessment of the long-term effects of simulated microgravity on cranial neural crest cells in zebrafish embryos with a focus on the adult skeleton. PLoS One. 9(2): e89296. DOI: <10.1371/journal.pone.0089296>

Edwards, C.M., and Mundy, G.R., 2008. Eph receptors and ephrin signaling pathways: a role in bone homeostasis. International Journal of Medical Sciences. 5(5) 263-272.

Eswarakumar, V.P., Özcan, F., Lew, E.D., Baw, J.H., Tomé, F., Booth, C.J., Adams, D.J., Lax, I., and Schlessinger, J., 2006. Attenuation of signaling pathways stimulated by pathologically activated FGF-receptor 2 mutants prevents craniosynostosis. Proceedings of the National Academy of Sciences of the United States of America. 103(49): 18603-18608.

Franz-Odendaal, T.A., 2011. Induction and patterning of intramembranous bone. Frontiers in Bioscience (Landmark Ed). 1(16): 2734-2746.

Franz-Odendaal, T.A., and Hall, B.K., 2007. Developmental and morphological variation in the teleost craniofacial skeleton reveals an unusual mode of ossification. Journal of Experimental Zoology. 308: 709-721.

Franz-Odendaal, T.A., Hall, B.K., and Witten, P.E., 2006. Buried alive: how osteoblasts become osteocytes. Developmental Dynamics. 235(1): 176-190.

Gart, M.S., Shoela, R.A., Tomaszewski, J.P., Favelevic, T.B.S., Topczewka, J.M., and Gosain, A.K. 2014. Zebrafish: advancing our understanding of the genetic basis of craniosynostosis. Plastic & Reconstructive Surgery. 134(4S-1): 2-3.

Gilbert, S.F., 2000. Developmental Biology, 6th Edition. Sinauer Associates. Sunderland, MA, USA.

Greenwald, J.A., Mehrara, B.J., Spector, J.A., Warren, S.M., Crisera, F.E., Fagenholz, P.J., Bouletreau, P.J., and Longaker, M.T., 2000. Regional differentiation of cranial suture-associated dura mater in vivo and in vitro: implications for suture fusion and patency. Journal of Bone and Mineral Research. 15(12): 2413-2430.

Gross, J.B., and Hanken, J., 2008. Review of fate-mapping studies of osteogenic cranial neural crest in vertebrates. Developmental Biology. 317(2): 389-400.

Grova, M., Lo, D.D., Montoro, D., Hyun, J.S., Chung, M.T., Wan, D.C., and Longaker, M.T., 2012. Animal models of cranial suture biology. Journal of Craniofacial Surgery. 23(701): 1954-1958.

Hall, B.K., 1986. The role of movement and tissue interactions in the development and growth of bone and secondary cartilage in the clavicle of the embryonic chick. Journal of Embryology exp. Morphology. 93: 133-152.

Hall, B.K., (Ed.) 2005. Bones and Cartilage: Developmental and Evolutionary Skeletal Biology. Elsevier Academic Press. San Diego, CA, 92101-4495, USA.

Hamburger, V., and Hamilton, H.L., 1951. A series of normal stages in the development of the chick embryo. Journal of Morphology. 88(1): 49-92.

Hammer, C., 2014. A comparative shape analysis of the oral jaws of the Mexican tetra (*Astyanax mexicanus*) and the zebrafish (*Danio rerio*) during development. Submitted to the Biology Department in partial fulfillment of the Bachelor of Sciences (Honours) degree at Mount Saint Vincent University. Halifax, NS.

Ishii, M., Merrill, A.E., Chan, Y.S., Gitelman, I., Rice, D.P.C., Sucov, H.M., and Maxson, R.E., 2003. Msx2 and Twist cooperatively control the development of the neural crest-derived skeletogenic mesenchyme of the murine skull vault. Development. 130: 6131-6142.

Iwata, H., and Ukai, Y., 2002. SHAPE: a computer program package for quantitative evaluation of biological shapes based on elliptic fourier descriptors. The Journal of Heredity. 93(5): 374-385.

Jiang, X., Iseki, S., Maxson, R.E., Sucov, H.M., and Morriss-Kay, G.M., 2002. Tissue origins and interactions in the mammalian skull vault. Developmental Biology. 241(1): 106-116.

Jones, T.L., Chong, L.D., Kim, J., Xu, R., Kung, H., and Daar, I.O., 1998. Loss of cell adhesion in *Xenopus* laevis embryos mediated by the cytoplasmic domain of XLerk, an erythropoietin-producing hepatocellular ligand. Proceedings of the National Academy of Sciences of the United States of America. 95(2): 576-581.

Kague, E., Gallagher, M., Burke, S., Parsons, M., Franz-Odendaal, T., and Fisher, S., 2012. Skeletogenic fate of zebrafish cranial and trunk neural crest. Public Library of Science. 7(11): e47394. DOI: <10.1371/journal.pone.0047394>

Kalo, M.S., Yu, H.H., Pasquale, E.B., 2001. *In vivo* tyrosine phosphorylation sites of activated ephrin-B1 and EphB2 from neural tissue. Journal of Biological Chemistry. 276: 38940-38948.

Kane, A.A., Lo, L.J., Vannier, M.W. and Marsh, J.L., 1996. Mandibular dysmorphology in unicoronal synostosis and plagiocephaly without synostosis. Cleft Palate Craniofacial Journal. 33(5): 418-423.

Kawahara, A., 2008. Meis1 regulates the development of endothelial cells in zebrafish. Biochemical and Biophysical Research Communications. 374(4): 647-652.

Kim, H.J., Rice, D.P.C., Kettunen, P.J., and Thesleff, I., 1998. FGF-, BMP- and Shh-mediated signalling pathways in the regulation of cranial suture morphogenesis and calvarial bone development. Development. 125: 1241-1251.

Kitamura, K., Takiguchi-Hayashi, K., Sezaki, M., Yamamoto, H., and Takeuchi, T., 1992. Avian neural crest cells express a melanogenic trait during early migration from the neural tube: observations with the new monoclonal antibody, "MEBL-1." Development. 114: 367-378.

Kumar, A.G.V., Agarwali, S.S., Bastia, B.K., Shivaramu M.G., and Honnungar, R.S., 2012. Fusion of skull vault sutures in relation to age - a cross sectional postmortem study done in 3rd, 4th & 5th decades of life. Journal of Forensic Research. 3:10

Laue, K., Pogoda, H., Daniel, P.B., van Haeringen, A., Alanay, Y., von Ameln, S., Rachwalski, M., Morgan, T., Gray, M.J., Breuning, M.H., Sawyer, G.M., Sutherland-Smith, A.J., Nikkels, P.G., Kubisch, C., Bloch, W., Wollnick, B., Hammerschmidt, M., and Robertson, S.P., 2011. Craniosynostosis and multiple skeletal anomalies in humans and zebrafish result from a defect in the localized degradation of retinoic acid. American Journal of Human Genetics. 89(5): 595-606.

LeClair, E.E., Mui, S.R., Huang, A., Topczewska, J.M., nd Topczewska, J., 2009. Craniofacial skeletal defects of adult zebrafish *Glypican 4 (knypek)* mutants. Developmental Dynamics. 238(10): 2550-2563.

Le Douarin, N., and Kalcheim, C., (Eds.) 1999. The Neural Crest, 2nd Edition. Cambridge University Press. Cambridge.

Le Lièvre, C.S., 1978. Participation of neural crest-derived cells in the genesis of the skull in birds. Journal of Embryology. 47: 17-37.

Levine, J.P., Bradley, J.P., Roth, D.A., McCarthy, J.G., and Longaker, M.T., 1998. Studies in cranial suture biology: regional dura mater determines overlying suture biology. Plastic Reconstructive Surgery. 101(6): 1441-1447.

Liu, Y., Tang, Z., Kundo, R.K., Wu, L., Luo, W., Zhu, D., Sangiorgi, F., Snead, M.L., and Maxson, R.E. Jr., 1999. Msx2 gene dosage influences the number of proliferative osteogenic cells in growth centers of the developing murine skull: a possible mechanism for msx2-mediated craniosynostosis in humans. Developmental Biology. 205(2): 260-274.

Lo, L.J., Marsh, J.L., Pilgram, T.K., and Vannier, M.W., 1996. Plagiocephaly: differential diagnosis based on endocranial morphology. Plastic and Reconstructive Surgery. 97(2): 282-291.

Markey, M.J., and Marshall, C.R., 2007. Linking form and function of the fibrous joints in the skull: a new quantification scheme for cranial sutures using extant fish *Polypterus endlicherii*. Journal of Morphology. 268: 89-102.

Menzel, P., Vlancia, F., Godement, P., Dodelet, V.C., and Pasquale, E.B., 2001. Ephrin-A6, a new ligand for EphA receptors in the developing visual system. Developmental Biology. 230(1): 74-88.

Monteiro, L.R., Duarte, L.C., and dos'Reis, S.F., 2003. Environmental correlates of geographical variation in skull and mandible shape of the punaré rat *Thrichomys apereoides* (Rodentia: Echimyidae). Journal of Zoology. 261(1): 47-57.

Monteiro-Filho, E.L.A., Monteiro, L.R., and Furtado de Reis, S., 2002. Skull shape and size divergence in dolphins of the genus *Sotalia*: a tridimensional morphometric analysis. Mammalogy. 83(1): 125-134.

Mooney, M.P., Burrows, A.M., Smith, T.D., Losken, H.W., Opperman, L.A., Dechant, J., Kreithan, A.M., Kapucu, R., Cooper, G.M., Ogle, R.C., and Siegel, M.I., 2001. Correction of coronal suture synostosis using suture and dura mater allografts in rabbits with familial craniosynostosis. Cleft Palate Craniofacial Journal. 38(3): 206-225.

Mooney, M.P., Losken, H.W,. Moursi, A.M., Shand, J.M., Cooper, G.M., Curry, C., Ho, L., Burrows, A.M., Stelnicki, E.J., Losee, J.E., Opperman, L.A., and Siegal, M.I., 2007. Postoperative anti-Tgf-beta2 antibody therapy improves intracranial volume and craniofacial growth in craniosynostotic rabbits. Journal of Craniofacial Surgery. 18(2): 336-346.

Morriss-Kay, G.M., 2001. Derivation of the mammalian skull vault. Journal of Anatomy. 199(1-2): 143-151.

Newberry, E.P., Boudreaux, J.M., and Towler, D.A., 1997. Stimulus-selective inhibition of rat osteocalcin promoter induction and protein-DNA interactions by the homeodomain repressor msx2. Journal of Biological Chemistry. 272: 29607-29613.

Noden, D.M., 1983. The role of neural crest in patterning of avian cranial skeletal, connective, and muscle tissues. Developmental Biology. 96(1): 144-165.

Noden, D.M., 1984. The use of chimeras in analysis of craniofacial development. N.M. Le Douarin, A. McLaren (Eds.), Chimeras in Developmental Biology. Academic Press. London. 241-280.

Onar, V., 2001. A morphometric study on the skull of the German shepherd dog (Alaskan). Anatomia Histologia Embryologia. 28(4): 253-256.

Opperman, L.A., 2000. Cranial sutures as intramembranous bone growth sites. Developmental Dynamics. 219(4): 472-485.

Parichy, D.M., Elizondo, M.R., Mills, M.G., Gordon, T.N., and Engeszer, R.E., 2009. Normal table of postembryonic zebrafish development: Staging by externally visible anatomy of the living fish. Developmental Dynamics. 238(12): 2975-3015.

Park, E.K., Warner, N., Bong, Y., Stapleton, D., Mueda, R., Pawson, T., and Daar, I.O., 2005. Ectopic EphA4 receptor induces posterior protrusions vis FGF signaling in *Zenopus* embryos. Molecular Biology of the Cell. 15(4): 1647-1655.

Parisi, M.A., 2002. Hirschsprung Disease Overview. GeneReviews. Access date: 22 October 2013. Available online: <http://www.ncbi.nlm.nih.gov/books/NBK1439/>

Pi-Roig, A., Martin-Blanco, E., and Minguillon, C., 2014. Distinct tissue-specific requirements for the zebrafish tbx5 genes during heart, retina and pectoral fin development. Open Biology. DOI: < 10.1098/rsob.140014>

Powder, K.E., Milch, K., Asselin, G., and Albertson, R.C., 2015. Constraint and diversification of developmental trajectories in cichlid facial morphologies**.** EvoDevo. 6(25). DOI <10.1186/s13227-015-0020-8>

Quarto, N., and Longaker, M.T., 2005. The zebrafish (*Danio rerio*): a model system for cranial suture patterning. Cells Tissues Organs. 181(2): 109-118.

Rayfield, E.J., 2005. Using finite-element analysis to investigate suture morphology. The Anatomical Record. 283A: 349-365.

Rice, D.P.C., Rice, R., and Thesleff, I., 2003. Molecular Mechanisms in calvarial bone and suture development, and their relation to craniosynostosis. The European Journal of Orthodontics. 25(2): 139-148.

Robin, N.H., Falk, M.J., and Halderman-Englert, C.R., 1998. FGFR-related craniosynostosis syndromes. GeneReviews. University of Washington, Seattle. Seattle, WA, USA.

Romanov, M.N., Farré, M., Lithgow, P.E., Fowler, K.E., Skinner, B.M., O'Connor, R., Foneska, G., Backström, N., Matsuda, Y., Nishida, C., Houde, P., Jarvis, E.D., Ellegren, H., Burt, D.W., Larkin, D.M., and Griffin, D.K., 2014. Reconstruction of gross avian genome structure, organization and evolution suggests that the chicken lineage most closely resembles the dinosaur avian ancestor. BMC Genomics. 15:1060.

Roth, D.A., Bradley, J.P., Levine, J.P., McMullen, H.F., McCarthy, J.G., and Longaker, M.T., 1996. Studies in cranial suture biology: part II. Role of the dura in cranial suture fusion. Plastic Reconstructive Surgery. 94(4): 693-699.

Sahar, D.E., Longaker, M.T., and Quarto, N., 2005. *Sox9* neural crest determinant gene controls patterning and closure of the posterior frontal cranial suture. Developmental Biology. 280(2): 344-361.

Sanatagi, F. and Rijli, F.M., 2003. Cranial neural crest and the building of the vertebrate head. Nature Reviews Neuroscience. 4: 806-818.

Schilling, T.F., and Kimmel, C.B., 1994. Segment and cell type lineage restrictions during pharyngeal arch development in the zebrafish embryo. Development. 120: 483-494.

Serbedzija, G.N., Bronner-Fraser, M., and Fraser, S.E., 1992. Vital dye analysis of cranial neural crest cell migration in the mouse embryo. Development 116: 297-307.

Skrzat, J., Walocha, J., and Zawiliński, J., 2004. A note on the morphology of the metopic suture in the human skull. Folia Morphologica. 63(4): 481-484.

Smith, A., Robinson, V., Patel, K., and Wilkinson, D.G., 1997. The EphA4 and EphB1 receptor tyrosine kinases and ephrin-B2 ligand regulate targeted migration of branchial neural crest cells. Current Biology. 7(8): 561-570.

Stamper, B.D., Park, S.S., Beyer, R.P., Bammler, T.K., Farin, F.M., Mecham, B., and Cunningham, M.L., 2011. Differential expression of extracellular matrix-mediated pathways in single-suture craniosynostosis. PLoS ONE 6(1): e26557. doi:10.1371/journal.pone.0026557

Stern, C.D., 2005. The chick: a great model system becomes even greater. Developmental Cell. 8(1): 9-17.

Stolfi, A., Wagner, E., Taliaferro, J.M., Chou, S., and Levine, M., 2011. Neural tube patterning by Ephrin, FGF and Notch signaling relays. Development. 138-5429-5439.

Walker, M.B., and Kimmel, C.B., 2007. A two-color acid-free cartilage and bone stain for zebrafish larvae. Biotechnic & Histochemistry. 82(1): 23-28.

Wieland, I., Jacubiczka, S., Muschke, P., Cohen, M., Thile, H., Gerlach, K.L., Adams, R.H., and Wiecker, P., 2004. Mutations of the ephrin-B1 gene cause craniofrontonasal syndrome. American Journal of Human Genetics. 74: 1209-1215.

Wilkie, A.O.M, and Morriss-Kay, G.M., 2001. Genetics of craniofacial development and malformation. Nature Reviews Genetics. 2:458-468.

Wilkinson, D.G., 2001. Multiple roles of eph receptors and ephrins in neural development. Nature Reviews Neuroscience. 2: 155-164.

Witten, P.E., Hansen, A., and Hall, B.K., 2001. Features of mono- and multinucleated bone resorbing cells of the zebrafish *Danio rerio* and their contribution to skeletal development, remodeling, and growth. Journal of Morphology. 250: 197-207.

Yokote, H., Fujita, K., Jing, X., Sawada, T., Liang, S., Yao, L., Yan, X., Zhang, Y., Schlessinger, J, and Sakagushi, K,. 2005. Trans-activation of EphA4 and FGF receptors mediated by direct interactions between their cytoplasmic domains. Proceedings of the National Academy of Sciences of the United States of America. 102(52): 18866-18871.

Zelditch, M.L., Wood, A.R., Bonnett, R.M., and Swiderski, D.L., 2008. Modularity of the rodent mandible: Integrating bones, muscles, and teeth. Evolution and Development. 10(6): 756-768.

Zhao, C., Irie, N., Takada, Y., Shimoda, K., Miyamoto, T., Nishiwaki, T., Suda, T., and Matsuo, K., 2006. Bidirectional ephrinB2-EphB4 signaling controls bone homeostasis. Cell Metabolism. 4(2): 111-121.

APPENDICES

APPENDIX A – SUMMARY OF SAMPLES

Table A1. Zebrafish samples and protocol used for Western analysis

Number of Zebrafish	Date of Birth	Age (dpf)	Fixation	Protocol
6	26-Nov-13	20	N/A	Western analysis
8	17-Jan-14	42	N/A	Western analysis
5	24-Jan-14	42	N/A	Western analysis
2	20-Feb-14	75	N/A	Western analysis
1	28-Feb-14	67	N/A	Western analysis
3	05-Mar-14	62	N/A	Western analysis
15	13-Mar-14	54	N/A	Western analysis
14	03-Apr-14	33	N/A	Western analysis
21	03-Apr-14	74	N/A	Western analysis
9	25-Apr-14	52	N/A	Western analysis
27	23-Apr-14	73	N/A	Western analysis

Table A2. Zebrafish samples and staining protocol to determine optimal stages for analysis

Number of Zebrafish	Date of Birth	Age (dpf)	Fixation	Protocol
2	26-Nov-13	20	10% NBF	Acid-free double stain
1	17-Jan-14	42	10% NBF	Acid-free double stain
1	20-Feb-14	28	10% NBF	Acid-free double stain
1	20-Feb-14	35	10% NBF	Acid-free double stain
1	20-Feb-14	35	10% NBF	Acid-free double stain
1	20-Feb-14	35	10% NBF	Acid-free double stain
7	28-Feb-14	45	10% NBF	Acid-free double stain
1	05-Mar-14	14	10% NBF	Acid-free double stain
1	13-Mar-14	7	10% NBF	Acid-free double stain

Table A3. Zebrafish samples and protocol used for morphometric analyses

Stage	Date of Birth	Age (dpf)	Fixation	Protocol
8 mm SL	9-Sep-14	65	4% PFA	Bone stain
n = 8	9-Sep14	65	4% PFA	Bone stain
	18-Sep-14	49	4% PFA	Bone stain
	18-Sep-14	49	4% PFA	Bone stain
	30-Oct-14	33	4% PFA	Bone stain
	30-Oct-14	33	4% PFA	Bone stain
	30-Oct-14	33	4% PFA	Bone stain
	25-Nov-14	42	4% PFA	Bone stain
10 mm SL	13-Mar-14	75	4% PFA	Bone stain
n = 8	13-Mar-14	75	4% PFA	Bone stain
	13-Mar-14	75	4% PFA	Bone stain
	8-Jul-14	70	4% PFA	Bone stain
	8-Jul-14	70	4% PFA	Bone stain
	8-Jul-14	70	4% PFA	Bone stain
	9-Sep-14	65	4% PFA	Bone stain
	18-Sep-14	49	4% PFA	Bone stain
12 mm SL	8-Jul-14	70	4% PFA	Bone stain
n = 8	8-Jul-14	70	4% PFA	Bone stain
	8-Jul-14	70	4% PFA	Bone stain
	8-Jul-14	70	4% PFA	Bone stain
	18-Sep-14	49	4% PFA	Bone stain
	18-Sep-14	49	4% PFA	Bone stain
	18-Sep-14	49	4% PFA	Bone stain
	30-Oct-14	33	4% PFA	Bone stain

Table A4. Zebrafish samples and protocol used for paraffin immunohistochemistry

Stage (mm SL)	Date of Birth	Age (dpf)	Fixation	Protocol
9	3-Apr-14	74	4% PFA	Paraffin IHC
9	3-Apr-14	74	4% PFA	Paraffin IHC
8	9-Sep-14	49	4% PFA	Paraffin IHC
10	9-Sep-14	49	4% PFA	Paraffin IHC
12	9-Sep-14	65	4% PFA	Paraffin IHC

Table A5. Zebrafish samples and protocol used for in situ hybridization

Stage	Date of Birth	Age (dpf)	Fixation	Protocol
8 mm SL	30-Jan-15	40	4% PFA (DepC)	ISH
n = 7	30-Jan-15	40	4% PFA (DepC)	ISH
	30-Jan-15	40	4% PFA (DepC)	ISH
	30-Jan-15	40	4% PFA (DepC)	ISH
	30-Jan-15	40	4% PFA (DepC)	ISH
	13-Feb-15	34	4% PFA (DepC)	ISH
	13-Feb-15	34	4% PFA (DepC)	ISH
10 mm SL	30-Jan-15	40	4% PFA (DepC)	ISH
n = 6	30-Jan-15	40	4% PFA (DepC)	ISH
	30-Jan-15	40	4% PFA (DepC)	ISH
	30-Jan-15	48	4% PFA (DepC)	ISH
	30-Jan-15	48	4% PFA (DepC)	ISH
	30-Jan-15	48	4% PFA (DepC)	ISH
12 mm SL	30-Jan-15	40	4% PFA (DepC)	ISH
n = 7	30-Jan-15	40	4% PFA (DepC)	ISH
	30-Jan-15	48	4% PFA (DepC)	ISH
	30-Jan-15	48	4% PFA (DepC)	ISH
	30-Jan-15	48	4% PFA (DepC)	ISH
	30-Jan-15	48	4% PFA (DepC)	ISH
	30-Jan-15	48	4% PFA (DepC)	ISH

APPENDIX B – RECIPES FOR SAMPLE FIXATION

1x PBS

- 8 g NaCl
- 0.2 g KCl
- 1.12 g Na_2HPO_4
- 2 g KH_2HPO_4
- 1000 mL dH2O
- pH 7.4

4% Paraformaldehyde

- 400 mL 0.01 M PBS
- 20 g PFA
- pH 7.40
- dH_2O to 500 mL

APPENDIX C – WHOLE-MOUNT STAINING

C1 – Acid-free Double Stain

By Sara Edsall (2011), modified from Walker and Kimmel (2007)

1. Fix embryos in 4% PFA in 0.01 M PBS (2 hrs room temperature with agitation, or overnight at 4°C)- store in 0.01 M PBS.
2. Put samples directly into 50% ethanol for 10 minutes at room temperature with agitation
3. Remove ethanol and add staining solution (see below) - agitate overnight at room temperature.
4. Rinse in distilled water (add water to tube with specimen and invert twice maximum).
5. Remove water and add bleach solution (below) to tubes for 20 minutes at room temperature, with LIDS OPEN (no agitation).
6. **If fish are >20 dpf, add a step here→ remove bleach and wash specimens in a 1% KOH solution for 1 hour at room temperature (agitation). The blue stain will stick to the outside of larger samples, covering the bone. This step does not completely solve the problem, but it helps. The remaining blue stuck on the specimens can be scraped off gently with forceps.
7. If fish are < 20 dpf, remove bleach and add 20% glycerol solution (made in 1% KOH) to tubes and agitate at room temperature for 30 min-overnight.
8. Replace 20% glycerol solution with a 40% glycerol solution (made in 1% KOH), agitate at room temperature for 2 hours-overnight.
9. Store in 100% Glycerol.

Solutions:

Staining Solution

- 1 ml of staining solution = 990 µl Part A+ 10 µl Part B
- Part A
    - 100 mL solution
    - Final concentrations: 0.02% Alcian Blue, 20 mM, $MgCl_2$, and 70% EtOH.
    - 5 ml 0.4% Alcian Blue in 70% ethanol (EtOH)
    - 70 ml 95% EtOH
    - 25 ml 20 mM $MgCl_2$
- Part B
    - 10 mL solution
    - 0.5% Alizarin Red in distilled water

Bleaching Solution

- Mix equal volumes 3% H_2O_2 (Life brand) and 2% KOH for a solution that is overall 1.5% H_2O_2 and 1% KOH.

C2 – Whole-mount Double Stain for Bone and Cartilage
Modified from Franz-Odendaal (2007)

1. Rinse 4% PFA-fixed specimen in tap water 30 minutes, or overnight for 10% NBF-fixed specimen
2. Remove brain and eyes from fixed chick embryo skull, careful not to damage the bones
3. Rinse in water for 30 minutes
4. Place specimen in an acetic acid/ethanol/Alcian blue solution overnight
    - 20 mL acetic acid
    - 80 mL 100% ethanol
    - 0.1g Alcian blue
5. Rehydrate specimen through graded ethanol series, 1 hour each
    - 100% ethanol
    - 70% ethanol
    - 50% ethanol
    - 25% ethanol
    - Water
6. Place specimen in 1% KOH with 3% hydrogen peroxide (about 5mL 3% hydrogen peroxide in 100 mL 1% KOH solution until the pigment is bleached and brown pigment is light brown (this step takes approximately 4-6 hours for a chick embryo skull, but can be left overnight if necessary)
7. Rinse specimen in tap water 30 minutes
8. Transfer specimen to 15 mL saturated sodium tetraborate in 35mL water overnight
9. Place specimen in 1% KOH with 1 mg/mL Alizarin red overnight (solution should be a deep purple colour)
10. Rinse specimen in tap water 30 minutes
11. Place specimen in 1% trypsin/2% borax for 3 nights at room temperature
12. Place specimen in fresh 1% trypsin/2% borax for 1 night at 37°C
13. Continue to place specimen in fresh 1% trypsin/2% borax each day until soft tissue has digested. When beak appears relaxed enough to drop open on its own, proceed to the next step. This may take several days, depending on the size of the specimen.
14. Transfer specimen through a series of glycerol/1% KOH solutions for 3-4 nights each.
    - 20% glycerol in 1% KOH
    - 40% glycerol in 1% KOH
1. Store in 70% glycerol in 70% ethanol
    - 35 mL 100% glycerol
    - 15 mL 70% ethanol

C3 – Whole-mount Bone Stain
Modified from Franz-Odendaal (2007)

2. Rinse 4% PFA-fixed specimen in tap water 30 minutes, or overnight for 10% NBF-fixed specimen
3. Remove brain and eyes from fixed chick embryo skull, careful not to damage the bones (NOTE: this step is not necessary for zebrafish).
4. Place specimen in 1% KOH with 3% hydrogen peroxide (about 5 mL 3% hydrogen peroxide in 100mL 1% KOH solution until the pigment is bleached and brown pigment is light brown (this step takes approximately 4-6 hours for a chick embryo skull, but can be left overnight if necessary)
5. Rinse specimen in tap water 30 minutes
6. Transfer specimen to 15 mL saturated sodium tetraborate in 35 mL water overnight
7. Place specimen in 1% KOH with 1mg/mL Alizarin red overnight (solution should be a deep purple colour)
8. Rinse specimen in tap water 30 minutes
9. Place specimen in 1% trypsin/2% borax for 3 nights (chicken) or 1 night (zebrafish) at room temperature
10. Place specimen in fresh 1% trypsin/2% borax for 1 night at 37°C
11. Continue to place specimen in fresh 1% trypsin/2% borax each day until soft tissue has digested. When beak appears relaxed enough to drop open on its own, proceed to the next step. This may take several days, depending on the size of the specimen. (NOTE: this step will likely be unnecessary for zebrafish).
12. Transfer specimen through a series of glycerol/1% KOH solutions for 3-4 nights each.
    - 20% glycerol in 1% KOH
    - 40% glycerol in 1% KOH
13. Store in 70% glycerol in 70% ethanol
    - 35 mL 100% glycerol
    - 15 mL 70% ethanol

APPENDIX D – MORPHOMETRICS

Morphometrics

Outline Morphometrics Protocol

- Download the SHAPE program
- Convert all images to a 24-Bitmap (.bmp) file type (this can be done easily in CorelPaint)
- Make sure that there is blank space around all edges of the shape
    - If the shape extends to the very edge of the image, the program will not be able to detect the outline of the shape
- Transfer images to be analyzed into a new, clearly labeled folder

Open "ChainCoder"

- Under "Config" Tab
    1. Object Colour
        - Select Bright (White) if image is lighter colour than background
        - Select Dark (Black) if image is darker colour than background
    2. Scale Included
        - Select yes or no depending on if a scale bar is included
        - Without a scale bar, the size differences between samples will be ignored
    3. Scale Size/ Scan Direction/ Scale Position
        - Select accordingly if scale bar included
    - Click "Proceed to Processing"
    - "Select Images"
        - Select the folder holding the images you wish to analyze
        - Use the double arrow button to transfer all images in that file into the program
        - You can also add one image at a time by using the single arrow
        - Hit "OK"
- Under "Processing" Tab
    1. "Load Image"
        - Brings up the first image file
    2. "Select Area"
        - If you want to crop image, hit this button
        - Click and drag a box over image to crop to proper dimensions
            - Note – Try to avoid this: Sometimes it can make program freeze!
        - If you do not need to crop, click the white box next to this button
            - This will allow the program to skip this step
    3. "Gray Scale"
        - In the drop down box, select the colour of your image (either Red, Green or Blue)

- Press the "Gray Scale Button"

4. "Make Histogram"
    - Based on this data, the program will decide which Binarize number is needed
5. "Binarize Image"
    - After making the histogram, a number will appear in the box beside this button
    - You can change it by selecting and typing, however normally it is more effective to simply use the number provided by clicking the "Binarize Image" button)
6. "Ero Filter" and "Dil Filter"
    - Can help to smooth out edges of an image
    - Should be avoided because it makes images inaccurate
7. "Labelling Object"
    - Use the dropdown box to select the minimum number of pixels in the image you want the program to detect
    - Automatically set to 500, which should be fine unless you are photographing something very small, in which case the number should be adjusted accordingly
8. "Chain Coding"
    - Can see chain code in white box at bottom of screen
9. "Save to file"
    - Select folder where you want file to be saved
    - Save as a ChainCode file (.chc)
10. Repeat steps 1-9 until all images have been processed

Open "CHC2NEF"

- "CHC File Name"
    - Select Chain Code File
- "NEF File Name"
    - Save as a NEF file (.nef)
- "Max Harmonic No"
    - Can be changed but is common to use 20
- "Normalization Method"
    - Select "based on First Harmonic" to normalize samples
        - Allows you to alter orientation by 180^{o}
    - Can also select "based on Longest Radius"
        - Manually alter orientation
        - Increases change of human error so normally is better to use the first option
- "OK" and then "Start"
- Orient image as desired by selecting the rotate buttons on the right side of the screen
- When finished hit "Save/Next Object"
- Repeat until all images have been processed

Open "PrinComp"

- Open NEF file
- Click "Analysis" Tab
- Click "Principal Components Analysis
- Hit "OK" and "Save"
- At bottom of output click "Make Report"
    - Save as a text file (".txt")
    - Among other information, this sheet provides the number of effective principal components with the corresponding amount of variation in shape accounted for by each PC
- Go back to the "Analysis" Tab
- Click "Calculate Prin Score"
    - Save file (".pcs")
- Select "Only on Effective Components" and then "OK"
- Provides sheet of all of the PC values that correspond to each sample
    - This can be copied and pasted into Excel and graphed
    - Before closing this sheet, hit "Save as" and save as a text file (".txt")
- Go back to "Analysis" Tab
- Select "Reconstruct Contour"
- Select "Effective Components Only"
- Hit Okay and Save file accordingly
- Opens up PrinPrint program
    - Shows pictorial representation of the shape changes occurring between the samples for each PC value, making interpretation of the data possible

- PCA results were imported into Microsoft Excel and used to create a scatterplot

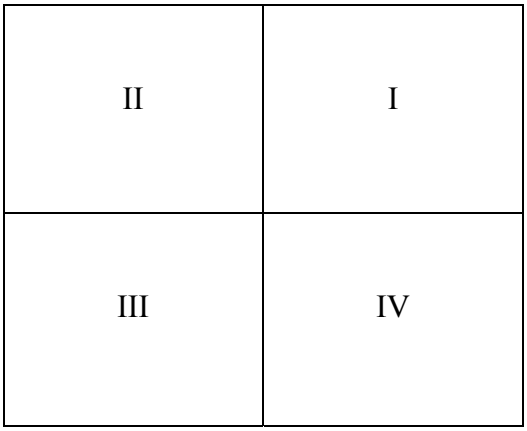

Figure D1. Quadrants of scatterplots.

APPENDIX E – MINITAB OUTPUTS

E1 – Chicken Analysis (all samples)

40 = HH 40
42 = HH 42
45 = HH 45

```
One-way ANOVA: PC1 versus GROUP

Source     DF       SS       MS     F      P
GROUP   2  0.08176  0.04088  4.37  0.026
Error      21  0.19630  0.00935
Total      23  0.27806

S = 0.09668   R-Sq = 29.40%   R-Sq(adj) = 22.68%


                             Individual 95% CIs For Mean Based on Pooled StDev
Level  N      Mean    StDev   --+---------+---------+---------+-------
40      8   0.05624  0.05179                      (---------*---------)
42      8   0.02420  0.14139                (---------*----------)
45      8  -0.08044  0.07328   (----------*---------)
                              --+---------+---------+---------+-------
                             -0.140    -0.070     0.000     0.070

Pooled StDev = 0.09668


Grouping Information Using Tukey Method

GROUP  N      Mean  Grouping
40          8   0.05624  A
42          8   0.02420  A B
45          8  -0.08044    B

Means that do not share a letter are significantly different.


Tukey 95% Simultaneous Confidence Intervals
All Pairwise Comparisons among Levels of GROUP

Individual confidence level = 98.00%


GROUP = 40 subtracted from:

GROUP     Lower    Center     Upper
42          -0.15373  -0.03204   0.08965
45          -0.25837  -0.13668  -0.01499

GROUP  -------+---------+---------+---------+--
42                (-------*-------)
45          (-------*-------)
           -------+---------+---------+---------+--
               -0.15      0.00      0.15      0.30


GROUP = 42 subtracted from:
```

```
GROUP     Lower    Center    Upper
45          -0.22633  -0.10464  0.01705

GROUP  -------+---------+---------+---------+--
45            (-------*-------)
           -------+---------+---------+---------+--
               -0.15      0.00      0.15      0.30
```

```
One-way ANOVA: PC2 versus GROUP

Source     DF       SS       MS     F      P
GROUP   2  0.06585  0.03292  4.01  0.033
Error      21  0.17229  0.00820
Total      23  0.23813

S = 0.09058   R-Sq = 27.65%   R-Sq(adj) = 20.76%


                            Individual 95% CIs For Mean Based on Pooled StDev
Level  N      Mean    StDev  ---------+---------+---------+---------+
40      8  -0.06551  0.06158  (---------*--------)
42      8   0.00282  0.13036            (--------*---------)
45      8   0.06270  0.06185                     (---------*--------)
                            ---------+---------+---------+---------+
                                  -0.070     0.000     0.070     0.140

Pooled StDev = 0.09058


Grouping Information Using Tukey Method

GROUP  N      Mean  Grouping
45          8   0.06270  A
42          8   0.00282  A B
40          8  -0.06551    B

Means that do not share a letter are significantly different.


Tukey 95% Simultaneous Confidence Intervals
All Pairwise Comparisons among Levels of GROUP

Individual confidence level = 98.00%


GROUP = 40 subtracted from:

GROUP     Lower   Center    Upper  ----+---------+---------+---------+-----
42          -0.04567  0.06833  0.18233            (---------*--------)
45           0.01421  0.12821  0.24222                 (---------*--------)
                                  ----+---------+---------+---------+-----
                                   -0.12      0.00      0.12      0.24


GROUP = 42 subtracted from:

GROUP     Lower   Center    Upper  ----+---------+---------+---------+-----
45          -0.05412  0.05988  0.17389           (---------*--------)
                                  ----+---------+---------+---------+-----
                                   -0.12      0.00      0.12      0.24
```

```
One-way ANOVA: PC3 versus GROUP

Source     DF       SS       MS     F      P
GROUP   2  0.03791  0.01895  4.27  0.028
Error      21  0.09316  0.00444
Total      23  0.13106

S = 0.06660   R-Sq = 28.92%   R-Sq(adj) = 22.15%


                            Individual 95% CIs For Mean Based on Pooled StDev
Level  N      Mean    StDev    -+---------+---------+---------+--------
40      8  -0.05568  0.04752    (---------*---------)
42      8   0.02120  0.09388                  (---------*---------)
45      8   0.03448  0.04730                     (---------*---------)
                            -+---------+---------+---------+--------
                           -0.100    -0.050    -0.000     0.050

Pooled StDev = 0.06660


Grouping Information Using Tukey Method

GROUP  N      Mean  Grouping
45          8   0.03448  A
42          8   0.02120  A B
40          8  -0.05568    B

Means that do not share a letter are significantly different.


Tukey 95% Simultaneous Confidence Intervals
All Pairwise Comparisons among Levels of GROUP

Individual confidence level = 98.00%


GROUP = 40 subtracted from:

GROUP     Lower   Center    Upper  ----+---------+---------+---------+-----
42          -0.00696  0.07687  0.16071               (-----------*-----------)
45           0.00633  0.09016  0.17399                 (-----------*-----------
)
                                      ----+---------+---------+---------+-----
                                       -0.070     0.000     0.070     0.140


GROUP = 42 subtracted from:

GROUP     Lower   Center    Upper  ----+---------+---------+---------+-----
45          -0.07055  0.01328  0.09711      (-----------*-----------)
                                      ----+---------+---------+---------+-----
                                       -0.070     0.000     0.070     0.140

One-way ANOVA: PC4 versus GROUP

Source     DF       SS       MS     F      P
GROUP   2  0.00032  0.00016  0.07  0.931
Error      21  0.04750  0.00226
Total      23  0.04782

S = 0.04756   R-Sq = 0.68%   R-Sq(adj) = 0.00%
```

```
                              Individual 95% CIs For Mean Based on Pooled StDev
Level  N      Mean    StDev  ---------+---------+---------+---------+
40      8  -0.00395  0.03898  (-----------------*-----------------)
42      8   0.00490  0.05398      (-----------------*-----------------)
45      8  -0.00095  0.04849   (-----------------*-----------------)
                              ---------+---------+---------+---------+
                                    -0.020     0.000     0.020     0.040

Pooled StDev = 0.04756


Grouping Information Using Tukey Method

GROUP  N      Mean  Grouping
42          8   0.00490  A
45          8  -0.00095  A
40          8  -0.00395  A

Means that do not share a letter are significantly different.


Tukey 95% Simultaneous Confidence Intervals
All Pairwise Comparisons among Levels of GROUP

Individual confidence level = 98.00%


GROUP = 40 subtracted from:

GROUP     Lower   Center    Upper
42          -0.05102  0.00884  0.06870
45          -0.05686  0.00299  0.06285

GROUP  ---------+---------+---------+---------+
42              (-----------------*-----------------)
45             (-----------------*-----------------)
           ---------+---------+---------+---------+
                 -0.035     0.000     0.035     0.070


GROUP = 42 subtracted from:

GROUP     Lower    Center    Upper
45          -0.06571  -0.00585  0.05401

GROUP  ---------+---------+---------+---------+
45          (-----------------*-----------------)
           ---------+---------+---------+---------+
                 -0.035     0.000     0.035     0.070One-way ANOVA: PC5 versus
GROUP

Source     DF       SS       MS     F      P
GROUP   2  0.01429  0.00715  6.30  0.007
Error      21  0.02382  0.00113
Total      23  0.03811

S = 0.03368   R-Sq = 37.50%   R-Sq(adj) = 31.55%


                              Individual 95% CIs For Mean Based on Pooled StDev
Level  N      Mean    StDev     +---------+---------+---------+---------
```

```
40      8   0.02256  0.03907                         (--------*-------)
42      8  -0.03390  0.03444     (--------*-------)
45      8   0.01134  0.02627                    (-------*-------)
                              +---------+---------+---------+---------
                           -0.060    -0.030     0.000     0.030

Pooled StDev = 0.03368


Grouping Information Using Tukey Method

GROUP  N      Mean  Grouping
40          8   0.02256  A
45          8   0.01134  A
2           8  -0.03390    B

Means that do not share a letter are significantly different.


Tukey 95% Simultaneous Confidence Intervals
All Pairwise Comparisons among Levels of GROUP

Individual confidence level = 98.00%


GROUP = 40 subtracted from:

GROUP     Lower    Center     Upper
42          -0.09885  -0.05646  -0.01407
45          -0.05361  -0.01122   0.03116

GROUP     +---------+---------+---------+---------
42             (--------*-------)
45                      (--------*-------)
               +---------+---------+---------+---------
           -0.100    -0.050     0.000     0.050


GROUP = 42 subtracted from:

GROUP    Lower   Center    Upper
45          0.00285  0.04523  0.08762

GROUP     +---------+---------+---------+---------
45                                (-------*--------)
               +---------+---------+---------+---------
           -0.100    -0.050     0.000     0.050


One-way ANOVA: PC6 versus GROUP

Source     DF       SS       MS     F      P
GROUP   2  0.00211  0.00105  0.69  0.511
Error      21  0.03189  0.00152
Total      23  0.03400

S = 0.03897   R-Sq = 6.19%   R-Sq(adj) = 0.00%


                              Individual 95% CIs For Mean Based on
                              Pooled StDev
Level  N      Mean    StDev  ------+---------+---------+---------+---
40      8   0.00046  0.03562       (----------*-----------)
```

```
42      8  -0.01169  0.04480  (----------*-----------)
45      8   0.01124  0.03578           (----------*-----------)
                              ------+---------+---------+---------+---
                                 -0.025     0.000     0.025     0.050

Pooled StDev = 0.03897


Grouping Information Using Tukey Method

GROUP  N      Mean  Grouping
45          8   0.01124  A
40          8   0.00046  A
42          8  -0.01169  A

Means that do not share a letter are significantly different.


Tukey 95% Simultaneous Confidence Intervals
All Pairwise Comparisons among Levels of GROUP

Individual confidence level = 98.00%


GROUP = 40 subtracted from:

GROUP     Lower    Center    Upper
42          -0.06120  -0.01215  0.03690
45          -0.03827   0.01078  0.05983

GROUP  --------+---------+---------+---------+-
42             (-----------*-----------)
45                  (------------*-----------)
           --------+---------+---------+---------+-
                -0.040     0.000     0.040     0.080


GROUP = 42 subtracted from:

GROUP     Lower   Center    Upper
45          -0.02612  0.02293  0.07198

GROUP  --------+---------+---------+---------+-
5                    (------------*-----------)
           --------+---------+---------+---------+-
                -0.040     0.000     0.040     0.080


One-way ANOVA: PC7 versus GROUP

Source     DF        SS        MS     F      P
GROUP   2  0.003491  0.001746  2.74  0.087
Error      21  0.013358  0.000636
Total      23  0.016849

S = 0.02522   R-Sq = 20.72%   R-Sq(adj) = 13.17%


                              Individual 95% CIs For Mean Based on
                              Pooled StDev
Level  N      Mean    StDev  ------+---------+---------+---------+---
40      8  -0.00363  0.03375       (--------*--------)
42      8   0.01625  0.02114                 (--------*--------)
```

```
45      8  -0.01262  0.01795  (---------*--------)
                              ------+---------+---------+---------+---
                                 -0.020     0.000     0.020     0.040

Pooled StDev = 0.02522


Grouping Information Using Tukey Method

GROUP  N      Mean  Grouping
42          8   0.01625  A
40          8  -0.00363  A
45          8  -0.01262  A

Means that do not share a letter are significantly different.


Tukey 95% Simultaneous Confidence Intervals
All Pairwise Comparisons among Levels of GROUP

Individual confidence level = 98.00%


GROUP = 40 subtracted from:

GROUP     Lower    Center    Upper
42          -0.01187   0.01988  0.05162
45          -0.04073  -0.00899  0.02276

GROUP  -------+---------+---------+---------+--
42                      (--------*--------)
45             (--------*---------)
           -------+---------+---------+---------+--
               -0.035     0.000     0.035     0.070


GROUP = 42 subtracted from:

GROUP     Lower    Center    Upper
45          -0.06061  -0.02887  0.00288

GROUP  -------+---------+---------+---------+--
45          (--------*--------)
           -------+---------+---------+---------+--
               -0.035     0.000     0.035     0.070


One-way ANOVA: PC8 versus GROUP

Source     DF        SS        MS     F      P
GROUP   2  0.000230  0.000115  0.21  0.809
Error      21  0.011262  0.000536
Total      23  0.011492

S = 0.02316   R-Sq = 2.00%   R-Sq(adj) = 0.00%


                            Individual 95% CIs For Mean Based on
                            Pooled StDev
Level  N      Mean    StDev  -------+---------+---------+---------+--
40      8  -0.00291  0.03589  (--------------*-------------)
42      8  -0.00138  0.00628    (-------------*-------------)
45      8   0.00428  0.01678        (--------------*-------------)
```

```
                              -------+---------+---------+---------+--
                                  -0.012     0.000     0.012     0.024

Pooled StDev = 0.02316


Grouping Information Using Tukey Method

GROUP  N      Mean  Grouping
45          8   0.00428  A
42          8  -0.00138  A
40          8  -0.00291  A

Means that do not share a letter are significantly different.


Tukey 95% Simultaneous Confidence Intervals
All Pairwise Comparisons among Levels of GROUP

Individual confidence level = 98.00%


GROUP = 40 subtracted from:

GROUP     Lower   Center    Upper  -------+---------+---------+---------+--
42          -0.02762  0.00153  0.03067     (--------------*-------------)
45          -0.02196  0.00719  0.03634        (--------------*-------------)
                                  -------+---------+---------+---------+--
                                      -0.020     0.000     0.020     0.040


GROUP = 42 subtracted from:

GROUP     Lower   Center    Upper  -------+---------+---------+---------+--
45          -0.02349  0.00566  0.03481       (--------------*-------------)
                                  -------+---------+---------+---------+--
                                      -0.020     0.000     0.020     0.040
```

E2 – Chicken Analysis (No Outlier)

40 = HH 40
42 = HH 42
45 = HH 45

```
One-way ANOVA: PC1 versus GROUP

Source     DF       SS       MS      F      P
GROUP   2  0.13966  0.06983  12.90  0.000
Error      20  0.10826  0.00541
Total      22  0.24792

S = 0.07357   R-Sq = 56.33%   R-Sq(adj) = 51.97%


                            Individual 95% CIs For Mean Based on
                            Pooled StDev
Level  N      Mean    StDev  --------+---------+---------+---------+-
40      8  -0.09037  0.05788  (------*-----)
42      7  -0.00666  0.10937            (------*------)
45      8   0.09619  0.04315                      (------*------)
                            --------+---------+---------+---------+-
                                 -0.080     0.000     0.080     0.160

Pooled StDev = 0.07357


Grouping Information Using Tukey Method

GROUP  N      Mean  Grouping
45          8   0.09619  A
42          7  -0.00666    B
40          8  -0.09037    B

Means that do not share a letter are significantly different.


Tukey 95% Simultaneous Confidence Intervals
All Pairwise Comparisons among Levels of GROUP

Individual confidence level = 98.01%


GROUP = 40 subtracted from:

GROUP     Lower   Center    Upper
42          -0.01268  0.08371  0.18010
45           0.09344  0.18656  0.27968

GROUP  -------+---------+---------+---------+--
42                      (-------*-------)
45                               (-------*------)
           -------+---------+---------+---------+--
               -0.12      0.00      0.12      0.24


GROUP = 2 subtracted from:
```

```
GROUP    Lower   Center    Upper  -------+---------+---------+---------+--
45         0.00646  0.10285  0.19924                    (-------*-------)
                                  -------+---------+---------+---------+--
                                      -0.12      0.00      0.12      0.24
```

One-way ANOVA: PC2 versus GROUP

Source	DF	SS	MS	F	P
GROUP	2	0.03263	0.01632	2.50	0.107
Error	20	0.13048	0.00652		
Total	22	0.16311			

S = 0.08077   R-Sq = 20.01%   R-Sq(adj) = 12.01%

```
                          Individual 95% CIs For Mean Based on
                          Pooled StDev
Level  N      Mean    StDev  --------+---------+---------+---------+-
40      8  -0.05095  0.05823  (---------*--------)
42      7   0.01938  0.10537            (---------*----------)
45      8   0.03399  0.07571               (---------*---------)
                          --------+---------+---------+---------+-
                               -0.060     0.000     0.060     0.120
```

Pooled StDev = 0.08077

Grouping Information Using Tukey Method

GROUP	N	Mean	Grouping
45	8	0.03399	A
42	7	0.01938	A
40	8	-0.05095	A

Means that do not share a letter are significantly different.

Tukey 95% Simultaneous Confidence Intervals
All Pairwise Comparisons among Levels of GROUP

Individual confidence level = 98.01%

GROUP = 40 subtracted from:

```
GROUP     Lower   Center    Upper  -----+---------+---------+---------+----
42          -0.03549  0.07033  0.17615            (------------*------------)
45          -0.01730  0.08493  0.18717              (------------*-----------)
                                  -----+---------+---------+---------+----
                                    -0.080     0.000     0.080     0.160
```

GROUP = 42 subtracted from:

```
GROUP     Lower   Center    Upper  -----+---------+---------+---------+----
45          -0.09122  0.01460  0.12042      (------------*------------)
                                  -----+---------+---------+---------+----
                                    -0.080     0.000     0.080     0.160
```

One-way ANOVA: PC3 versus GROUP

```
Source     DF       SS       MS     F      P
GROUP   2  0.00489  0.00244  0.56  0.581
Error      20  0.08763  0.00438
Total      22  0.09252

S = 0.06619   R-Sq = 5.28%   R-Sq(adj) = 0.00%


                              Individual 95% CIs For Mean Based on Pooled StDev
Level  N      Mean    StDev  ---------+---------+---------+---------+
40      8   0.01767  0.05691            (-------------*-------------)
42      7  -0.00045  0.05969       (--------------*--------------)
45      8  -0.01728  0.07890  (-------------*-------------)
                              ---------+---------+---------+---------+
                                    -0.035     0.000     0.035     0.070

Pooled StDev = 0.06619


Grouping Information Using Tukey Method

GROUP  N      Mean  Grouping
40          8   0.01767  A
42          7  -0.00045  A
45          8  -0.01728  A

Means that do not share a letter are significantly different.


Tukey 95% Simultaneous Confidence Intervals
All Pairwise Comparisons among Levels of GROUP

Individual confidence level = 98.01%


GROUP = 40 subtracted from:

GROUP     Lower    Center    Upper
42          -0.10484  -0.01811  0.06861
45          -0.11873  -0.03495  0.04884

GROUP     +---------+---------+---------+---------
2                (-------------*-------------)
5             (-------------*-------------)
              +---------+---------+---------+---------
           -0.120    -0.060     0.000     0.060


GROUP = 42 subtracted from:

GROUP     Lower    Center    Upper
45          -0.10355  -0.01683  0.06989

GROUP     +---------+---------+---------+---------
45               (-------------*--------------)
              +---------+---------+---------+---------
           -0.120    -0.060     0.000     0.060

One-way ANOVA: PC4 versus GROUP

Source     DF       SS       MS     F      P
GROUP   2  0.01491  0.00746  6.33  0.007
```

```
Error      20  0.02356  0.00118
Total      22  0.03848

S = 0.03432   R-Sq = 38.76%   R-Sq(adj) = 32.64%


                            Individual 95% CIs For Mean Based on
                            Pooled StDev
Level  N      Mean    StDev  -----+---------+---------+---------+----
40      8  -0.02104  0.04132  (-------*-------)
42      7   0.03810  0.03918                    (--------*--------)
45      8  -0.01229  0.01852    (--------*-------)
                            -----+---------+---------+---------+----
                              -0.030     0.000     0.030     0.060

Pooled StDev = 0.03432


Grouping Information Using Tukey Method

GROUP  N      Mean  Grouping
42          7   0.03810  A
45          8  -0.01229    B
40          8  -0.02104    B

Means that do not share a letter are significantly different.


Tukey 95% Simultaneous Confidence Intervals
All Pairwise Comparisons among Levels of GROUP

Individual confidence level = 98.01%


GROUP = 0 subtracted from:

GROUP     Lower   Center    Upper
42          0.01418  0.05915  0.10411
45         -0.03469  0.00875  0.05219

GROUP  ---------+---------+---------+---------+
42                            (--------*--------)
45                    (--------*-------)
           ---------+---------+---------+---------+
                 -0.050     0.000     0.050     0.100


GROUP = 42 subtracted from:

GROUP     Lower    Center     Upper
45         -0.09536  -0.05040  -0.00543

GROUP  ---------+---------+---------+---------+
45          (--------*--------)
           ---------+---------+---------+---------+
                 -0.050     0.000     0.050     0.100



One-way ANOVA: PC5 versus GROUP

Source     DF       SS       MS     F      P
GROUP   2  0.00117  0.00059  0.35  0.708
```

```
Error      20  0.03344  0.00167
Total      22  0.03461

S = 0.04089   R-Sq = 3.39%   R-Sq(adj) = 0.00%


                            Individual 95% CIs For Mean Based on Pooled StDev
Level  N      Mean    StDev     +---------+---------+---------+---------
40      8   0.00365  0.03628            (--------------*--------------)
42      7   0.00682  0.04686            (---------------*----------------)
45      8  -0.00962  0.03973     (--------------*--------------)
                              +---------+---------+---------+---------
                            -0.040    -0.020     0.000     0.020

Pooled StDev = 0.04089


Grouping Information Using Tukey Method

GROUP  N      Mean  Grouping
42          7   0.00682  A
40          8   0.00365  A
45          8  -0.00962  A

Means that do not share a letter are significantly different.


Tukey 95% Simultaneous Confidence Intervals
All Pairwise Comparisons among Levels of GROUP

Individual confidence level = 98.01%


GROUP = 40 subtracted from:

GROUP     Lower    Center    Upper
42          -0.05040   0.00317  0.05674
45          -0.06502  -0.01327  0.03848

GROUP  --------+---------+---------+---------+-
42               (-------------*------------)
45            (------------*------------)
           --------+---------+---------+---------+-
                -0.040     0.000     0.040     0.080


GROUP = 42 subtracted from:

GROUP     Lower    Center    Upper
45          -0.07001  -0.01644  0.03713

GROUP  --------+---------+---------+---------+-
45           (-------------*------------)
           --------+---------+---------+---------+-
                -0.040     0.000     0.040     0.080



One-way ANOVA: PC6 versus GROUP

Source     DF        SS        MS     F      P
GROUP   2  0.003206  0.001603  2.32  0.124
Error      20  0.013829  0.000691
```

```
Total      22  0.017035

S = 0.02630   R-Sq = 18.82%   R-Sq(adj) = 10.70%


                            Individual 95% CIs For Mean Based on
                            Pooled StDev
Level  N      Mean    StDev  ------+---------+---------+---------+---
0      8  -0.00259  0.03373       (---------*--------)
2      7   0.01681  0.02401                 (---------*----------)
5      8  -0.01212  0.01854  (---------*---------)
                            ------+---------+---------+---------+---
                               -0.020     0.000     0.020     0.040

Pooled StDev = 0.02630


Grouping Information Using Tukey Method

GROUP  N      Mean  Grouping
42          7   0.01681  A
40          8  -0.00259  A
45          8  -0.01212  A

Means that do not share a letter are significantly different.


Tukey 95% Simultaneous Confidence Intervals
All Pairwise Comparisons among Levels of GROUP

Individual confidence level = 98.01%


GROUP = 40 subtracted from:

GROUP     Lower    Center    Upper
42          -0.01505   0.01940  0.05385
45          -0.04281  -0.00953  0.02376

GROUP  --------+---------+---------+---------+-
42                      (---------*--------)
45              (--------*---------)
           --------+---------+---------+---------+-
                -0.035     0.000     0.035     0.070


GROUP = 42 subtracted from:

GROUP     Lower    Center    Upper
45          -0.06338  -0.02892  0.00553

GROUP  --------+---------+---------+---------+-
45          (---------*---------)
           --------+---------+---------+---------+-
                -0.035     0.000     0.035     0.070



One-way ANOVA: PC7 versus GROUP

Source     DF        SS        MS     F      P
GROUP   2  0.000223  0.000112  0.20  0.822
Error      20  0.011297  0.000565
```

```
Total      22  0.011520

S = 0.02377   R-Sq = 1.94%   R-Sq(adj) = 0.00%


                            Individual 95% CIs For Mean Based on
                            Pooled StDev
Level  N      Mean    StDev  --------+---------+---------+---------+-
40      8   0.00366  0.03603        (--------------*--------------)
42      7   0.00017  0.00543     (---------------*---------------)
45      8  -0.00381  0.01704  (--------------*-------------)
                            --------+---------+---------+---------+-
                                 -0.012     0.000     0.012     0.024

Pooled StDev = 0.02377


Grouping Information Using Tukey Method

GROUP  N      Mean  Grouping
40          8   0.00366  A
42          7   0.00017  A
45          8  -0.00381  A

Means that do not share a letter are significantly different.


Tukey 95% Simultaneous Confidence Intervals
All Pairwise Comparisons among Levels of GROUP

Individual confidence level = 98.01%


GROUP = 40 subtracted from:

GROUP     Lower    Center    Upper
42          -0.03462  -0.00348  0.02765
45          -0.03754  -0.00746  0.02262

GROUP  ---------+---------+---------+---------+
42            (--------------*---------------)
45          (--------------*--------------)
           ---------+---------+---------+---------+
                 -0.020     0.000     0.020     0.040


GROUP = 42 subtracted from:

GROUP     Lower    Center    Upper
45          -0.03512  -0.00398  0.02716

GROUP  ---------+---------+---------+---------+
45            (---------------*---------------)
           ---------+---------+---------+---------+
                 -0.020     0.000     0.020     0.040



One-way ANOVA: PC8 versus GROUP

Source     DF        SS        MS     F      P
GROUP   2  0.000848  0.000424  0.91  0.417
Error      20  0.009278  0.000464
```

```
Total      22  0.010126

S = 0.02154   R-Sq = 8.38%   R-Sq(adj) = 0.00%


                           Individual 95% CIs For Mean Based on
                           Pooled StDev
Level  N      Mean    StDev  --------+---------+---------+---------+-
40      8  -0.00530  0.01745  (-------------*------------)
42      7   0.00902  0.02616             (--------------*-------------)
45      8  -0.00260  0.02084     (------------*------------)
                           --------+---------+---------+---------+-
                                -0.012     0.000     0.012     0.024

Pooled StDev = 0.02154


Grouping Information Using Tukey Method

GROUP  N      Mean  Grouping
42          7   0.00902  A
45          8  -0.00260  A
40          8  -0.00530  A

Means that do not share a letter are significantly different.


Tukey 95% Simultaneous Confidence Intervals
All Pairwise Comparisons among Levels of GROUP

Individual confidence level = 98.01%


GROUP = 40 subtracted from:

GROUP     Lower   Center    Upper  ------+---------+---------+---------+---
42          -0.01390  0.01432  0.04254            (-----------*----------)
45          -0.02456  0.00270  0.02996        (----------*----------)
                                       ------+---------+---------+---------+---
                                          -0.025     0.000     0.025     0.050


GROUP = 42 subtracted from:

GROUP     Lower    Center    Upper
45          -0.03984  -0.01162  0.01660

GROUP  ------+---------+---------+---------+---
45          (----------*-----------)
           ------+---------+---------+---------+---
              -0.025     0.000     0.025     0.050
```

E3 – Chicken Analysis (No HH 42)

40 = HH 40
42 = HH 42
45 = HH 45

```
One-way ANOVA: PC1 versus GROUP

Source     DF       SS       MS      F      P
GROUP   1  0.17331  0.17331  71.05  0.000
Error      14  0.03415  0.00244
Total      15  0.20746

S = 0.04939   R-Sq = 83.54%   R-Sq(adj) = 82.36%


                            Individual 95% CIs For Mean Based on
                            Pooled StDev
Level  N      Mean    StDev  --------+---------+---------+---------+-
40      8   0.10408  0.06093                              (----*----)
45      8  -0.10408  0.03416  (----*----)
                            --------+---------+---------+---------+-
                                 -0.080     0.000     0.080     0.160

Pooled StDev = 0.04939


Grouping Information Using Tukey Method

GROUP  N      Mean  Grouping
40          8   0.10408  A
45          8  -0.10408    B

Means that do not share a letter are significantly different.


Tukey 95% Simultaneous Confidence Intervals
All Pairwise Comparisons among Levels of GROUP

Individual confidence level = 95.00%


GROUP = 40 subtracted from:

GROUP     Lower    Center     Upper
45          -0.26112  -0.20815  -0.15518

GROUP  ---+---------+---------+---------+------
45          (------*------)
           ---+---------+---------+---------+------
           -0.240    -0.160    -0.080     0.000



One-way ANOVA: PC2 versus GROUP

Source     DF       SS       MS     F      P
GROUP   1  0.00035  0.00035  0.05  0.823
Error      14  0.09379  0.00670
```

```
Total      15  0.09414

S = 0.08185   R-Sq = 0.37%   R-Sq(adj) = 0.00%


                              Individual 95% CIs For Mean Based on Pooled StDev
Level  N      Mean    StDev  ---------+---------+---------+---------+
40      8  -0.00467  0.06857  (-----------------*----------------)
45      8   0.00467  0.09326     (----------------*-----------------)
                              ---------+---------+---------+---------+
                                    -0.035     0.000     0.035     0.070

Pooled StDev = 0.08185


Grouping Information Using Tukey Method

GROUP  N      Mean  Grouping
45          8   0.00467  A
40          8  -0.00467  A

Means that do not share a letter are significantly different.


Tukey 95% Simultaneous Confidence Intervals
All Pairwise Comparisons among Levels of GROUP

Individual confidence level = 95.00%


GROUP = 40 subtracted from:

GROUP     Lower   Center    Upper
45          -0.07843  0.00934  0.09712

GROUP  --------+---------+---------+---------+-
45            (-----------------*----------------)
           --------+---------+---------+---------+-
                -0.050     0.000     0.050     0.100



One-way ANOVA: PC3 versus GROUP

Source     DF       SS       MS     F      P
GROUP   1  0.00003  0.00003  0.01  0.926
Error      14  0.05385  0.00385
Total      15  0.05389

S = 0.06202   R-Sq = 0.06%   R-Sq(adj) = 0.00%


                              Individual 95% CIs For Mean Based on Pooled StDev
Level  N      Mean    StDev  ---------+---------+---------+---------+
40      8   0.00148  0.05123   (------------------*-----------------)
45      8  -0.00148  0.07119  (-----------------*------------------)
                              ---------+---------+---------+---------+
                                    -0.025     0.000     0.025     0.050

Pooled StDev = 0.06202


Grouping Information Using Tukey Method
```

```
GROUP  N      Mean  Grouping
40          8   0.00148  A
45          8  -0.00148  A

Means that do not share a letter are significantly different.


Tukey 95% Simultaneous Confidence Intervals
All Pairwise Comparisons among Levels of GROUP

Individual confidence level = 95.00%


GROUP = 40 subtracted from:

GROUP     Lower    Center    Upper
45          -0.06946  -0.00295  0.06356

GROUP     +---------+---------+---------+---------
45              (------------------*------------------)
              +---------+---------+---------+---------
            -0.070    -0.035     0.000     0.035

One-way ANOVA: PC4 versus GROUP

Source     DF       SS       MS     F      P
GROUP   1  0.00037  0.00037  0.22  0.648
Error      14  0.02384  0.00170
Total      15  0.02421

S = 0.04126   R-Sq = 1.53%   R-Sq(adj) = 0.00%


                            Individual 95% CIs For Mean Based on
                            Pooled StDev
Level  N      Mean    StDev  --------+---------+---------+---------+-
40      8  -0.00481  0.05454  (---------------*--------------)
45      8   0.00481  0.02074       (--------------*---------------)
                            --------+---------+---------+---------+-
                                 -0.020     0.000     0.020     0.040

Pooled StDev = 0.04126


Grouping Information Using Tukey Method

GROUP  N      Mean  Grouping
45          8   0.00481  A
40          8  -0.00481  A

Means that do not share a letter are significantly different.


Tukey 95% Simultaneous Confidence Intervals
All Pairwise Comparisons among Levels of GROUP

Individual confidence level = 95.00%


GROUP = 40 subtracted from:

GROUP     Lower   Center    Upper
```

```
45          -0.03463  0.00962  0.05387

GROUP  --------+---------+---------+---------+-
45              (-----------------*-----------------)
           --------+---------+---------+---------+-
                -0.025     0.000     0.025     0.050



One-way ANOVA: PC5 versus GROUP

Source     DF        SS        MS     F      P
GROUP   1  0.000170  0.000170  0.20  0.658
Error      14  0.011696  0.000835
Total      15  0.011866

S = 0.02890   R-Sq = 1.44%   R-Sq(adj) = 0.00%


                            Individual 95% CIs For Mean Based on
                            Pooled StDev
Level  N      Mean    StDev  -------+---------+---------+---------+--
40      8   0.00326  0.03351       (-------------*--------------)
45      8  -0.00326  0.02340  (--------------*-------------)
                            -------+---------+---------+---------+--
                                -0.015     0.000     0.015     0.030

Pooled StDev = 0.02890


Grouping Information Using Tukey Method

GROUP  N      Mean  Grouping
40          8   0.00326  A
45          8  -0.00326  A

Means that do not share a letter are significantly different.


Tukey 95% Simultaneous Confidence Intervals
All Pairwise Comparisons among Levels of GROUP

Individual confidence level = 95.00%


GROUP = 40 subtracted from:

GROUP     Lower    Center    Upper
45          -0.03752  -0.00653  0.02447

GROUP  ---------+---------+---------+---------+
45          (---------------*--------------)
           ---------+---------+---------+---------+
                 -0.020     0.000     0.020     0.040



One-way ANOVA: PC6 versus GROUP

Source     DF        SS        MS     F      P
GROUP   1  0.000251  0.000251  0.35  0.563
Error      14  0.010010  0.000715
Total      15  0.010262
```

```
S = 0.02674   R-Sq = 2.45%   R-Sq(adj) = 0.00%


                           Individual 95% CIs For Mean Based on
                           Pooled StDev
Level  N      Mean    StDev  ------+---------+---------+---------+---
40      8   0.00396  0.02278       (-------------*------------)
45      8  -0.00396  0.03018  (------------*-------------)
                           ------+---------+---------+---------+---
                              -0.015     0.000     0.015     0.030

Pooled StDev = 0.02674


Grouping Information Using Tukey Method

GROUP  N      Mean  Grouping
40          8   0.00396  A
45          8  -0.00396  A

Means that do not share a letter are significantly different.


Tukey 95% Simultaneous Confidence Intervals
All Pairwise Comparisons among Levels of GROUP

Individual confidence level = 95.00%


GROUP = 40 subtracted from:

GROUP     Lower    Center    Upper
45          -0.03660  -0.00793  0.02075

GROUP  --------+---------+---------+---------+-
45          (-------------*-------------)
           --------+---------+---------+---------+-
                -0.020     0.000     0.020     0.040



One-way ANOVA: PC7 versus GROUP

Source     DF        SS        MS     F      P
GROUP   1  0.000334  0.000334  0.68  0.423
Error      14  0.006866  0.000490
Total      15  0.007201

S = 0.02215   R-Sq = 4.64%   R-Sq(adj) = 0.00%


                           Individual 95% CIs For Mean Based on
                           Pooled StDev
Level  N      Mean    StDev  --------+---------+---------+---------+-
40      8  -0.00457  0.02811  (-------------*-------------)
45      8   0.00457  0.01381           (-------------*-------------)
                           --------+---------+---------+---------+-
                                -0.012     0.000     0.012     0.024

Pooled StDev = 0.02215
```

```
Grouping Information Using Tukey Method

GROUP  N      Mean  Grouping
45          8   0.00457  A
40          8  -0.00457  A

Means that do not share a letter are significantly different.


Tukey 95% Simultaneous Confidence Intervals
All Pairwise Comparisons among Levels of GROUP

Individual confidence level = 95.00%


GROUP = 40 subtracted from:

GROUP     Lower   Center    Upper  ------+---------+---------+---------+---
45          -0.01461  0.00914  0.03289        (---------------*---------------)
                                        ------+---------+---------+---------+---
                                           -0.015     0.000     0.015     0.030



One-way ANOVA: PC8 versus GROUP

Source     DF        SS        MS     F      P
GROUP   1  0.000003  0.000003  0.01  0.938
Error      14  0.005841  0.000417
Total      15  0.005844

S = 0.02043   R-Sq = 0.04%   R-Sq(adj) = 0.00%


                             Individual 95% CIs For Mean Based on Pooled StDev
Level  N      Mean    StDev     +---------+---------+---------+---------
40      8  -0.00040  0.01861     (-------------------*-------------------)
45      8   0.00040  0.02209      (-------------------*-------------------)
                                 +---------+---------+---------+---------
                             -0.0160   -0.0080    0.0000    0.0080

Pooled StDev = 0.02043


Grouping Information Using Tukey Method

GROUP  N      Mean  Grouping
45          8   0.00040  A
40          8  -0.00040  A

Means that do not share a letter are significantly different.


Tukey 95% Simultaneous Confidence Intervals
All Pairwise Comparisons among Levels of GROUP

Individual confidence level = 95.00%


GROUP = 40 subtracted from:

GROUP     Lower   Center    Upper
45          -0.02110  0.00081  0.02271
```

```
GROUP  --------+---------+---------+---------+-
45          (-----------------*-----------------)
           --------+---------+---------+---------+-
               -0.012      0.000     0.012     0.024
```

E4 – Zebrafish Analysis

8 = 8 mm SL
10 = 10 mm SL
12 = 12 mm SL

```
One-way ANOVA: PC1 versus Group

Source  DF       SS       MS      F      P
Group    2  0.86351  0.43175  68.69  0.000
Error   21  0.13199  0.00629
Total   23  0.99550

S = 0.07928   R-Sq = 86.74%   R-Sq(adj) = 85.48%


                             Individual 95% CIs For Mean Based on Pooled StDev
Level  N      Mean    StDev     +---------+---------+---------+---------
10      8   0.01133  0.04781                    (---*---)
12      8  -0.23777  0.11039     (---*---)
 8      8   0.22644  0.06621                                 (---*---)
                               +---------+---------+---------+---------
                             -0.30     -0.15      0.00      0.15

Pooled StDev = 0.07928


Grouping Information Using Tukey Method

Group  N      Mean  Grouping
8      8   0.22644  A
10      8   0.01133    B
12      8  -0.23777      C

Means that do not share a letter are significantly different.


Tukey 95% Simultaneous Confidence Intervals
All Pairwise Comparisons among Levels of Group

Individual confidence level = 98.00%


Group = 10 subtracted from:

Group     Lower    Center     Upper  ---------+---------+---------+---------+
12      -0.34889  -0.24911  -0.14932         (---*--)
 8       0.11532   0.21510   0.31489                         (--*--)
                                    ---------+---------+---------+---------+
                                          -0.30      0.00      0.30      0.60


Group = 12 subtracted from:

Group    Lower   Center    Upper  ---------+---------+---------+---------+
8      0.36442  0.46421  0.56400                                   (--*---)
                                 ---------+---------+---------+---------+
                                       -0.30      0.00      0.30      0.60
```

```
One-way ANOVA: PC2 versus Group

Source  DF      SS      MS     F      P
Group    2  0.0031  0.0015  0.10  0.907
Error   21  0.3290  0.0157
Total   23  0.3320

S = 0.1252   R-Sq = 0.92%   R-Sq(adj) = 0.00%


                          Individual 95% CIs For Mean Based on
                          Pooled StDev
Level  N     Mean   StDev  --------+---------+---------+---------+-
10     8   0.0103  0.0796      (---------------*--------------)
12     8  -0.0158  0.1905  (--------------*---------------)
 8     8   0.0054  0.0661      (--------------*--------------)
                          --------+---------+---------+---------+-
                               -0.060     0.000     0.060     0.120

Pooled StDev = 0.1252


Grouping Information Using Tukey Method

Group  N     Mean  Grouping
10     8   0.0103  A
 8     8   0.0054  A
12     8  -0.0158  A

Means that do not share a letter are significantly different.


Tukey 95% Simultaneous Confidence Intervals
All Pairwise Comparisons among Levels of Group

Individual confidence level = 98.00%


Group = 10 subtracted from:

Group    Lower   Center   Upper  --------+---------+---------+---------+-
12     -0.1836  -0.0261  0.1315  (--------------*---------------)
 8     -0.1624  -0.0049  0.1527    (---------------*--------------)
                                --------+---------+---------+---------+-
                                     -0.10      0.00      0.10      0.20


Group = 12 subtracted from:

Group    Lower  Center   Upper  --------+---------+---------+---------+-
8      -0.1363  0.0212  0.1787      (---------------*---------------)
                                --------+---------+---------+---------+-
                                     -0.10      0.00      0.10      0.20


One-way ANOVA: PC3 versus Group

Source  DF       SS       MS     F      P
Group    2  0.02298  0.01149  1.39  0.272
Error   21  0.17416  0.00829
Total   23  0.19714

S = 0.09107   R-Sq = 11.66%   R-Sq(adj) = 3.24%
```

```
                           Individual 95% CIs For Mean Based on
                           Pooled StDev
Level  N      Mean    StDev  -------+---------+---------+---------+--
10     8  -0.03724  0.06976  (----------*----------)
12     8  -0.00128  0.11855        (----------*----------)
 8     8   0.03852  0.07720              (----------*----------)
                           -------+---------+---------+---------+--
                               -0.060     0.000     0.060     0.120

Pooled StDev = 0.09107


Grouping Information Using Tukey Method

Group  N      Mean  Grouping
 8     8   0.03852  A
12     8  -0.00128  A
10     8  -0.03724  A

Means that do not share a letter are significantly different.


Tukey 95% Simultaneous Confidence Intervals
All Pairwise Comparisons among Levels of Group

Individual confidence level = 98.00%


Group = 10 subtracted from:

Group     Lower   Center    Upper  -----+---------+---------+---------+----
12      -0.07866  0.03596  0.15058         (-----------*----------)
 8      -0.03886  0.07577  0.19039             (-----------*----------)
                                  -----+---------+---------+---------+----
                                    -0.10      0.00      0.10      0.20


Group = 12 subtracted from:

Group     Lower   Center    Upper  -----+---------+---------+---------+----
8       -0.07481  0.03981  0.15443         (----------*----------)
                                  -----+---------+---------+---------+----
                                    -0.10      0.00      0.10      0.20



One-way ANOVA: PC4 versus Group

Source  DF       SS       MS     F      P
Group    2  0.02250  0.01125  2.68  0.092
Error   21  0.08818  0.00420
Total   23  0.11068

S = 0.06480   R-Sq = 20.33%   R-Sq(adj) = 12.74%


                           Individual 95% CIs For Mean Based on
                           Pooled StDev
Level  N      Mean    StDev  --------+---------+---------+---------+-
10     8  -0.04329  0.08665  (--------*---------)
12     8   0.02099  0.06770              (--------*---------)
```

```
8      8   0.02230  0.02251               (--------*---------)
                                 --------+---------+---------+---------+-
                                      -0.050     0.000     0.050     0.100

Pooled StDev = 0.06480


Grouping Information Using Tukey Method

Group  N      Mean  Grouping
 8     8   0.02230  A
12     8   0.02099  A
10     8  -0.04329  A

Means that do not share a letter are significantly different.


Tukey 95% Simultaneous Confidence Intervals
All Pairwise Comparisons among Levels of Group

Individual confidence level = 98.00%


Group = 10 subtracted from:

Group     Lower   Center    Upper  ----+---------+---------+---------+-----
12      -0.01728  0.06429  0.14585             (-------------*------------)
 8      -0.01597  0.06559  0.14716             (-------------*-------------)
                                  ----+---------+---------+---------+-----
                                   -0.060     0.000     0.060     0.120


Group = 12 subtracted from:

Group     Lower   Center    Upper  ----+---------+---------+---------+-----
8       -0.08026  0.00130  0.08287   (------------*-------------)
                                  ----+---------+---------+---------+-----
                                   -0.060     0.000     0.060     0.120



One-way ANOVA: PC5 versus Group

Source  DF       SS       MS     F      P
Group    2  0.02535  0.01268  4.68  0.021
Error   21  0.05694  0.00271
Total   23  0.08229

S = 0.05207   R-Sq = 30.81%   R-Sq(adj) = 24.22%


                            Individual 95% CIs For Mean Based on Pooled StDev
Level  N      Mean    StDev    -+---------+---------+---------+--------
10     8  -0.04583  0.07506    (---------*--------)
12     8   0.01984  0.03928                  (---------*---------)
 8     8   0.02599  0.03094                    (--------*---------)
                              -+---------+---------+---------+--------
                            -0.080    -0.040     0.000     0.040

Pooled StDev = 0.05207


Grouping Information Using Tukey Method
```

```
Group  N      Mean  Grouping
 8     8   0.02599  A
12     8   0.01984  A
10     8  -0.04583    B

Means that do not share a letter are significantly different.


Tukey 95% Simultaneous Confidence Intervals
All Pairwise Comparisons among Levels of Group

Individual confidence level = 98.00%


Group = 10 subtracted from:

Group    Lower   Center    Upper   --+---------+---------+---------+-------
12     0.00013  0.06567  0.13120               (----------*----------)
 8     0.00628  0.07181  0.13735                (----------*----------)
                                  --+---------+---------+---------+-------
                                 -0.060     0.000     0.060     0.120


Group = 2 subtracted from:

Group     Lower   Center    Upper   --+---------+---------+---------+-------
8      -0.05939  0.00615  0.07169     (----------*----------)
                                    --+---------+---------+---------+-------
                                   -0.060     0.000     0.060     0.120



One-way ANOVA: PC6 versus Group

Source  DF       SS       MS     F      P
Group    2  0.00226  0.00113  0.75  0.486
Error   21  0.03172  0.00151
Total   23  0.03398

S = 0.03887   R-Sq = 6.64%   R-Sq(adj) = 0.00%


                           Individual 95% CIs For Mean Based on
                           Pooled StDev
Level  N      Mean    StDev  -------+---------+---------+---------+--
10     8  -0.01320  0.04199  (-----------*----------)
12     8   0.00983  0.03994           (-----------*----------)
 8     8   0.00337  0.03425         (----------*-----------)
                           -------+---------+---------+---------+--
                               -0.025     0.000     0.025     0.050

Pooled StDev = 0.03887


Grouping Information Using Tukey Method

Group  N      Mean  Grouping
12     8   0.00983  A
 8     8   0.00337  A
10     8  -0.01320  A

Means that do not share a letter are significantly different.
```

```
Tukey 95% Simultaneous Confidence Intervals
All Pairwise Comparisons among Levels of Group

Individual confidence level = 98.00%


Group = 10 subtracted from:

Group     Lower   Center    Upper  ------+---------+---------+---------+---
12      -0.02589  0.02303  0.07195           (-------------*-------------)
 8      -0.03235  0.01657  0.06549         (-------------*-------------)
                                   ------+---------+---------+---------+---
                                      -0.035     0.000     0.035     0.070


Group = 12 subtracted from:

Group     Lower    Center    Upper  ------+---------+---------+---------+---
8       -0.05537  -0.00645  0.04247  (-------------*-------------)
                                    ------+---------+---------+---------+---
                                       -0.035     0.000     0.035     0.070



One-way ANOVA: PC7 versus Group

Source  DF       SS       MS     F      P
Group    2  0.00068  0.00034  0.29  0.751
Error   21  0.02445  0.00116
Total   23  0.02512

S = 0.03412   R-Sq = 2.69%   R-Sq(adj) = 0.00%


                            Individual 95% CIs For Mean Based on Pooled StDev
Level  N      Mean    StDev  ---------+---------+---------+---------+
10     8  -0.00497  0.02974  (---------------*---------------)
12     8   0.00736  0.04550          (---------------*---------------)
 8     8  -0.00239  0.02319    (---------------*---------------)
                            ---------+---------+---------+---------+
                                  -0.016     0.000     0.016     0.032

Pooled StDev = 0.03412


Grouping Information Using Tukey Method

Group  N      Mean  Grouping
12     8   0.00736  A
 8     8  -0.00239  A
10     8  -0.00497  A

Means that do not share a letter are significantly different.


Tukey 95% Simultaneous Confidence Intervals
All Pairwise Comparisons among Levels of Group

Individual confidence level = 98.00%
```

```
Group = 10 subtracted from:

Group     Lower   Center    Upper  --------+---------+---------+---------+-
12      -0.03061  0.01233  0.05527          (-------------*-------------)
 8      -0.04037  0.00258  0.04552       (-------------*-------------)
                                    --------+---------+---------+---------+-
                                         -0.030     0.000     0.030     0.060


Group = 12 subtracted from:

Group     Lower    Center    Upper  --------+---------+---------+---------+-
8       -0.05270  -0.00975  0.03319  (--------------*-------------)
                                     --------+---------+---------+---------+-
                                          -0.030     0.000     0.030     0.060
```

APPENDIX F – ALL P-VALUES FOR MORPHOMETRIC ANALYSIS

Table F1. Principle components and respective p-values for the first chicken morphometric analysis (including all data points). Statistically significant p-values are marked with an asterisk.

Principle Component	p-value
1	0.026*
2	0.033*
3	0.028*
4	0.931
5	0.007*
6	0.511
7	0.087
8	0.809

Table F2. Principle components and respective p-values for the second chicken morphometric analysis (after removal of the HH 42 outlier). Statistically significant p-values are marked with an asterisk.

Principle Component	p-value
1	0.000*
2	0.107
3	0.581
4	0.007*
5	0.708
6	0.124
7	0.822
8	0.417

Table F3. Principle components and respective p-values for the third chicken morphometric analysis (after removal of all HH 42 samples). Statistically significant p-values are marked with an asterisk.

Principle Component	p-value
1	0.000*
2	0.823
3	0.926
4	0.648
5	0.658
6	0.563
7	0.423
8	0.938

Table F4. Principle components and respective p-values for the zebrafish morphometric analysis. Statistically significant p-values are marked with an asterisk.

Principle Component	p-value
1	0.000*
2	0.907
3	0.272
4	0.092
5	0.021*
6	0.486
7	0.751

APPENDIX G – WESTERN ANALYSIS

WESTERN ANALYSIS
Adapted from existing lab protocols

G1 – ZEBRAFISH COLLECTION

½ Ginzburg Fish Ringer's – No Ca^{2+}

- 3.25 g NaCl
- 0.125 g KCl
- H_2O up to almost 1 L
- 0.1 g $NaHCO_3$
- dH_2O up to 1 L
- add half a EDTA-free protease inhibitor tablet per 25 mL before use

1. Euthanize previously measured zebrafish by placing them in 0.1% MS-222 for 5-10 minutes
2. Place in new petri dish with ½ Ginzburg Fish Ringer's with protease inhibitor, and keep on ice
3. Label two eppendorf tubes for HEAD tissue and BRAIN tissue and keep these on ice as well
4. Dissect under microscope, with fish in ½ Ginzburg Fish Ringer's with protease inhibitor
5. HEAD
    - Remove eyes from head one at a time
    - Sever head and place in labeled tube on ice
6. BRAIN
    - Cut incision along pigment boundary on dorsal side of head
    - Tear forward to remove the skull roof
    - Remove brain tissue (may come out in several chunks)
    - Place in labeled tube on ice
7. When all fish have been dissected, flash freeze the labeled tubes in liquid nitrogen – float tubes in liquid nitrogen for 45-60 seconds and remove carefully using long forceps
8. Quickly relocate to the -80°C freezer, where they are to be kept until the next step

G2 – LYSIS & SAMPLE PREP

RIPA Buffer

- 1.25 mL Tris-HCl pH 8.0
- 0.2451 g NaCl

- 0.25 mL Triton X-100
- 0.0137 g Sodium Deoxycholate
- 0.25 mL 10% SDS
- dH_2O up to 2 5mL
- Store at -4^oC
- add half a EDTA-free protease inhibitor tablet per 25 mL before use

Laemmli Buffer

- 900uL Laemmli buffer stock
    - 0.3785g Tris
    - 5mL glycerol
    - 10mL 10% SDS
    - dH_2O up to 25mL
- 100uL 2-mercaptoethanol

1. Keep frozen samples and RIPA buffer on ice
2. Homogenize samples separately using blue plastic homogenizer in eppendorf tubes
3. Add RIPA buffer to cover sample during homogenization (50 uL for brain, 150 uL for head)
4. Homogenization is complete when sample can be pipetted with P100 tip
5. When homogenization is complete, add an amount of Laemmli buffer that is equal to the amount of RIPA buffer previously added and mix by inversion
6. Boil tubes for 10 minutes
7. Centrifuge tubes for 5 minutes at 9,100 x gravity at room temperature
8. Remove supernatant, place in clean eppendorf tube and freeze at -80^oC (unless immediately continuing to next step)

G3 – LOADING AND RUNNING PAGE GEL

10x Running Buffer

- 15.175 g Tris
- 72.127 g glycine
- 5 mL 10% SDS in 400 mL dH_2O
- dH_2O up to 50 0mL
- pH 8.69

1. Fill cooling tank from transfer rig with H_2O and freeze
2. Retrieve 6x loading dye and protein ladder and keep on ice
3. Prepare 1x running buffer
    - 75 mL 10x running buffer
    - 675 mL dH2O

4. Keeping everything on ice as much as possible, make up samples to load onto gel
    - Ephrin samples
        - 20 uL head protein + 6 uL loading dye
        - 10 uL brain protein + 3 uL loading dye
    - β-tubulin samples
        - 20 uL head protein + 6 uL loading dye
        - 10 uL brain protein + 3 uL loading dye
    - Control
        - 10 uL brain protein + 3 uL loading dye
5. Spin samples 5 seconds to mix
6. Prepare gel running apparatus as follows:
    - Retrieve PAGE gel and remove green tape and plastic
    - Lock gel and dam into place
    - Fill exterior of running rig with 1x running buffer up to "2 gels" line
    - Fill interior of running rig with 1x running buffer up to submerge wells
7. Load wells as follows:
    1. –
    2. head (ephrin)
    3. brain (ephrin)
    4. –
    5. –
    6. head (β-tubulin)
    7. brain (β-tubulin)
    8. –
    9. brain (no primary control)
    10. -
8. Place nick in corner near lane #1 for orientation
9. Run 45 minutes @ 147 volts at room temperature, do not let colour pass the black line

G4 – TRANSFER

Transfer buffer

- 5.8230 g tris base
- 2.9339 g glycine
- 4 mL 10% SDS
- 600 mL dH2O
- 200 mL methanol
- H_2O up to 1 L dH2O
- pH 9.43

1. Remove gel

2. Fill three tupperwares with transfer buffer for soaking transfer components in transfer buffer
    1. Gel
    2. Scotchbrite pads
    3. Nitrocellulose membrane and filter papers
3. Soak gel, scotchbrite pads, nitrocellulose membrane, and filter papers in transfer buffer for 5 minutes
4. Make gel sandwich
    - Black side of cassette
    - Scotchbrite pad
    - Filter paper
    - Nitrocellulose membrane
    - Gel
    - Filter Paper
    - Scotchbrite pad
    - Transparent side of cassette
5. Place gel in transfer rig with membrane/black side nearest the red positive terminal
6. Insert frozen cooling tank, stir bar, fill rig almost to top (there are holes in the very top, so just high enough that there isn't any danger of leaking)
7. Run at ~30V overnight in walk-in fridge, stirring moderately

PONCEAU ROUGE TRANSFER CHECK

1. Carefully turn off transfer and remove components from fridge one at a time
2. Disassemble cassette on a few layers of paper towel
3. Incubate nitrocellulose membrane in 0.1% Ponceau Rouge in 5% acetic acid for approximately 5 minutes, then rinse with dH_2O

G5 – IMMUNOBLOT

1. Keep membrane in dH_2O while preparing for blot
2. Prepare ephrin-B2 and β -tubulin WB-1 antibody solutions as follows:
    - Ephrin-B2 WB-1 solution
        - 25uL ephrin-B2 antibody (not diluted)
        - 50uL WB-1 from kit
    - β -tubulin WB-1 solution
        - 7.2uL β -tubulin antibody
        - 50uL WB-1 from kit
3. Spin 3-5 sec after addition
4. Incubate 40 minutes at room temperature
5. Prepared 1x wash buffer (enough for 3 membranes x 6 washes x 12.5mL per wash)
    - 40mL 5x wash buffer

- 200mL dH_2O

6. Prepare pre-treat solution when there are 5 minutes left in incubation time for the WB-1 solution
    - 15 mL part A from kit
    - 15 mL part B from kit
7. Remove membrane from dH2O and separate into strips that will be tested with the same antibody (one ephrin-B2, one β-tubulin, one control), each strip in a different petri dish
8. Remember to add nicks in the top left corner for orientation
9. Place membranes in pre-treat solution for 5 minutes with gentle agitation at room temperature
10. Remove pre-treat solution and add ~12.5mL 1x wash buffer to each for 5 minutes at room temperature with gentle agitation 3 times
11. During these washes, prepare three WB-2 solutions
12. Ephrin-B2 WB-2 solution
    - 10 mL WB-2 solution from kit
    - Ephrin-B2 WB-1 solution (75 uL)
13. β-tubulin WB-2 solution
    - 10 mL WB-2 solution from kit
    - β-tubulin WB-1 solution (57.2 uL)
14. No-1^o control WB-2 solution
    - 10 mL WB-2 solution from kit
15. Removed third wash from membranes and added appropriate WB-2 solution to each
16. Leave for 1.5 hours at room temperature with gentle agitation
17. Remove WB-2 solution and add 1x wash buffer 3 times with gentle agitation
18. Remove final wash and add ~1 mL TMB (from kit) to each membrane and observe colour reaction

Products:

- Gels: BioRad 400079749
- Kit: GenScript L00204T
- Zebrafish Anti-β-tubulin primary antibody: Abcam AB6046
- Zebrafish Anti-ephrin-B2 primary antibody: Anaspec 55744
- Chicken Anti-β-tubulin primary antibody: Abcam AB6046
- Chicken Anti-ephrin-B2 primary antibody: Abcam AB140077

G6 – Results and troubleshooting

Table G1. Troubleshooting of Western analysis protocol for detecting ephrin-B2 in zebrafish and chicken.

Issue	Modification	Result
Very faint β-tubulin band	New Western kits	Clearer β-tubulin bands in anlyses with new kits
No β-tubulin band for zebrafish skull roof sample	Kept samples on ice during preparation	No discernible difference in results
No β-tubulin band for zebrafish skull roof sample	Flash-froze samples with liquid nitrogen between collection and homogenization steps	No discernible difference in results
No β-tubulin band for zebrafish skull roof sample	Increased amount of skull roof sample and anti-ephrin-B2 antibody concentration	No discernible difference in results
Blurry/unclear β–tubulin bands	More thorough mixing of antibodies prior to incubation	Clearer β-tubulin bands

APPENDIX H – PARAFFIN SECTION IMMUNOHISTOCHEMISTRY

H1 – APTES Coated Slides

1. Place new slides in silver trays
2. Dip in 100% EtOH
3. Dip in tap water
4. Dry overnight in 37°C oven
5. Remove slides from oven and allow to cool
6. Prepare solutions in large histology jars (make up to 300mL)
    a) 2% 3-aminopropylthioethoxy silane in acetone
    b) 100% acetone
    c) 100% acetone
    d) distilled water
7. Dip slides in jars in order
8. Dry overnight in 37°C oven
9. Put slides in labeled box for storage

H2 – Wax Embedding

1. Dissect the fixed samples if necessary
2. If stored in 70% ethanol, rehydrate to water through graded ethanol series
3. Platce samples in 10% EDTA (pH 7.4) for 1-5 days to decalcify (soften) the tissue (decalcification time depends on the sample)
4. Dehydrate through an ethanol series to absolute ethanol (25%, 50%, 70%, 80%, 90%, 100%, 45 minutes each, time depending on size of sample)
5. Place sample in glass vials in Citrosolv 2 x 1hr
6. Keep metal trays in the wax oven to warm them up
7. Place in low melting point wax at 54°C for 2 hours
8. Change wax and leave overnight at 54°C. Change the wax after 2 hours and replace with fresh wax.
9. Warm up forceps for embedding
10. With a pencil, label plastic block holder with sample name and your initials
11. Put sample with the correct orientation on the tray. Then place the tray on the ice block, cover with the plastic block holder and gently pout hot wax over it.
12. Keep the block on ice to set and leave in freezer overnight
13. Store at room temperature (or at -20°C if intending to do immune staining) in paper envelopes (NOT plastic bag)
14. Place in freezer day before intended use

H3 – Sectioning

- All sectioning was done using a Leitz 1512 wax sectioning apparatus
- All sections were 6μm in depth
- 9mm SL and 10mm SL zebrafish were oriented frontally, with their nose facing the top of the block, for embedding

H4 – Hall Brunt Quadruple Stain
By Hall (1986)

Hydration

1. Citrosolv 2x5 minutes
2. 100% ethanol 1 minute
3. 90% ethanol 1 minute
4. 80% ethanol 1 minute
5. 70% ethanol 1 minute
6. 50% ethanol 1 minute
7. H_2O 2'

Stain

1. Celestine blue 5 minutes
2. Wash in H_2O 1 minute
3. Mayer's Haemotoxylyn 5 minutes
4. Wash in H_2O 1 minutes
5. Alcian blue 5 minutes
6. Wash in H_2O 2 minutes
7. Phosphomolybdic acid 1 minute
8. Wash in H_2O 1 minutes
9. Direct red 5 minutes
10. Wash in H_2O (let sit in this and take through next steps one at a time
11. 100% ethanol <20 seconds
12. 100% ethanol <20 seconds
13. 100% ethanol <20 seconds
14. 100% ethanol <20 seconds

Clearing

1. Citrosolv 1 minute
2. Citrosolv 1 minute
3. Citrosolv 1 minute
4. Citrosolv 1 minute

Coverslip with distyrene plasticizer xylene (DPX), may take several days to completely dry

H5 – Paraffin section IHC for Ephrin-B2a in zebrafish
Adapted from existing lab protocols

1. Deparaffinize slides and rehydrate as follows:
    - 2x5 minutes Citrisolv
    - 2x2 minutes 100% EtOH

- 2 minutes 90% EtOH
- 2 minutes 70% EtOH
- 2 minutes 50% EtOH
- 2 minutes dH_2O

2. Permeabilize tissue (the following ways were used)
    - 0.1% Triton X-100/0.1% sodium citrate at 90°C, 8 minutes
    - 0.1% Triton X-100/0.1% sodium citrate at 60°C, 8 minutes
    - 0.1% Triton X-100/0.1% sodium citrate at room temperature, 8 minutes
    - 0.1% Tween/0.1% sodium citrate at 60°C, 8 minutes
3. Rinse 2x5 minutes in 1x PBS
4. Block endogenous peroxidases by 3% H_2O_2/1x PBS, 10 minutes
5. Rinse 5 minutes in 1x PBS
6. Block in 10% rabbit serum/1% bovine serum in 1x PBS for 1 hour in humidity chamber at 37°C
7. Apply primary antibody diluted 1:500 in 1% BSA/1x PBS overnight at 4C in humidity chamber
8. Rinse 2x5 minutes in 1x PBS
9. Apply secondary antibody for 2 hours in humidity chamber at room temp
    - Various dilutions included 1:200, 1:500, 1:1000, 1:2000, 1:5000
10. Rinse 2x5 minutes in 1x PBS
11. Prepare detection buffer by dissolving Sigmafast DAB tablets D0426 (one gold, one silver) in 5mL dH2O
12. Apply DAB solution to slides and monitor progress for 5-10 minutes
13. Rinse slides gently in tap water
14. Coverslip with Fluoroshield and observe the following day

Antibodies:

- Zebrafish anti-ephrin-B2 primary antibody (polyclonal goat IgG): R&D Systems AF1088
- Rabbit anti-Goat IgG (HRP) secondary antibody: Abcam AB6741

H6 – Results and troubleshooting

Table H1. Troubleshooting of Paraffin IHC protocol for visualizing ephrin-B2 in zebrafish skull sections.

Issue	Modification	Result
All slides except no-secondary control too dark in background, implying over-staining or under-rinsing of secondary antibody	Increased washes after secondary incubation from 2x5 minutes to 3x20 minutes	No discernible difference in results
All slides except no-secondary control too dark in background, implying over-staining or under-rinsing of secondary antibody	Decreased secondary antibody concentration to 1:1000 and 1:2000	Background of all slides consistently lighter at both new concentrations
Staining not distinguishable from background	Added block in 10% rabbit serum/1% bovine serum in 1x PBS for 1 hour at 37°C before secondary incubation	No discernible difference in results
Staining not distinguishable from background	Increased peroxidase blocking from 10 minutes to 30 minutes	No discernible difference in results
No distinguishable staining, suspected over-permeabilization	Decreased permeabilization temperature from 90°C to 60°C and room temperature	No discernible difference in results
No distinguishable staining, suspected over-permeabilization	Used 0.1% Tween instead of 0.1% Triton	No discernible difference in results

APPENDIX I – WHOLE-MOUNT IMMUNOHISTOCHEMISTRY

I1 – Whole-mount IHC for ephrin-B2a in zebrafish

Adapted from existing lab protocols

1. Fix 36 hpf embryos in 4% PFA at 4°C overnight and store in 1x PBS
2. Dechorionate fixed embryos
3. Rinse 3x15 minutes in 1x PBS at room temperature with gentle agitation
4. Permeabilize in 4% triton x-100 in 0.1% sodium citrate overnight at room temperature
    - Also tested 2% and 1% triton x-100
5. Rinse 3x15 minutes in 1x PBS at room temperature with gentle agitation
6. Bleach 30 minutes in 3% H_2O_2/1x PBS
    - Also tested 3% H_2O_2/MeOH
7. Rinse 2x10 minutes in 1x PBS at room temperature with gentle agitation
8. Block 1 hour in 10% rabbit serum / 1% bovine serum in 1x PBS at 37C
9. Prepare primary antibody diluted 1:500 in 1% bovine serum albumin / 1x PBS
10. Incubate in primary antibody 3 nights at 4°C
11. Rinse 2x20 minutes in 1x PBS at room temperature with gentle agitation
12. Block 1 hour in 10% rabbit serum / 1% bovine serum in 1x PBS at 37C
13. Prepare secondary antibody diluted 1:1000 in 1% bovine serum albumin / 1x PBS
14. Incubate in secondary antibody 2 nights at 4°C
15. Rinse 2x20 minutes in 1x PBS at room temperature with gentle agitation
16. Prepare detection buffer by dissolving Sigmafast DAB tablets D0426 (one gold, one silver) in 5mL dH2O
17. Apply DAB solution and monitor progress for 5-10 minutes
18. Remove DAB solution and store in 1x PBS at 4°C

Antibodies:

- Zebrafish anti-ephrin-B2 primary antibody (polyclonal goat IgG): R&D Systems AF1088
- Rabbit anti-Goat IgG (HRP) secondary antibody: Abcam AB6741

I2 – Results and Troubleshooting

Table I1. Toubleshooting of whole-mount IHC protocol for visualizing ephrin-B2 in 36hpf zebrafish embryos.

Issue	Modification	Result
Antibodies unable to permeate egg	Dechorionate embryos before beginning protocol	Antibodies and other chemicals able to reach embryo directly
Embryos very small and susceptible to being lost during solution changes	Moved protocol from eppendorf tubes to well plates and used P100 tips for all solution changes	It became much easier to keep track of the very small embryos
All samples except no-secondary control too dark in background, implying over-staining or under-rinsing of secondary antibody	Increased washes after secondary incubation from 2x20' to 4x10'	No discernible difference in results

I3 – Whole-mount IHC for ephrin-B2a in zebrafish – Protocol #2
Retrieved from ABCAM

1. Fix 36hpf embryos in 4% PFA at 4°C overnight and store in 1x PBS
2. Dechorionate fixed embryos
3. Rinse 4x5 minutes in 1x PBS/1% triton at room temperature
4. Permeabilize in ice cold acetone 8 minutes only
5. Rinse 4x5 minutes in 1x PBS/1% triton at room temperature
6. Wash 2x1 hour in 1xPBS/1% triton/10% bovine serum at room temperature
7. Peroxidase block in 0.1% H_2O_2 in 10% rabbit serum/1% bovine serum overnight at 4°C
8. Wash 2x30 minutes 10% rabbit serum/1% bovine serum
9. Prepare primary antibody diluted 1:500 in 1% bovine serum albumin / 1x PBS
10. Incubate in primary antibody 4 nights at 4°C
11. Wash 3x1 hour in 1xPBS/1% triton/10% bovine serum at room temperature
12. Wash 3x10 minutes 1xPBS/1% triton
13. Prepare secondary antibody diluted 1:1000 in 1% bovine serum albumin / 1x PBS
14. Incubate in secondary antibody 3 nights at 4°C
15. Wash 3x1 hour in 1xPBS/1% triton/10% bovine serum at room temperature
16. Wash 3x10 minutes 1xPBS/1% triton

17. Prepare detection buffer by dissolving Sigmafast DAB tablets D0426 (one gold, one silver) in 5mL dH2O
18. Apply DAB solution and monitor progress for 5-10 minutes
19. Remove DAB solution and store in PBS at 4°C

Antibodies:

- Zebrafish anti-ephrin-B2 primary antibody (polyclonal goat IgG): R&D Systems AF1088
- Rabbit anti-Goat IgG (HRP) secondary antibody: Abcam AB6741

APPENDIX J – *IN SITU* HYBRIDIZATION

IN SITU HYBRIDIZATION

J1 – Anti-*efnB2a* probe

Digoxigenin-labelled, single-stranded RNA probes were made using DIG RNA labeling kit (Roche 11175025910). cDNA used for preparation of these probes was prepared using a cloning vector. This was done by Dr. Jochen Weigele.

J2 – Prep Day (Collection of embryos and fish) (Approx 2 hours + Overnights)
Collect Embryos
Dechorinate 24 and 48 hpf embryos. For older embryos – anesthetise in 0.1% MS222.
Fix in 4% PFA (RNAase free) for 2 hours at room temperature or overnight at 4^{o}C.

Dehydrate in series

25% MeOH in PBS	30 min at RT	1X
50% MeOH in PBS	30 min at RT	1X
75% MeOH in PBS	30 min at RT	1X
100% MeOH	At Least Overnight	Store in -20^{o}C

Notes
MS222 is a powder that should be made into 0.01% and 0.1% solutions fresh for each day.
PFA is found in the -20^{o}C freezer

J3 – Day 1: Bleach Day (Approx 1.5 hours, longer if older fish)
Rehydrate embryos

75% MeOH in PBS	5 min at RT	1X
50% MeOH in PBS	5 min at RT	1X
25% MeOH in PBS	5 min at RT	1X

Wash

PBST	5 min at RT	1x

Transfer embryos to sterile 24 well plate. Use sterile baskets and tweezers to move basket from well to well. RNAase zap basket and tweezers before use.

Bleach
Bleach according to times below, or until the embryo is a creamy white. Ensure eyes don't become bulgy.

General timeline for fish

Age	Approx Bleach Time
24 hpf	10 min
48 hpf	25 min
72 hpf	40 min
5 dpf	50 min
6.7mm	1h15
8.0mm	1h30

Bleach Recipe – Make Fresh on the day of…

Total Amount	5ml	Total Amount	20ml
KOH (0.5%)	0.025g	KOH (0.5%)	.1050g
H_2O_2 (3% of 30%)	150ul	H_2O_2 (3% of 30%)	600 ul
DepC treated H_2O	To 5ml	DepC treated H_2O	To 20mls

Wash

PBS	5 min at RT	1x

Note: Embryo's can be very sticky in PBS/MeOH solutions

Dehydrate in series

25% MeOH in PBS	5 min at RT	1X
50% MeOH in PBS	5 min at RT	1X
75% MeOH in PBS	5 min at RT	1X

Transfer into 1.5ml eppendorff tube

100% MeOH	Store in -20^{o}C Overnight

Embryos can now be stored in 100% MeOH at -20^{o}C for several weeks or at minimum of 2 hours before continuing on

J4 – Day 2: Pro-K and Treatment Day (Approx 5 hours, longer if older fish)

Rehydrate embryos in 1.5ml eppendorf tubes

75% MeOH in PBS	5 min at RT	1X
50% MeOH in PBS	5 min at RT	1X
25% MeOH in PBS	5 min at RT	1X

Wash

PBST 5 min at RT 4x

Permeabilize: With Proteinase K (10ug/ml in DepC)
If using a 10mg/ml stock, dilute by adding 1ul of stock solution to 1000ul ul of DepC treated H_2O
Note: Pro-K in lower part of -20°C

Age	Approx Pro-K Time
24 hpf	10 min
48 hpf	23 min
72 hpf	30 min
5 dpf	42 min
6.7mm	1 h
8.0mm	1 h 15 min

Wash
PBST 5 min at RT 2x

Fix (In fume hood)
4% PFA (DepC Treated) 20 min at RT 1x
Note: PFA is found in the -20°C freezer

Wash
PBST 5 min at RT 2x

Treat (In fume hood) – Make fresh on the day of…
Acetic Anhydride 30 min at RT 1x

Acetic Anhydride Recipe	6ml Batch
DepC treated H_2O	4.5 ml
Triethanolamamine (upstairs lab cabinet)	79.9 ul
pH to 7.0	
DepC treated H_2O	To 6 ml
Acidic anhydride (under fume hood)	15 ul

Wash
PBST 10 min at RT 2x

Prehybridize
Hyb (-) 2 hours at 70°C/35 rpm
Note: See last page for Hyb(-) recipe. There should be a premade stock in the -20°C at all times.

Stop Point: Embryo's can be stored in Hyb (-) for several weeks, or you can continue to the next step.

J5 – Day (1/3): Hyb(+) – Adding the probe (Approx 2 hours)

Pre Hyb(-)
Hyb (-) 2 hours at 70°C/35rpm

Note: We re-do this stage to ensure the embryos are at the same permeability/solubility as previous

Adding Hyb (+)
Add 1 ml of Hyb (+) to each sample

Hyb (+) Recipe	Per tube (1ml)	For 4 ml
Hyb (-)	890 ul	3560 ul
Yeast tRNA (5mg/ml)	100 ul of 50mg/ml stock	400 ul
Heparin (50ug/ml)	10 ul of 5mg/ml stock	40 ul
pH to 6.0 with Citric Acid	9.2 ul of 1M citric acid	36.8 ul

Note: Multiply each reagent by the number of samples you have.

Adding probe
Add 2-3 ul of probe (depending on strength) to each of the sample tubes.

Notes
Probe should not be left out of the freezer long. Putting them on ice is recommended.
Ensure probe is mixed – flick with finger and centrifuge liquid back down for 2-3 seconds.
If using Fast Red probes – ensure samples are not exposed to light. Cover using tinfoil.

Incubate overnight at 70°C/35rpm

J6 – Day (2/4): Washes and Antibody (Approx 7 hours, with 3-4 hour break in middle)

Washes

75% Hyb (-) + 25% 2xSSC	15 mins at 70°C/35rpm	1x
50% Hyb (-) + 50% 2xSSC	15 mins at 70°C/35rpm	1x
25% Hyb (-) + 75% 2xSSC	15 mins at 70°C/35rpm	1x

Note: These solutions should be premade and stored in the -20°C freezer

Change to fresh eppendorf tubes – Hyb (-) is very slippery and the tube caps tend not to stay in place at this point. The tubes will also likely have white precipitate

throughout.

Note: Going into this next stage – Embryo's can become very sticky! Check pipette tip after each
changeover!

2xSSC	10 mins at 70°C/35rpm	2x
0.2xSSC	30 mins at 70°C/35rpm	3x

Start sheep serum inactivation 30 mins at 60°C (amount based on Blocking Buffer Recipe)

75% 0.2xSSC + 25% PBST	10 mins at Room temp/60rpm	1x
50% 0.2xSSC + 50% PBST	10 mins at Room temp/60rpm	1x
25% 0.2xSSC + 75% PBST	10 mins at Room temp/60rpm	1x
100% PBST	10 mins at Room temp/60rpm	1x

Incubate in blocking buffer for 3-4 hours
Add 1 ml of Blocking buffer to each tube
Make Fresh on the day of…

Blocking Buffer recipe	1 ml/Sample	For 4 ml
1 x PBST	980 ul	3920 ul
2% Heat inactivated Sheep serum	20ul	80 ul
Bovine serum albumin (2 mg/ml)	0.002 g	0.008 g

Note: Save at least 10 ul of blocking buffer. It is required in making the antibody recipe.

Adding antibody

Antibody Recipe	
Blocking Buffer (saved from before)	9 ul
Anti-Dig Antibody	1 ul
Optional – Fish powder	A few pieces

Allow antibody to sit in blocking buffer for at least 10 minutes before adding the antibody solution to the samples. This allows preabsorption to occur, and reduces background.
Add 1 ul of above antibody recipe to each sample tube already containing the 1 ml of blocking buffer from 4-5 hours prior.

Incubate overnight at 4°C while shaking
Note: The incubator in the lower lab works well for this. Ensure the incubator is properly set and on early in the day, as it takes time to cool down.
The small "Mandel" shaker works well for this stage.

J7 – Day (3/5): Antibody and Color Reaction (Approx 4 hours then overnight)

Remove samples from incubator and discard antibody solution

Washes
PBST 5 min at RT

PBST 15 min at RT on same "Mandel" Shaker
12x

Place embryos in sterile glass vials – Ensure proper labeling

Incubate TRIS Staining Buffer
Add 1ml of TRIS Staining Buffer to each sample 5 mins at room temp 3x

Make Fresh on the day of…

Reagent	Stock	Final	20 ml Batch	10 ml Batch
TRIS pH 9.0	1 M	100 mM	2 ml	1 ml
$MgCl_2$	1 M	50 mM	1 ml	0.5 ml
NaCl	5 M	100mM	400 ul	200 ul
Tween	10%	0.1%	20 ul	10 ul
Levamisole		2mM	0.019 g	0.0095 g
DepC treated H_2O			To 20 ml	To 10 ml

Note: When determining batch size, allow for three change-over's per tube as well as enough for mixing NBT/BCIP staining solution

Add Color Reaction Solution
Very Important! – Ensure staining solution remaining in dark. It is a light sensitive reagent.

NBT/BCIP Staining Solution	Amount needed per single sample	Amount for 4 tubes
TRIS staining buffer (from above)	1.2 ml	4.8 ml
BCIP	4.25 ul (50mg/mL)	17 ul
NBT	3.03 ul (50mg/mL)	12.12 ul

Remove TRIS staining buffer and Add Color Reaction Solution

Approximately 1.2 ml per sample
Place samples in incubator at 4°C overnight or at 37°C until expression shows.
Best results have been attained at 4°C overnight

J8 – Day (4/6): Stopping Color Reaction (Approx 2 hours)

Wash		
PBST	5 min at Room Temperature	6x

Fix (in fume hood)		
4% PFA	20 mins at room temperature	1x

Dehydrate (for NBT/BCIP Color reactions only!)

25% MeOH in PBS	10 min at RT	1X
50% MeOH in PBS	10 min at RT	1X
75% MeOH in PBS	10 min at RT	1X
100% MeOH	Store in 4°C in sample box	

Note: Photos should be taken while sample is in 25% or 50% MeOH/PBS

J9 – Reagent recpies

Hyb(-)

Reagent	% in final solution	50 ml Batch	250 ml Batch (ideal)
Deionized Formamide 100%	50	25 ml	125 ml
SSC 20x	5x	12.5 ml	62.5 ml
Tween 10% (stock solution)	0.1	50ul	250 ul
DepC treated H_2O		Top to 50ml	Top to 250 ml

Note: Make in fume hood. Ensure contents are well mixed. Aliquot into 50ml flacon tube and store in -20°C.

PBS

Reagent for 500 ml Batch	
NaCl	4.0 g
KCl	0.1 g
Na_2PO_4	0.693 g
KH_2PO_4	0.1 g
Top to 500ml with DepC treated H_2O	
pH to 7	

To make PBST
add 50 ul of Tween-10 to 50 ml of PBS DepC treated H_2O Per 1 L of water add 100 ul of DepC (found in upstairs fridge). Carry out in fume hood. Shake for 30 minutes vigorously. Autoclave

APPENDIX K – CATALOGUE NUMBERS

Table K1. Catalogue and supplier number of all products used for staining, Western analysis, IHC, and ISH.

Product	Supplier and Catalogue Number
Acetic acid	Fisher A38 212
Acetic anhydride	Sigma A6405
Acetone	Fisher A18-4
Acidic anhydride	Sigma A6405
Alcian blue GX	Sigma A3157
Alizarin red S	Sigma A5533
Aminopropyl triethoxy-silane (APTES)	Sigma A3648
Antibody – anti-dioxigenin	Roche 13680323
Antibody – Chicken anti-ephrin-B2 (WESTERN)	Abcam AB140077
Antibody – Rabbit anti-Goat IgG (HRP) (IHC)	Abcam AB6741
Antibody – Zebrafish anti-ephrin-B2 (IHC)	R&D Systems AF1088
Antibody – Zebrafish anti-ephrin-B2 (WESTERN)	Anaspec 55744
Antibody – Zebrafish/Chicken anti-β-tubulin (WESTERN)	Abcam AB6046
Bovine serum albumin	Sigma A9647
Citric acid	Acros Organics 220341000
Citrosolv	Fisher 22143975
Complete EDTA-free protease inhibitor	Roche 11873580001
Deionized formamide	Amresco 606
Diethylpyrocarbonate (DepC)	Sigma D5758
DIG RNA labeling kit	Roche 11175025910
Di-sodium hydrogen phosphate	Fluka 71636
DPX Mountant	Fluka 44581
Ethylenediaminetetraacetic acid	Gibco 15575-038
Glycerol	VWR CABDH1172
Glycine	VWR CA97061
Heparin sodium salt	Sigma H3393
Hydrochloric acid	Sigma 258148
Hydrogen peroxide	VWR BDH3742-1
Levamisole (Tetramisole hydrochloride)	Sigma L9756
Magnesium chloride	Fisher 930963
Mercaptopethanol	VWR CA EM6010
Methanol	Fisher A412-4
One-Hour Western Complete Kit	Genscript L00204T
Paraformaldehyde	Sigma P6148
Potassium chloride	Sigma P217-10

Product	Company and Catalogue Number
Potassium hydroxide	Sigma 221473
Potassium phosphate	Sigma P5655
Proteinase K	Sigma P8044
Rabbit serum	Sigma R9133
Saline sodium citrate buffer	Sigma S6639
Sheep serum	Sigma S2263
Sigma Fast 3.3' diaminobenzidine tetrahydrochloride with metal enhancer tablet sets	Sigma D-0426
Sodium chloride	Sigma S5881
Sodium citrate	Sigma S1804
Sodium deoxycholate	VWR CASX0480
Sodium phosphate	EMD SX0720-1
Sodium dodecyl sulfate	Sigma L4390
Sodium tetraborate	Sigma B9876
SSC buffer 20x concentrate	Sigma S6639-1L
Triethanolamamine	Sigma T58300
Tris base	Tupper 3118142001
Triton X-100	Aldrich 234729-100ml
Trypsin	Fisher T360-500
Tween 20	Sigma P9416
Western running gels	BioRad 400079749
Yeast tRNA	Roche 10 109 223 001